STUDIES OF THE MOLECULAR MECHANISMS UNDERLYING CANCER STEM CELLS AND THE TRANSFORMED METABOLIC PHENOTYPE

A Dissertation

Presented to the Faculty of the Graduate School

of Cornell University

in Partial Fulfillment of the Requirements for the Degree of

Doctor of Philosophy

by

Kelly Elizabeth Sullivan

August 2015

STUDIES OF THE MOLECULAR MECHANISMS UNDERLYING CANCER STEM CELLS AND THE TRANSFORMED METABOLIC PHENOTYPE

Kelly Elizabeth Sullivan, Ph.D.

Cornell University 2015

Intense research throughout recent decades has significantly expanded our knowledge of the complexities that make cancer a highly diverse and therapeutically challenging disease. Recently, cancer stem cells (CSCs) and de-regulated cellular metabolism have become appreciated for their crucial roles in the development, growth, and therapy resistance of tumors, and are now being pursued as therapeutic targets for the treatment of cancer. To better understand how these oncogenic events contribute to tumor malignancy, I carried out a mechanistic analysis of the CSC marker aldehyde dehydrogenase 1A3 (ALDH1A3) and the GTP-binding protein/crosslinking enzyme tissue transglutaminase (tTG), two proteins suspected to have key roles in tumor initiation and the development of the malignant state, in glioma stem cells (GSCs). Additionally, I examined the contributions of two isoforms of glutaminase (GLS), given the critical role of elevated glutamine metabolism in maintaining the transformed state.

In delineating the role of ALDH1A3 in GSCs, I discovered that it is an important regulator of gene expression through the production of retinoic acid (RA). Specifically, I demonstrated that the expression of tTG is induced downstream of ALDH1A3 via RA in highly aggressive GSCs. Furthermore, targeting tTG results in a dramatic reduction in the self-renewal of these cells, suggesting that it may be a viable therapeutic target in ALDH1A3^{+} GSCs. Finally,

I showed that combination therapies including a tTG inhibitor and radiation or chemotherapy are cytotoxic, indicating that tTG inhibitors enhance the effects of standard glioma therapies.

Work described in this thesis has also been directed toward understanding the roles of different splice variants of the metabolic enzyme GLS in cancer cell growth. An important question in the field has concerned whether the two known GLS splice variants, glutaminase C (GAC) and kidney-type glutaminase (KGA), have redundant or opposing functions. This becomes especially relevant when considering the importance of targeting one or both of these enzymes when designing strategies to inhibit the metabolic reprogramming of cancer cells. Here, I show that although KGA is expressed at low levels in cancer cells relative to GAC, these isoforms are functionally redundant in their abilities to support the transformed metabolic phenotype.

BIOGRAPHICAL SKETCH

Kelly was born and raised in the beautiful Hudson Valley in New York. Her parents encouraged her to work hard in school, and she came to love science at a young age. The loss of her beloved dog, Taffy, to brain cancer inspired her to become a cancer researcher. After graduating from high school, Kelly attended the University of Rochester in Rochester, NY, where she studied biochemistry and history. It was there that she was first exposed to scientific research as an undergraduate research assistant in the laboratory of Dr. Mark Dumont. Under Dr. Dumont's guidance, Kelly investigated the oligomerization of the Ste2 α-factor receptor in yeast. She later went on to work with Dr. A. James Mason at King's College London while studying abroad, where she investigated the biophysical properties of novel antimicrobial peptides. After graduating from college, Kelly enrolled in the Biochemistry, Molecular and Cell Biology graduate program at Cornell University, where she was fortunate to be accepted as a student in the laboratory of Dr. Richard Cerione. Her graduate research has focused on understanding the molecular mechanisms that drive the initiation and maintenance of cancer, particularly the roles of cancer stem cells and an altered metabolic phenotype. Kelly enjoyed her five years at Cornell in the Cerione lab, and learned a great deal about becoming a scientist. After getting her Ph.D., Kelly will enroll in the College of Veterinary Medicine at Cornell, where she will become a veterinarian. She hopes to continue pursuing cancer research as a veterinary scientist.

For my family, my mentors, and my friends.

ACKNOWLEDGEMENTS

To my parents, Julie, and Erin, thank you for your constant love and support, for always believing in me, and for teaching me to never give up.

To James, thank you for your endless love and support, for always encouraging me to follow my passions, and for having more faith in me than I have in myself.

To Rick, my deepest gratitude for taking me as a student, for all of your dedication, patience, and support these five years, and for teaching me to think like a scientist.

To Kristin, thank you for your patience, guidance, and support throughout my journey towards becoming a scientist.

Thank you to my committee members, Maurine and Scott, for your helpful comments and advice.

To the members of the Cerione lab, past and present, thank you for creating a warm and welcoming environment where I have always felt comfortable asking questions, and for all of the engaging discussions about science and life.

To the Department of Molecular Medicine, especially Cindy and Debbie, thank you for your superb administrative support, and for always putting a smile on my face.

Thank you to all of my friends who have supported me through this journey, for always making me laugh, and for reminding me that there is life outside of the lab.

TABLE OF CONTENTS

LIST OF FIGURES

LIST OF TABLES

LIST OF ABBREVIATIONS

3'UTR: 3' untranslated region
αKG: α-ketoglutarate
ABC: ATP-binding cassette superfamily protein
ABCG2/BCRP: ATP-binding cassette sub-family G member 2/breast cancer resistance protein
ACL: ATP-citrate lyase
ALDH: aldehyde dehydrogenase
ALDH1A3: aldehyde dehydrogenase 1 family, member A3
AML: Acute myeloid leukemia
AMPK: AMP-activated protein kinase
ALT: alanine aminotransferase
APA: alternative polyadenylation
APC: Adenomatous polyposis coli
ARF/p14: alternate reading frame, cyclin-dependent kinase inhibitor 2A
AST: aspartate aminotransferase
ATM: Ataxia telangiectasia mutated
BMI1: B lymphoma Mo-MLV insertion region 1 homolog
BPA: biotinylated pentylamine
BPTES: Bis-2-(5-phenylacetamido-1,3,4-thiadiazol-2-yl)ethyl sulfide
C/EBPβ: CCAAT-enhancer-binding protein β
CIMP: CpG island methylator phenotype
CK1: Casein kinase 1
CNS: central nervous system
CRABP: cellular retinoic acid binding protein
CRBP: cellular retinol binding protein
CSCs: cancer stem cells
CXCR4: C-X-C chemokine receptor type 4
CYP26: cytochrome P450 26
DEAB: diethylaminobenzaldehyde
dm-αKG: dimethyl-α-ketoglutarate
DMSO: dimethyl sulfoxide
ECM: extracellular matrix
EGF: epidermal growth factor
EGFR: epidermal growth factor receptor
EGFRvIII: epidermal growth factor receptor variant type III
EMT: epithelial-mesenchymal transition
ERK: extracellular signal-regulated kinase
FAK: focal-adhesion kinase
FAS: fatty acid synthase
FGF: fibroblast growth factor
FOXO: forkhead box protein O
GAC: glutaminase C
GABA: γ-aminobutyric acid

GBM: glioblastoma multiforme
GDH: glutamate dehydrogenase
GEF: guanine nucleotide exchange factor
GLI: glioma-associated oncogene
GLS: glutaminase
GLS2: glutaminase 2
GLUT3: glucose transporter 3
GPCR: G protein-coupled receptor
GSCs: glioma stem cells
GSK3β: glycogen synthase kinase 3 β
HGG: high grade glioma
HH: hedgehog
HIF1α/β: hypoxia-inducible factor 1 α/β
HK: hexokinase
IDH1: isocitrate dehydrogenase 1
IL-6: interleukin 6
INK4A/p16: cyclin-dependent kinase inhibitor 2A
IR: ionizing radiation
JAK: Janus kinase
JNK: c-Jun N-terminal kinase
KGA: kidney-type glutaminase
L1CAM: L1 cell adhesion molecule
LDHA: lactate dehydrogenase A
LEF/TCF: lymphoid enhancer factor/T-cell factor
LGA: liver-type glutaminase
LKB1: liver kinase B1
MAP kinase: mitogen-activated protein kinase
MES: mesenchymal
MDC: monodansyl cadaverine
MMP-9: matrix metallopeptidase 9
mTOR: mammalian target of rapamycin
mTORC1: mammalian target of rapamycin complex 1
NF-κB: nuclear factor kappa-light-chain-enhancer of activated B cells
OCT4: octamer-binding transcription factor 4
PAG: phosphate-activated glutaminase
PDGFRα: platelet-derived growth factor receptor α
PDI: protein disulfide isomerase
PDH: pyruvate dehydrogenase
PDK1: pyruvate dehydrogenase kinase 1
PEP: phosphoenolpyruvate
PFK2: phosphofructokinase 2
PFKFB3: phosphofructokinase 2 isoform FB3
PI3K: phosphoinositide 3-kinase
PIP_3: phosphatidylinositol (3,4,5)-trisphosphate
PKM1: pyruvate kinase isoform M1
PKM2: pyruvate kinase isoform M2

PLCδ1: phospholipase C δ1
PN: proneural
PNS: peripheral nervous system
PTEN: phosphatase and tensin homolog
RA: retinoic acid
RAR: retinoic acid receptor
RARE: retinoic acid response element
Rb: retinoblastoma
RDH: retinol dehydrogenase
ROCK: Rho-associated, coiled-coil containing protein 1
ROS: reactive oxygen species
RTK: receptor tyrosine kinase
RXR: retinoid X receptor
SC: stem cell
Sirt5: Sirtuin 5
SOX2: sex determining region Y-box 2
SSEA-1: stage-specific embryonic antigen 1
STAT: signal transducer and activator of transcription
SVZ: subventricular zone
TAZ: tafazzin
TCA cycle: tricarboxylic acid cycle
TERT: telomerase reverse transcriptase
TG: transglutaminase
TGF-β: transforming growth factor β
TMZ: temozolomide
TNF: tumor necrosis factor
TSC2: tuberous sclerosis 2
tTG/TGM2: tissue transglutaminase/transglutaminase 2
VEGF: vascular endothelial growth factor
VHL: von Hippel-Lindau tumor suppressor

CHAPTER 1

Overview

Over the past thirty to forty years, rapidly accumulating studies of cancer have made significant advancements in uncovering the vast complexities and diverse characteristics associated with this disease. Comprehensive analyses of the ever-expanding cancer biology literature have led to the synthesis of a set of "rules" for the development of cancer, encompassing the hallmarks that are exhibited by and required for nearly all malignant neoplastic transformations. In recent years, cancer stem cells (CSCs) and de-regulated cellular metabolism have come to the forefront of cancer research, with countless studies highlighting their diverse roles in supporting these hallmarks (1). These studies have uncovered the pleiotropic functions of a novel stem cell-like population of cancer cells, as well as shed light on a previously under-appreciated alternative metabolic phenotype that is crucial for the growth and expansion of neoplasias (2-8). In this thesis, I set out to better understand the molecular mechanisms underlying these oncogenic events by examining the regulated expression of a protein often implicated in metastatic disease, tissue transglutaminase (tTG), by aldehyde dehydrogenase 1A3 (ALDH1A3), a major marker of glioma stem cells (GSCs) (9-12). I have also examined two splice variants of the mitochondrial enzyme glutaminase (GLS), which is thought to have a critical role in the metabolic reprogramming of cancer cells and in the maintenance of their malignant state (13, 14).

In this chapter, I will provide an overview of CSCs, ALDH1A3, and tTG, as well as our current understanding of the transformed metabolic phenotype and the role of GLS in normal and neoplastic cells. I will begin with a discussion of the characteristics and diverse roles of CSCs in

cancer, as well as those of GSCs, the model system that I have used for my studies detailed in Chapter 2. Next, I will recount the known roles of ALDH1A3 and tTG in normal and transformed cells, and suggest a potential link between these enzymes that I will later explore in Chapter 2. The second part of this chapter will introduce the phenomenon of aerobic glycolysis, commonly referred to as "the Warburg effect," as well as the glutamine dependence exhibited by many cancer cells (5-8). Finally, I will discuss the roles of GLS in both normal and transformed cells, and our current mechanistic understanding of GLS catalysis.

Identification and characterization of cancer stem cells

The notion that tumors are clonally derived from a single malignant and undifferentiated cell has been explored for nearly 75 years, and the joint efforts of cancer and stem cell biologists have gradually given rise to the concept that CSCs lay the foundation for tumor initiation (15). Although CSCs, also referred to as tumor-initiating cells, were suspected to exist for many decades, this rare population of cancer cells was not successfully isolated until 1994 by John Dick and colleagues. In a study of acute myeloid leukemia (AML), they determined that only an immature population of human leukemic cells with a hematopoietic stem cell-like marker signature ($CD34^{+}CD38^{-}$) was capable of recapitulating this disease in mice (16). They then went on to develop what is now considered the "gold standard" assay for the detection of CSCs, in which potential CSC populations were isolated from mice engrafted with human patient samples, and assayed for the ability of limiting cell dilutions to regenerate the disease in secondary mouse recipients, as well as differentiate into non-CSC leukemic blasts (Figure 1.1A) (17). The subsequent use of this transplantation assay, in addition to the sphere-forming assay (adapted from the neurosphere assay for neural stem cell self-renewal; see Figure 1.1B) and extensive

Figure 1.1. Methods for confirming the presence and self-renewal of cancer stem cells.

(A) The "gold standard" for confirming the presence of CSCs involves isolating putative CSCs from patient-derived samples, and orthotopically injecting them into mice. Tumors are allowed to develop, and are then harvested for the re-isolation of CSCs. Limiting dilutions of these cells are injected into a secondary mouse recipient, and tumor formation indicates that self-renewing CSCs were present in the secondary injection.

(B) As a secondary method of analyzing CSCs for self-renewal, they may be cultured *in vitro* as non-adherent spheres. Following the formation of primary spheres, they are dissociated into single cells, then allowed to re-establish secondary spheres. The ability to indefinitely regenerate these spheres indicates the presence of CSCs.

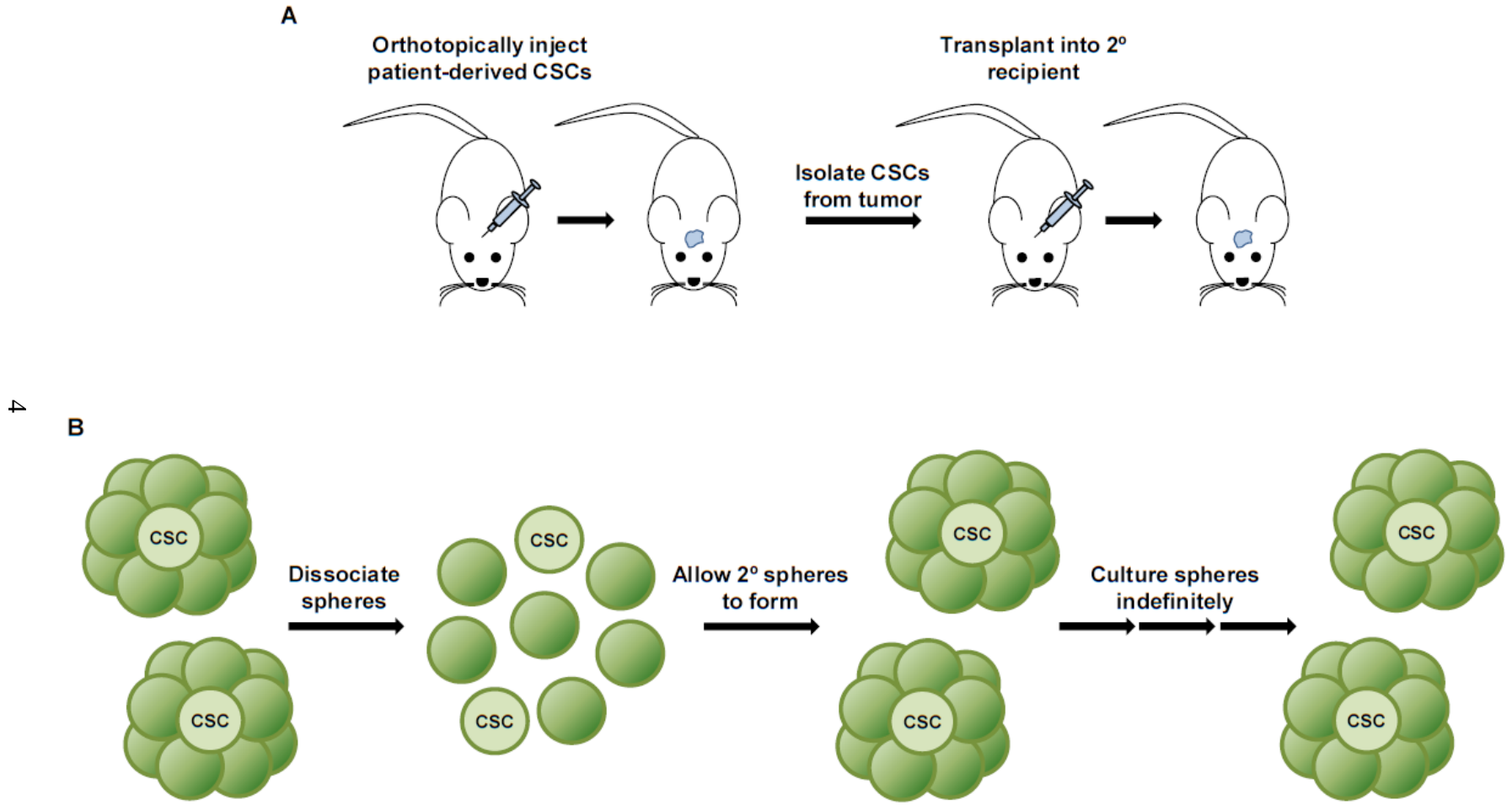
A
Orthotopically inject patient-derived CSCs
Isolate CSCs from tumor
Transplant into 2º recipient
B
CSC
Dissociate spheres
Allow 2º spheres to form
Culture spheres indefinitely

marker analysis (outlined in Table 1.1), has led to the prospective identification of CSCs in many solid tumors, including those of the breast, brain, colon, liver, lung, pancreas, and prostate, among others (4, 18-25). The widespread presence of CSCs in many different types of cancer suggests that they are crucial for neoplastic growth and propagation, and has thus led to extensive studies into the characterization of these cells.

By definition, CSCs are a population of cancer cells that are capable of undergoing self-renewal, have unlimited proliferative potential, and can initiate the formation of a tumor. Furthermore, their ability to differentiate is thought to be responsible for the high degree of heterogeneity that is commonly observed in tumors. These characteristics, particularly the capacity for self-renewal and differentiation, have led to broad comparisons between CSCs and normal stem cells (SCs). Indeed, many SC properties are exploited by CSCs, and they commonly rely on the oncogenic potentiation of key signaling pathways that promote stemness (see below) (2-4). Perhaps the most clinically relevant aspect of CSCs, though, is their enhanced ability to evade standard cancer therapies, including chemotherapy and radiation, as described below (26-28). This resistance is now thought to be a major mechanism of tumor recurrence, and as such, therapies that specifically target and eliminate CSCs are the focus of intense research.

Key signaling pathways in cancer stem cells

Many critical signaling pathways that promote the CSC phenotype are dependent on the oncogenic activation of normal SC signaling and that of their niche. These pathways are summarized in Table 1.2, along with the cancers within which they are often de-regulated, and their SC-related targets. In particular, Wnt signaling has been heavily implicated in promoting stemness in normal SCs and in CSCs (3, 19, 29). The normal SC niche has been shown to

Table 1.1. Markers for the isolation of cancer stem cells.

Common CSC markers and the tumors in which they identify CSCs are listed. {Adapted and compiled from (4, 11, 19, 30-32)}

Tumor type	CSC markers
Brain	$A2B5^+$, $ABCG2^+$, $ALDH1^+$, $CD133^+$, $SSEA\text{-}1^+$
Breast	$ALDH1^+$, $CD44^+$, $CD24^{-/low}$, ESA^+, $Lineage^-$
Colon	$ALDH1^+$, CEA^+, $CD24^+$, $CD44^+$, $CD133^+$, $CD166^+$, $CK20^+$, $CXCR4^+$, $EpCAM^{high}$, $LGR5^+$
Head and neck	$ALDH1^+$, $BMI1^+$, $CD44^+$, $YAP1^+$
Leukemia	$ALDH1^+$, $CD34^+$, $CD38^-$, $CD71^-$, $CD90^-$, $CD117^-$, $CD123^+$, $HLA\text{-}DR^-$
Liver	$ALDH1^+$, $CD49f^+$, $CD90^+$, $CD133^+$
Lung	$ALDH1^+$, $CD133^+$, $ABCG2^{high}$
Melanoma	$ALDH1^+$, $ABCB5^+$
Mesenchymal	Side population ($Hoechst\ dye^-$)
Multiple myeloma	$CD138^-$
Pancreas	$ALDH1^+$, $ABCG2^{high}$, $CD24^+$, $CD44^+$, $CD133^+$, $EpCAM^+$, ESA^+
Prostate	$ALDH1^+$, $CD44^+$, $CD133^+$, $\alpha2\beta1^{high}$

Table 1.2. Commonly altered signaling pathways in cancer stem cells.

Commonly altered signaling pathways in CSCs, the tumors they are often de-regulated in, and their stem cell-related targets are listed. {Adapted and compiled from (3, 19, 29)}

Signaling pathway	Cancer	Targets
Wnt/β-catenin	Colorectal, gastric, gastrointestinal, glioma, hepatocellular carcinoma, lymphoblastic leukemia, medulloblastoma, pilomatricoma	LEF/TCF transcription factors, Myc, cyclin D1, LGR5, AXIN2, survivin, TERT
Notch	Breast, glioma, lymphoblastic leukemia, NSCLC, ovarian, pancreatic, small cell lung	Hes1, Hey1, cyclin D, SOX9
HH	Basal cell carcinoma, glioma, medulloblastoma, pancreatic	GLI1-3, Nanog, BMI1, ABCG2
BMI1	AML, B-cell lymphomas	Inhibits INK4A and ARF, activating cyclin D and repressing Rb and p53
JAK/STAT	Colorectal, gastric, gastrointestinal, hepatocellular carcinoma, pancreatic	Nanog, OCT4
TGF-β	Glioma, NSCLC	SMAD transcription factors, PDGF-β pathway, SOX2, SOX4, LIF, ID1, ID3
Hippo	Breast, colon, esophageal	Represses YAP/TAZ, TEAD-induced transcription, and SOX9

produce Wnt ligands that regulate the self-renewal of neighboring SCs, and can influence asymmetric SC division based on proximity to the daughter cells: the daughter cell proximal to Wnt ligands is maintained in its SC state, while the distal daughter cell undergoes differentiation (19, 33). There is evidence to suggest that the CSC niche and stromal cells within a tumor may also produce Wnt, and GSC-like cells have been shown to exhibit elevated Wnt signaling following radiation (34, 35). Upon binding to their cell-surface receptors (e.g. Frizzled), Wnt ligands induce the stabilization of β-catenin, which is otherwise targeted for degradation by the APC/Axin/CK1/GSK3β complex. β-catenin can then translocate into the nucleus, where it binds and activates the LEF/TCF transcription factors, and promotes the induction of genes that regulate self-renewal, proliferation, survival, and migration (19). Interestingly, Wnt signaling has been shown to directly activate the expression of TERT, the catalytic subunit of telomerase, in normal SCs as well as embryonal and colorectal carcinoma cells (36). Thus, it is likely that telomerase is up-regulated downstream of Wnt signaling in CSCs, and potentially contributes to the enhanced proliferative potential observed in these cells.

The hedgehog (HH) signaling pathway is also thought to be critical for the maintenance of self-renewal in both SCs and CSCs, and may promote chemoresistance in CSCs. Signaling induced by the Sonic, Indian, and Desert ligands promotes the activation of the Smoothened receptor and the subsequent stabilization of glioma-associated oncogene (GLI) family transcription factors, resulting in the expression of self-renewal-related target genes (e.g. *Nanog*) (19, 37, 38). In CSCs derived from glioblastoma multiforme (GBM) and pancreatic cancer, HH signaling was shown to be necessary for maintaining self-renewal (39, 40). Furthermore, inhibition of this pathway in pancreatic CSCs led to the downregulation of BMI1 and the multi-drug resistance transporter ABCG2, restoring sensitivity to the chemotherapeutic agent

gemcitabine (40). Similarly, HH signaling was reported to modulate resistance to ionizing radiation (IR) in esophageal cancer cells (41). Thus, targeting HH signaling in CSCs may be a powerful means of inhibiting stemness, as well as enhancing patient responses to chemo- and radiotherapy.

In addition to Wnt and HH, several other signaling pathways are recognized for their contributions to the CSC phenotype. Like Wnt and HH signaling, the activation of Notch, BMI1, JAK/STAT, and TGF-β, and the repression of Hippo, have been shown to promote self-renewal in SCs and CSCs. In some cases, signaling through these pathways also promotes the epithelial-mesenchymal transition (EMT), and mediates resistance to chemotherapy and radiation (3, 19, 29). As all of these pathways are integral to maintaining the CSC phenotype, they provide a multitude of targets that may be exploited for the therapeutic targeting of CSCs. A major challenge that must now be overcome is identifying those targets that can selectively inhibit the growth and survival of CSCs, while sparing normal SCs.

Role of cancer stem cells in therapy resistance

CSCs have been repeatedly shown to exhibit resistance to chemo- and radiotherapy, and are likely the drivers of tumor recurrence and metastatic disease (19, 26, 27, 42). Most clinically-used therapies are selected based on their ability to reduce overall tumor mass, and are relatively successful in treating primary tumors (28). However, the cure rate for these therapies is extremely low, with 90% of cancer-related deaths estimated to result from metastatic and recurrent tumors (42). These outcomes have led to the search for therapies that specifically target CSCs, with the hope that these treatments will induce tumor reduction, if not elimination, and prevent tumor recurrence (Figure 1.2).

Figure 1.2. Cancer stem cell-targeted therapies may permanently cure cancer.

(A) Cancer therapies currently in use are effective at shrinking a primary tumor, but spare CSCs. CSCs may then initiate the formation of a recurrent or metastatic tumor.

(B) Therapies that specifically target CSCs may result in the degeneration of a tumor, and eliminate the possibility of tumor recurrence.

{Adapted from (2)}

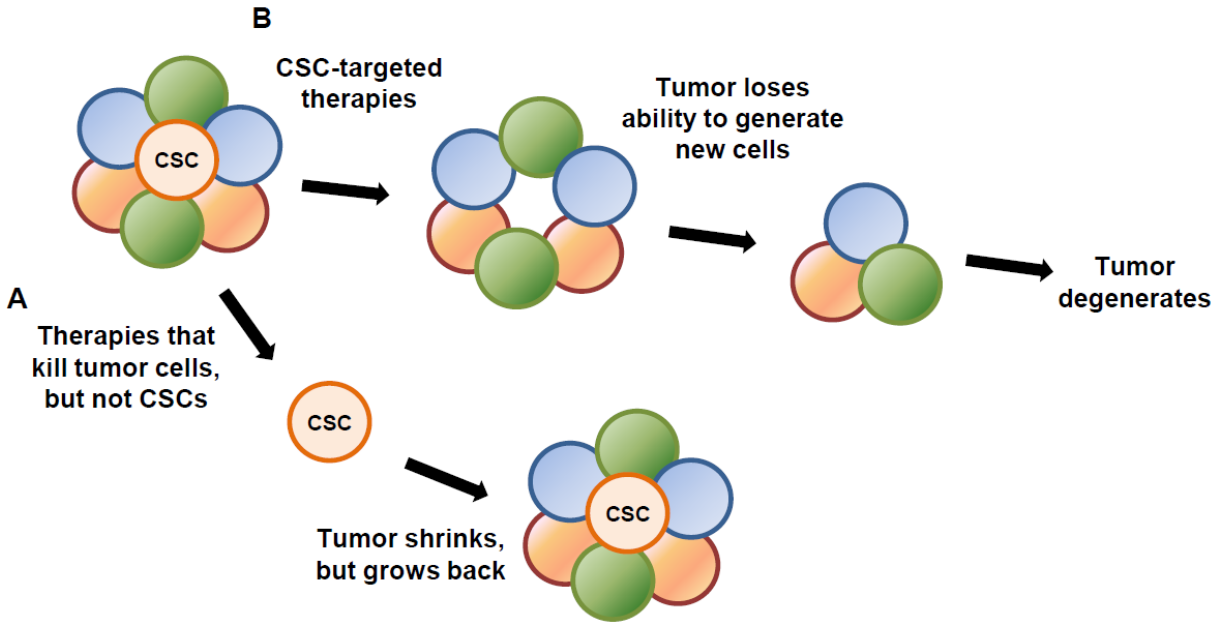
B
CSC-targeted therapies
CSC
Tumor loses ability to generate new cells
Tumor degenerates
A
Therapies that kill tumor cells, but not CSCs
CSC
CSC
Tumor shrinks, but grows back

Among the mechanisms for enhanced CSC resistance to chemotherapy are the over-expression of multi-drug resistance transporters and the metabolism of chemotherapeutic compounds by ALDH isozymes (11, 12, 26). Like most normal SCs, CSCs commonly over-express members of the ATP-binding cassette (ABC) family of drug transporters, including ABCB1, ABCC1, and ABCG2 (also known as breast cancer resistance protein, BCRP) (26). These proteins promote the efflux of a wide variety of chemotherapeutic agents, such as doxorubicin, paclitaxel, and cisplatin, resulting in the limited efficacy of these drugs against CSCs (43). The finding that *Abcb1*, *Abcc1*, and *Abcg2* knockout mice develop normally makes these transporters attractive targets for therapeutic intervention (26). Members of the ALDH superfamily have also been shown contribute to drug resistance in CSCs. In particular, ALDH1A1 and ALDH3A1 are capable of converting the alkylating agent cyclophosphamide to an inactive state, protecting cells from its DNA-damaging effects. ALDH1 isozymes appear to metabolize other agents as well, such as hydrogen peroxide, and have been used clinically to predict chemotherapy resistance (11).

CSCs also display enhanced resistance to IR, and this is thought to be achieved through the up-regulation of DNA damage repair pathways. In a recent study of CSCs derived from high grade gliomas (HGGs), a subpopulation of radiation-resistant GSCs was shown to express significantly higher levels of genes involved in DNA damage repair, including *ATM*, *BRCA1*, and *RAD51*, compared with more radiation-sensitive GSCs (44). Additionally, a study of radiation-resistant $CD133^+$ GSCs found that DNA checkpoint proteins including ATM, Rad17, Chk1, and Chk2 were activated following IR, and a Chk1/2 inhibitor could resensitize them to this therapy (45). Signaling through Wnt, HH, Notch, the epidermal growth factor receptor (EGFR), and TGF-β, as well as the loss of PTEN, have also been shown to promote

radioresistance in CSCs, and present further targets that may be exploited for resensitization to IR (27, 29).

Cancer stem cell model versus clonal evolution model

Despite the extensive work that has been done to isolate and characterize CSCs, a consensus has still not been reached as to which population of cells is responsible for tumor propagation and heterogeneity. Two models currently exist to explain these phenomena: the clonal evolution model, and the CSC model. The clonal evolution model predicts that all tumor cells are capable of undergoing self-renewal and propagating a tumor, and may stochastically acquire mutations that result in intratumoral heterogeneity. These mutations may bestow a cell with a growth advantage relative to other cells in the tumor, leading to clonal expansion and the development of a dominant population within the tumor (Figure 1.3A). By contrast, the CSC model is defined by the hierarchical organization of cancer cells, in which only a small subset of cells possesses unlimited proliferative potential, undergoes self-renewal, and is capable of initiating a tumor in a secondary recipient. By definition, this CSC population must be able to differentiate into cells with reduced proliferative potential, with these variable lineages resulting in tumor heterogeneity (Figure 1.3B) (2, 4, 15). While these two models are often presented as distinct philosophies for the development of cancer, they are likely not mutually exclusive. The extensive characterization of CSCs over the past two decades provides strong evidence for these cells as a distinct subset of tumor-initiating cancer cells, but they are likely subject to clonal selection as outlined by the clonal evolution model. That is, one population of CSCs may initiate the formation of a tumor, but the stochastic acquisition of mutations over time may result in several distinct CSCs with variable properties and myriad lineages (4). The ensuing intratumoral

Figure 1.3. Two models for tumor propagation and heterogeneity.

(A) The clonal evolution model deems that all cancer cells have the capacity to undergo self-renewal (small curved arrows) and initiate tumor formation (large curved arrows). Stochastic mutations (red arrow) may lead to a growth advantage and expansion of a new clonal population, leading to tumor heterogeneity.

(B) The CSC model is defined by the hierarchical organization of a tumor, with only a subset of cells (CSCs) capable of undergoing self-renewal and tumor initiation. The differentiation of CSCs leads to the expansion of multiple lineages and tumor heterogeneity.

{Adapted from (2)}

A

Clonal evolution model

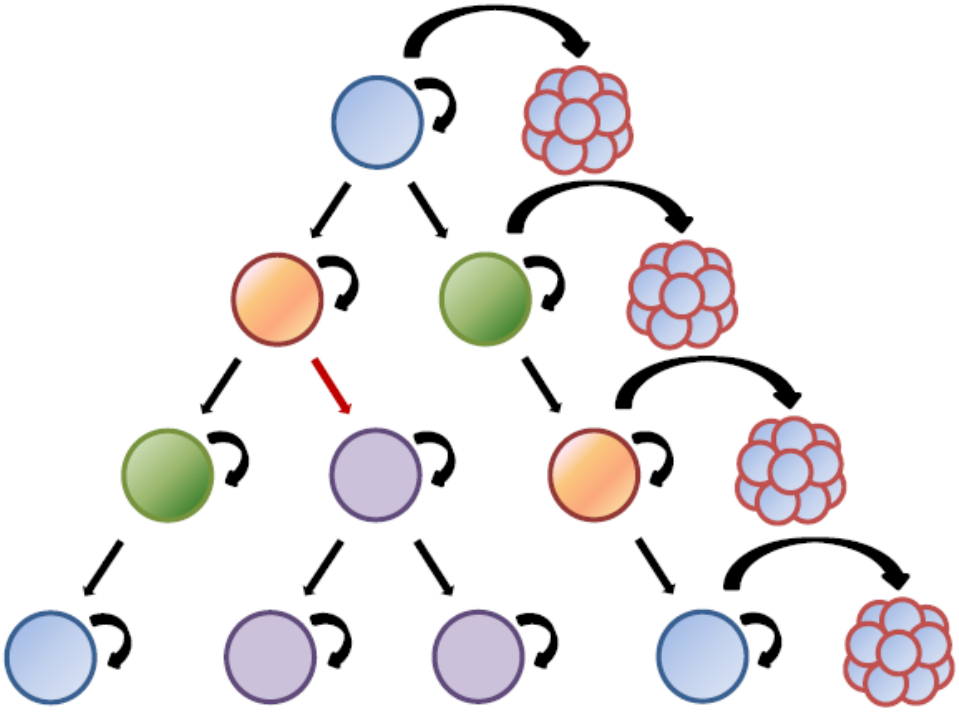

B

Cancer stem cell model

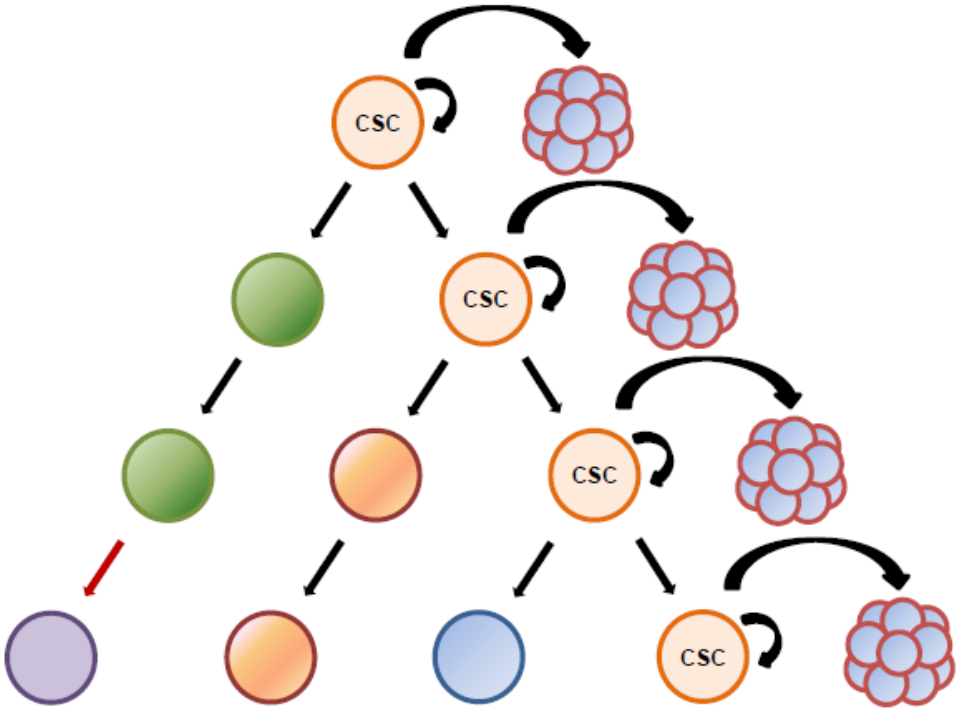

heterogeneity is often manifested in several clinical challenges, complicating the diagnosis as well as the treatment of many cancers, and further study will be required to determine the best course of action for eliminating CSCs.

High grade glioma

For my study of CSCs detailed in Chapter 2, I used GSCs that were isolated from HGGs. HGGs encompass both grade III and grade IV gliomas, with the latter also referred to as grade IV astrocytoma or Glioblastoma multiforme (GBM), as designated by the World Health Organization (WHO). GBM is a highly aggressive disease with a median survival time of 14.6 months, and patient outcomes have only improved by a few months over the past fifty years. The standard of care currently consists of surgery, radiation, and chemotherapy (temozolomide, TMZ), and the lack of effective targeted therapies highlights the need for further molecular research in this field of cancer biology (29, 46).

HGGs are characterized by high cell density and heterogeneity, elevated vascularity and necrosis, and are highly invasive in the brain. They have been classified into three distinct subtypes, referred to as proneural (PN), mesenchymal (MES), and classical, and each exhibits discrete mutations and gene expression signatures. Additionally, PN tumors are found in either a CpG island methylator phenotype ($CIMP^+$) or $CIMP^-$ state, with $CIMP^-$ tumors associated with a worse prognosis, similar to that of MES and classical tumors. Moreover, $CIMP^+$ PN tumors commonly bear mutations in *IDH1*, *TP53*, and *ATRX*, and exhibit altered isocitrate dehydrogenase 1 (IDH1) metabolic activity, whereas $CIMP^-$ PN tumors are often characterized by elevated receptor tyrosine kinase (RTK) activity, PDGFRα amplification/over-expression, mutations in *TP53* and *CDK4*, and the deletion of *CDKN2A*, which encodes INK4A and ARF

(the targets of BMI1). These PN signatures are mutually exclusive from those of MES tumors, which are mutated in *NF1*, have altered signaling through STAT3, C/EBPβ, and TAZ, and are resistant to radiation therapy. However, classical signatures bear some resemblance to both PN and MES tumors, and are characterized by the deletion of *CDKN2A*, elevated signaling through RTKs, PI3K/Akt, and mammalian target of rapamycin (mTOR), and exhibit resistance to radiation (47).

Identification and characterization of glioma stem cells

In recent years, the identification and isolation of GSCs from HGGs have led to their extensive characterization in the hope of developing better treatment options for HGG patients. These cells were isolated through the use of many different markers, including CD133, ALDH1, SSEA-1, A2B5, and ABCG2 (see Table 1.1), and they were also found to express elevated levels of Nanog, OCT4, SOX2, nestin, BMI1, Musashi-1, integrin-α6, and L1CAM, as well as the inactivation of PTEN (19, 29, 30). Like their parent HGGs, these GSCs were very recently categorized through gene expression profiling as either PN or MES, with PN GSCs found in both grade III HGG and GBM, and MES GSCs predominantly found in GBM (44, 47). These two GSC subtypes also exhibit diverse phenotypes *in vitro* and in an orthotopic mouse model of HGG, with MES GSCs appearing much more aggressive, proliferative, invasive, angiogenic, and resistant to radiation than PN GSCs. Additionally, these GSC sub-populations could be separated based on differentially expressed markers, with CD133 and CD15 found in PN GSCs, and ALDH1A3 marking MES GSCs (44). Moreover, they exhibit different signaling and metabolic patterns, with Notch, PDGFRα, and GLUT3 altered in PN GSCs, and MES GSCs characterized by de-regulated activity in ALDH1A3, NF-κB, glycolysis, and the inflammasome. As with a

majority of cultured CSCs, though, each of these subtypes responds to epidermal growth factor (EGF) and fibroblast growth factor (FGF) stimulation (47). The PN and MES GSCs first characterized by Mao and colleagues will be the model system for my work described in Chapter 2 (44).

Understanding the glioma stem cell niche

Interestingly, GSCs appear to have highly specialized niches within HGGs. Gliomas are thought to arise near the subventricular zone (SVZ), where normal neural SCs reside, and many tumors have been observed to form near this region both clinically and in mouse models of glioma. The glioma cell-of-origin has not been definitively determined, but studies suggest that the accumulation of mutations in neural SCs or progenitor cells, combined with the SC microenvironment, may allow GSCs and HGGs to arise (46, 48). The perivascular niche is also well-known to promote the growth of GSCs, which appear to associate closely with endothelial cells (49). Notch signaling from these endothelial cells has been shown to support GSC self-renewal, and GSCs secrete vascular endothelial growth factor (VEGF) to induce further angiogenesis (50, 51). Furthermore, GSCs can maintain the perivascular niche through their own trans-differentiation into endothelial cells and pericytes, resulting in highly vascularized tumors (52, 53). Clinically, this vascularity has been found to correlate with the number of GSCs in a tumor as well as with patient prognosis, suggesting that this niche may be a target for therapeutic intervention (54, 55).

Similar to the perivascular niche, the hypoxic niche at the site of tumor necrosis may also promote GSC expansion. Hypoxia has been shown to stimulate the expression of HIF1α and HIF2α in GSCs, which can ultimately promote neo-vascularization and the development of a

new perivascular niche (56, 57). Additionally, the tumor edge/invasion niche appears to promote GSC expansion and invasion of the surrounding parenchyma. Tumor-associated macrophages in this microenvironment secrete TGF-β, and local astrocytes may promote HH signaling, both of which can contribute to GSC self-renewal (see Table 1.2) (39, 58). Furthermore, the chemokine receptor CXCR4 is often over-expressed in GSCs, promoting their invasion and migration toward endothelial cells, where they can establish a new perivascular niche (59). Altogether, the rapidly accumulating understanding of GSC niches may lead to the development of niche-targeted therapies that could indirectly halt the self-renewal and tumor-initiating capacity of these cells.

Overview of aldehyde dehydrogenases

The search for CSC markers has led to the identification of many proteins that are enriched in CSC populations (see Table 1.1) (4, 11, 19, 30-32). Among the numerous cancers for which CSCs have been identified, ALDH1 isozymes have been found to be markers for nearly all of them, suggesting that these enzymes may be universally expressed by CSCs. These findings have sparked renewed interest in these proteins, and they were subsequently shown to mediate CSC resistance to both chemo- and radiotherapy (11, 12). ALDH1A3 will be the focus of my research in Chapter 2, but I will begin with an overview of the ALDH superfamily.

The human ALDH superfamily consists of 19 distinct isozymes that belong to 11 subfamilies, and are characterized by a wide variety of subcellular localizations, tissue distributions, substrate specificities, and associated diseases and pathologies (Table 1.3) (11, 60). However, each of them catalyzes the $NAD(P)^+$-dependent, irreversible oxidation of aliphatic and aromatic aldehydes to their corresponding carboxylic acids. These enzymes play critical roles in

Table 1.3. Human aldehyde dehydrogenase superfamily isozymes.

The 19 isozymes of the ALDH superfamily are listed, along with their subcellular localization, major substrates, and associated diseases and pathologies. {Adapted from (11, 60)}

Family	Gene	Subcellular localization	Tissue distribution	Major substrates	Associated diseases and pathologies
ALDH1	*ALDH1A1*	Cytosol	Liver, kidney, RBCs, skeletal muscle, lung, breast, lens, stomach mucosa, brain, pancreas, testis, prostate, ovary	Retinal, aldophosphamide, acetaldehyde, lipid peroxidation-derived aldehydes	Drug resistance, alcohol sensitivity, cancer
	ALDH1A2	Cytosol	Testis, liver, kidney	Retinal	Spina bifida, cancer
	ALDH1A3	Cytosol	Kidney, skeletal muscle, lung, breast, testis, stomach mucosa, salivary glands	Retinal	Perinatal lethality, cancer
	ALDH1B1	Mitochondria	Liver, kidney, heart, skeletal muscle, brain, prostate, lung, testis, placenta	Acetaldehyde, lipid peroxidation-derived aldehydes	Various phenotypes
	ALDH1L1	Cytosol	Liver, skeletal muscle, kidney	10-Formyltetrahydrofolate	Cancer
	ALDH1L2	Cytosol		Unknown	
ALDH2	*ALDH2*	Mitochondria	Liver, kidney, heart, skeletal muscle, lens, brain, pancreas, prostate, spleen	Acetaldehyde, nitroglycerin	Alcohol sensitivity, ethanol-induced cancers, hypertension
ALDH3	*ALDH3A1*	Cytosol, nucleus	Stomach mucosa, cornea, breast, lung, lens, esophagus, salivary glands, skin	Medium-chain aliphatic and aromatic aldehydes	Cancer, various phenotypes
	ALDH3A2	Microsomes, peroxisomes	Liver, kidney, heart, skeletal muscle, lung, brain, pancreas, placenta, most tissues	Long-chain aliphatic aldehydes	Sjögren–Larsson syndrome
	ALDH3B1	Cytosol, mitochondria	Kidney, lung, pancreas, placenta	Lipid peroxidation-derived aldehydes	Paranoid schizoprenia
	ALDH3B2	Mitochondria	Parotid gland	Unknown	

Table 1.3 continued

Family	Gene	Subcellular localization	Tissue distribution	Major substrates	Associated diseases and pathologies
ALDH4	*ALDH4A1*	Mitochondria	Liver, kidney, heart, skeletal muscle, brain, placenta, lung, pancreas, spleen	Proline metabolism	Type II hyperprolinemia
ALDH5	*ALDH5A1*	Mitochondria	Liver, kidney, heart, skeletal muscle, brain	Succinic semialdehyde	Neurological disorders, γ-hydroxybutyric aciduria
ALDH6	*ALDH6A1*	Mitochondria	Liver, kidney, heart, skeletal muscle	Methylmalonate semialdehyde	Elevated levels in urine of β-alanine, 3-hydroxypropionic acid, 3-amino acids, and 3-hydroxyisobutyric acids, developmental delay
ALDH7	*ALDH7A1*	Cytosol, nucleus, mitochondria	Fetal liver, kidney, heart, lung, brain, ovary, eye, cochlea, spleen, adult spinal cord	Betaine aldehyde, lipid-peroxidation derived aldehydes	Hyperosmotic stress, pyridoxine-dependent epilepsy
ALDH8	*ALDH8A1*	Cytosol	Liver, kidney, brain, breast, testis	Retinal	
ALDH9	*ALDH9A1*	Cytosol	Liver, kidney, heart, skeletal muscle, brain, pancreas, adrenal gland, spinal cord	γ-Aminobutyraldehyde, aminoaldehydes	Various phenotypes
ALDH16	*ALDH16A1*	Unknown	Neuronal cells	Unknown	
ALDH18	*ALDH18A1*	Mitochondria	Kidney, heart, skeletal muscle, pancreas, testis, prostate, spleen, ovary, thymus	Glutamatic γ-semialdehyde	Hypoprolinemia, hypoornithinemia, hypocitrullinemia, hypoargininemia, hyperammonemia with cataract formation, neurodegeneration, connective tissue anomalies

the detoxification of endogenous and exogenous aldehydes (e.g. lipid peroxidation-induced aldehydes and aldophosphamide, respectively), which are highly reactive and can damage proteins and nucleic acids if not oxidized. Furthermore, ALDH catalysis is necessary for the generation of molecules involved in normal cellular physiology, such as the transcriptional activator retinoic acid (RA), the osmolyte betaine, and the neurotransmitter γ-aminobutyric acid (GABA) (11, 12, 60).

In addition to these enzymatic functions, ALDH isozymes have many non-catalytic and tissue-specific roles. For example, ALDH isozymes make up 5-20% of the water soluble fraction in the cornea and lens of the eye (and are thus deemed crystallins), providing critical structural support for this organ. They can also promote transparency and absorb UV light in the eye, prevent oxidative damage by scavenging hydroxyl radicals and generating NAD(P)H to reduce glutathione, catalyze the hydrolysis of esters, and bind hormones and other small molecules (12, 60).

Aldehyde dehydrogenase 1A subfamily

The ALDH1A subfamily is comprised of three isozymes, namely ALDH1A1, ALDH1A2, and ALDH1A3. These enzymes share > 60% amino acid identity and are all localized to the cytosol, where they catalyze the oxidation of all-*trans*- and 9-*cis*-retinal to all-*trans*- and 9-*cis*-RA, respectively (though ALDH1A1 has other substrates, as well, such as aldophosphamide) (Figure 1.4A). In this manner, ALDH1A isozymes are crucial for the metabolism of retinoids and RA-induced gene expression (see below) (12, 60). They are enzymatically active as homotetramers, and the crystal structures of ALDH1A1 and ALDH1A2 reveal that these isozymes each contain three major domains: an N-terminal NAD^+-binding

Figure 1.4. Enzymatic catalysis and structure of ALDH1A3.

(A) Retinal is converted to RA in an NAD^+-dependent reaction catalyzed by ALDH1A enzymes.

(B) The domain structure of ALDH1A isozymes is depicted. They contain an N-terminal NAD^+-binding domain (NBD) that is divided by a region of the oligomerization domain (OD). The remainder of the OD is located C-terminal to the catalytic domain.

(C) A three-dimensional model of ALDH1A3 is shown. α-helices are shown in red, β-sheets are shown in green, and the catalytic Cys314 and NAD^+ are represented in ball-and-stick format (61).

(D) Retinal and NAD^+ are shown in relation to the catalytic Cys314 and Glu280 in the hydrophobic substrate-binding tunnel of ALDH1A3 (61).

(E) A model of the ALDH1A3 Cys314-retinal tetrahedral intermediate is depicted. Asn181 and the Cys314 amide group stabilize the intermediate through hydrogen bonding, and Glu280 functions as a base to activate the attacking water molecule (61).

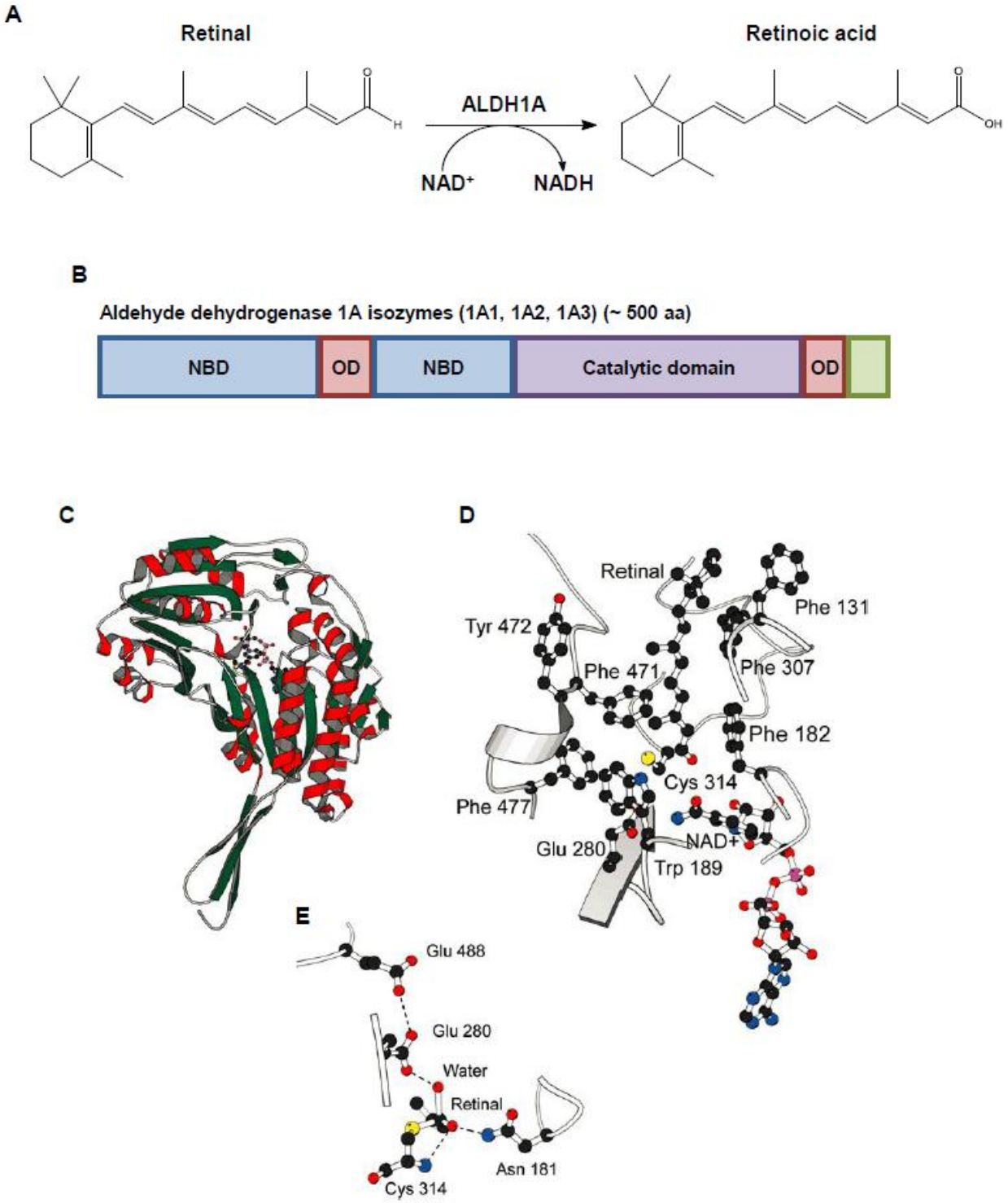
A
Retinal
Retinoic acid
ALDH1A
NAD+
NADH
B
Aldehyde dehydrogenase 1A isozymes (1A1, 1A2, 1A3) (~ 500 aa)
NBD
OD
NBD
Catalytic domain
OD
C
D
Retinal
Tyr 472
Phe 131
Phe 471
Phe 307
Phe 182
Cys 314
Phe 477
Glu 280
NAD+
Trp 189
E
Glu 488
Glu 280
Water
Retinal
Asn 181
Cys 314

domain containing a five-stranded parallel β sheet, a catalytic domain with a six-stranded parallel β sheet, and an oligomerization domain comprised of a three-stranded antiparallel β sheet (Figure 1.4B) (62-65). The crystal structure of ALDH1A3 has not yet been solved, but a three-dimensional model of mouse ALDH1A3 has been computationally generated using sheep ALDH1A1 as a template, since these two isozymes share 70% sequence identity. This model strongly suggests that ALDH1A3 has a similar domain structure as ALDH1A1 and ALDH1A2, but will need to be confirmed with a crystal structure (Figure 1.4C). It also depicts the hydrophobic substrate-binding tunnel, which is optimized for an eight-carbon chain, and the positioning of the catalytic cysteine (Cys314) in relation to retinal and the co-factor NAD^+ (Figure 1.4D). Moreover, the authors have illustrated the enzymatic mechanism of the catalytic triad, composed of Cys314, Asn181, and Glu280: the nucleophilic Cys314 thiol attacks the electrophilic carbonyl carbon in the aldehyde group of retinal, Asn181 stabilizes the transition state through hydrogen bonding, and Glu280 acts as a base to activate a water molecule for product release (Figure 1.4E). It has also been demonstrated that the thyroid hormone 3,3',5-tri-iodothyronine (T_3) can compete with NAD^+ binding and inhibit the activity of ALDH1A1 and ALDH1A3, but is five times more potent at inhibiting the former (61). This hormonal regulation may be physiologically relevant to RA-induced gene expression, and may underlie the tissue-specific expression of ALDH1A isozymes.

Aldehyde dehydrogenase 1A isozymes regulate gene expression through retinoic acid

The production of RA by ALDH1A isozymes is critical for many physiological processes, particularly in the central nervous system (CNS) (66, 67). Following the oxidation of retinol (vitamin A) to retinal and the subsequent conversion of retinal to RA by ALDH1A

enzymes, RA can diffuse into the nucleus or into a neighboring cell, acting in an autocrine or paracrine fashion to regulate gene expression (Figure 1.5A). As depicted in Figure 1.5B, the effects of RA are mediated by a heterodimer of the RA receptor (RAR) and retinoid X receptor (RXR), which binds to RA response elements (RAREs) in the promoter region of a gene. In the absence of RA, the RAR/RXR heterodimer recruits a co-repressor complex that leads to histone deacetylation, and thus represses transcription. However, in the presence of RA, the heterodimer instead recruits a co-activator complex that promotes histone acetylation and activates transcription (68). There are over 100 genes that appear to be induced by RA in this manner, suggesting that it can act as a master transcriptional regulator (69).

Perhaps the most well-characterized function of RA is the regulation of anteroposterior patterning in the CNS of developing embryos. Many of its effects are mediated by the RARE-containing *Hox* genes, which encode transcription factors that determine patterning in the neural tube. The de-regulation of RA metabolism can result in pronounced developmental defects, such as the expansion of the hindbrain and spinal cord and the loss of the forebrain when the RA concentration is too high (66, 68). Additionally, RA induces the differentiation of adult neural stem cells into neurons, and is involved in the regeneration of damaged nerves in the peripheral nervous system (PNS). It has also been shown to play a role in neuronal plasticity, particularly spatial learning and memory, and the aging-related decrease in RA signaling seems to be responsible for impaired spatial memory and long-term potentiation (67).

Aldehyde dehydrogenases in normal and cancer stem cells

The diverse roles of RA in the CNS have been well-established, but recent investigations of ALDH activity in other tissues suggest that it may also be important for various SCs (12, 60).

Figure 1.5. Mechanisms of retinoid metabolism and RA-induced gene regulation.

(A) The cellular metabolism of retinoids is shown. Upon its release from CRBP, retinol (vitamin A) is metabolized to retinal by RDH. Members of the ALDH1A family oxidize retinal to RA, which is then bound by CRABP, or further oxidized by CYP26.

(B) RA-regulated gene transcription is potentiated through the RAR/RXR heterodimer, which binds to a RARE in the promoter region of a gene (e.g. *Hox1*). In the absence of RA, the heterodimer recruits a co-repressor complex that promotes histone deacetylation and the subsequent repression of transcription. Upon binding of RA to RAR, the RAR/RXR heterodimer instead recruits a co-activator complex that leads to histone acetylation and the activation of transcription.

CRBP: cellular retinol binding protein; CRABP: cellular retinoic acid binding protein; RDH: retinol dehydrogenase; ALDH1: aldehyde dehydrogenase 1; retinaldehyde dehydrogenase; CYP26: cytochrome P450 26; RA: retinoic acid; RAR: retinoic acid receptor; RXR: retinoid X receptor; RARE: retinoic acid response element.

{Adapted from (68)}

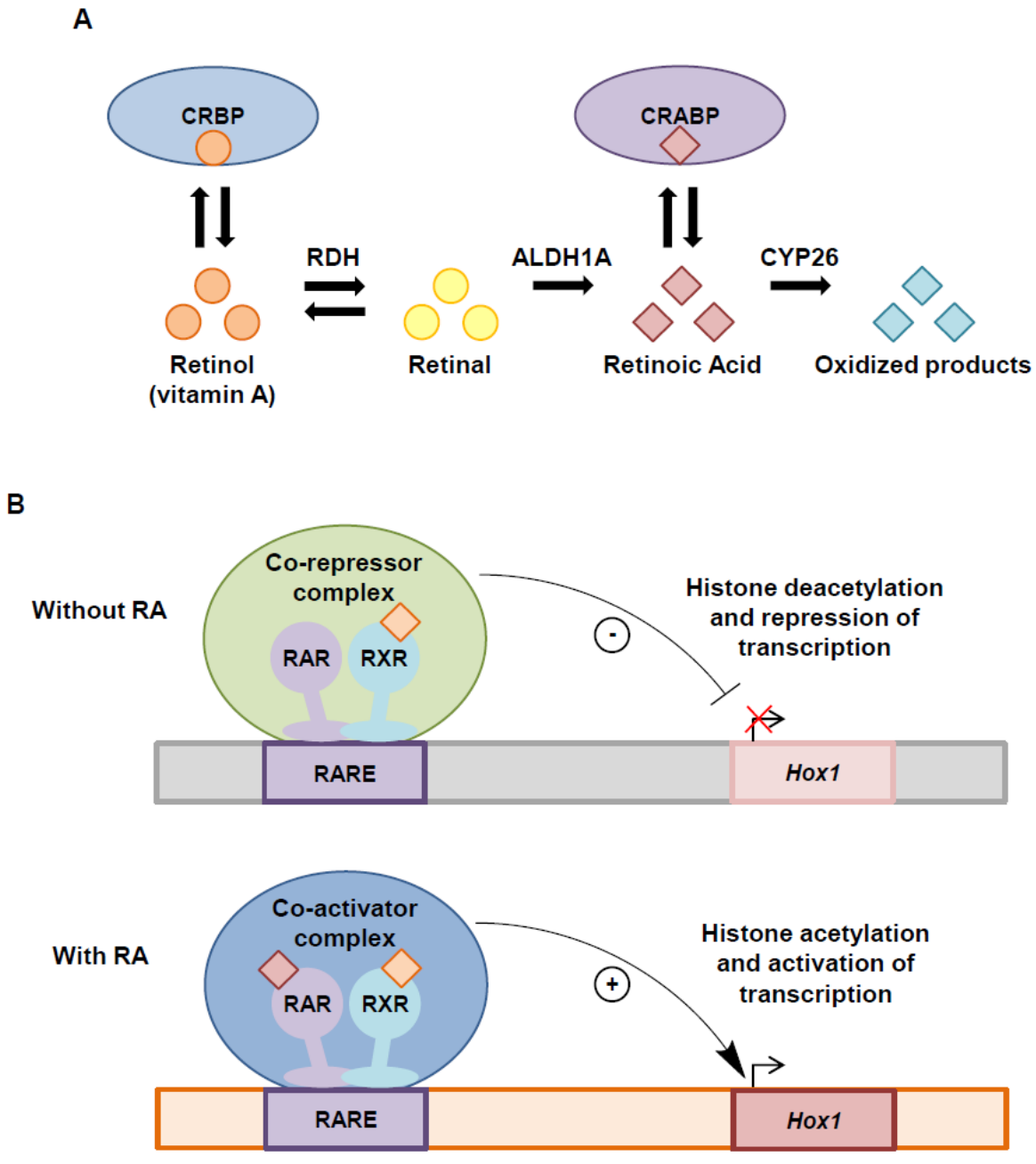
A
CRBP
CRABP
RDH
ALDH1A
CYP26
Retinol
(vitamin A)
Retinal
Retinoic Acid
Oxidized products
B
Without RA
Co-repressor
complex
RAR
RXR
Histone deacetylation
and repression of
transcription
RARE
Hox1
With RA
Co-activator
complex
RAR
RXR
Histone acetylation
and activation of
transcription
RARE
Hox1

The development of the Aldefluor assay for the detection of ALDH1 activity has led to the identification of $ALDH^+$ cells in many different tissues, but the results of these assays must be carefully interpreted. Though the Aldefluor assay was designed to specifically detect the activity of ALDH1A isozymes, the cross-reactivity of some other isozymes (e.g. ALDH2, ALDH3A1, and ALDH9A1) may also contribute to the observed activity (60, 70). Nevertheless, ALDH activity has been detected in a number of cell types, including mammary epithelial cells, where 8% of the total cells exhibited ALDH activity, high ALDH1 expression, and the ability to self-renew and differentiate; cells localized to the crypts of the colon and stomach (where SCs are located); hematopoietic SCs; central-acinar/terminal duct cells of the pancreas; and prostate cells (71-76). The mechanistic role of ALDH proteins in these cells is just starting to be explored.

In addition to these studies of ALDH in normal SCs, the Aldefluor assay has been used extensively to identify CSCs (see Table 1.1). ALDH activity has been reported in a majority of CSCs, and appears to contribute to their stemness and tumorigenicity (11, 12). For example, the knockdown of ALDH1A expression in melanoma CSCs led to a reduction in cell viability, increased apoptosis, and decreased tumorigenesis *in vivo* (31). Similarly, a study of MES GSCs that express high levels of ALDH1A3 found that the knockdown or inhibition of this enzyme significantly reduced cell proliferation (44). $ALDH^+$ cells isolated from breast tumors were also found to be tumorigenic and self-renewing, and $ALDH^+$ cells derived from AML were more tumorigenic *in vivo* than $ALDH^-$ AML cells (71, 77).

While ALDH activity thus appears to be involved in CSC self-renewal and tumorigenesis, ALDH isozymes also play a crucial role in therapy resistance. ALDH1A1 and ALDH3A1 are well-known for their abilities to metabolize and deactivate aldophosphamide, the active form of the chemotherapeutic agent cyclophosphamide (11, 60, 70, 78). Indeed, a

retrospective analysis of breast cancer patient samples found that ALDH1A1 expression was predictive of patient response to cyclophosphamide (79). Additionally, CSCs were enriched in colorectal cancer xenografts following cyclophosphamide treatment, and exhibited enhanced ALDH1A1 expression and activity (80). ALDH isozymes may also contribute to CSC radioresistance by scavenging radiation-induced free radicals, and by producing NAD(P)H, which can reduce the antioxidant glutathione (12, 60).

ALDH1A1 was originally thought to be the key ALDH isozyme regulating CSC tumorigenesis and therapy resistance, but accumulating evidence suggests that other ALDH isozymes may be more important for these phenotypes (12, 70). A panel of breast cancer patient samples examined for the expression of various ALDH isozymes found that ALDH1A3 correlated the best with tumor grade and metastasis, whereas ALDH1A1 did not significantly correlate with either. Correspondingly, an examination of three breast cancer cell lines with high ALDH activity found that this activity was unaffected by the knockdown of ALDH1A1, but was instead dependent on the expression of ALDH1A3 (81). A study of MES GSCs also showed that ALDH1A3 was the predominantly expressed ALDH isozyme, suggesting that this enzyme may play more of a role in CSCs than ALDH1A1 (44). However, the expression of these isozymes may be cancer-specific, and further studies will be necessary to determine the individual contributions of each isozyme in CSCs.

Given the pleiotropic roles of ALDH isozymes in CSC tumorigenesis, self-renewal, and therapy resistance, we became very interested in understanding the molecular mechanisms underlying their various functions. I hypothesized that genes up-regulated in response to RA may potentiate the CSC phenotype, so I made use of the ALDH1A3-expressing MES GSCs to analyze the expression of a known RA-regulated gene, namely *TGM2*, which encodes tTG (9,

44). As tTG will be a major focus of my research detailed in Chapter 2, I will provide a brief overview of the enzymatic activities and roles of tTG in both normal cells and in cancer cells.

The transglutaminase family of enzymes

Transglutaminases (TGs) comprise a family of enzymes that catalyze the irreversible Ca^{2+}-dependent transamidation (or crosslinking) of a peptide-bound glutamine and either a peptide-bound lysine or free amine. Additionally, they can post-translationally modify proteins through the deamidation of glutamine, in which it is converted to a glutamate residue (Figure 1.6A) (9, 10). Enzymes exhibiting TG activity are expressed in a wide variety of organisms, including unicellular organisms, invertebrates, fish, mammals, and plants (9). The human family of TGs is comprised of nine members, referred to as TG1-7, FXIIIa, and Band 4.2, and all contain a conserved active site and exhibit transamidation activity, with the exception of Band4.2 (Table 1.4). These enzymes have various tissue distributions and functions, and have been shown to act as scaffolds and adaptors, maintain membrane integrity, regulate the extracellular matrix (ECM) and cell adhesion, mediate signal transduction, and modulate gene expression. TG2, also referred to as tTG, is the most widely expressed and well-characterized of these enzymes (9, 10).

Overview of tissue transglutaminase

tTG is a multifunctional protein with a wide variety of roles both inside the cell and in the extracellular microenvironment. Its expression is regulated by a number of factors, including RA (through a RARE, as described above), IL-6, TGF-β1, vitamin D, TNF, NF-κB, EGF, phorbol ester, oxidative stress, and Hox-A7. Upon translation, tTG localizes primarily to the cytosol, but

Figure 1.6. Transglutaminase-catalyzed reactions and structure of tissue transglutaminase.

(A) Three distinct TG-catalyzed transamidation/deamidation reactions are depicted. In reaction 1, a primary amine is crosslinked onto the γ-carbon of a glutamine residue in protein 1 (P_1). Reaction 2 illustrates the crosslinking of two proteins (P_1 and P_2) through the γ-carbon of a glutamine residue in P_1, and the ε-amine of a lysine residue in P_2. Reaction 3 depicts the deamidation of glutamine to glutamate in P_1. Each reaction is accompanied by the release of ammonia. {Adapted from (9)}

(B) The domain structure of tTG is shown. It contains an N-terminal β-sandwich, followed by a catalytic core and two C-terminal β-barrels.

(C) The X-ray crystal structures of tTG in the closed conformation (PDB: 1KV3) and open conformation (PDB: 2Q3Z) are shown, and represented as cartoons. Ca^{2+} drives tTG into the open conformation, whereas the binding of GTP/GDP allows tTG to adopt the closed conformation. βS, β-sandwich; core, catalytic core; β1, β-barrel 1; β2, β-barrel 2 (82, 83).

A

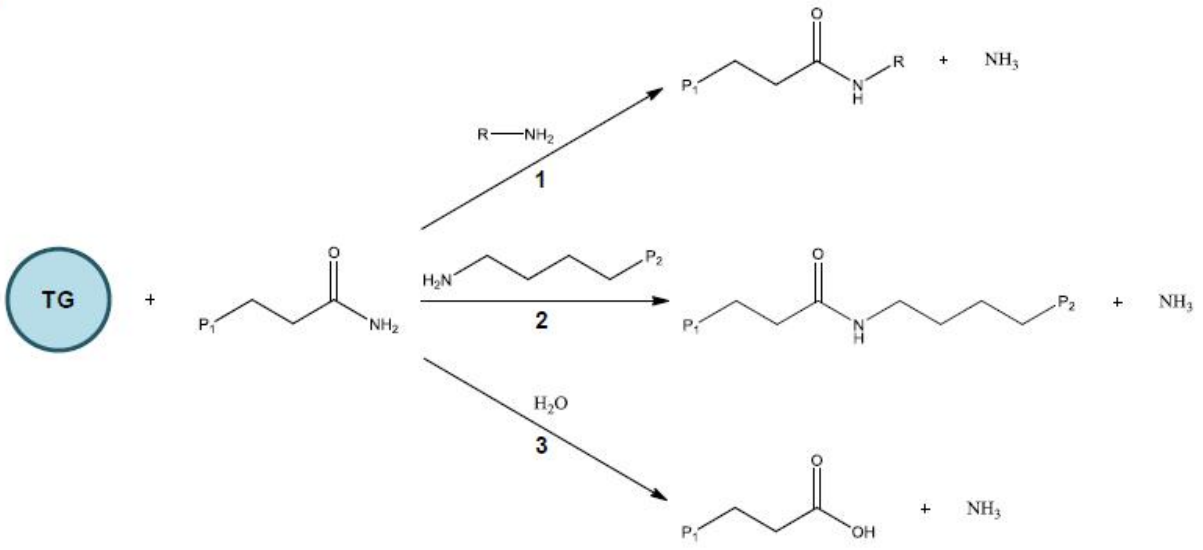
TG
+
R—NH2
1
H2N
P2
2
H2O
3
P1
NH2
R
N
H
OH
NH3
O

B


Tissue transglutaminase (tTG): 687 aa
β-sandwich
Catalytic core
β-barrel 1
β-barrel 2

C

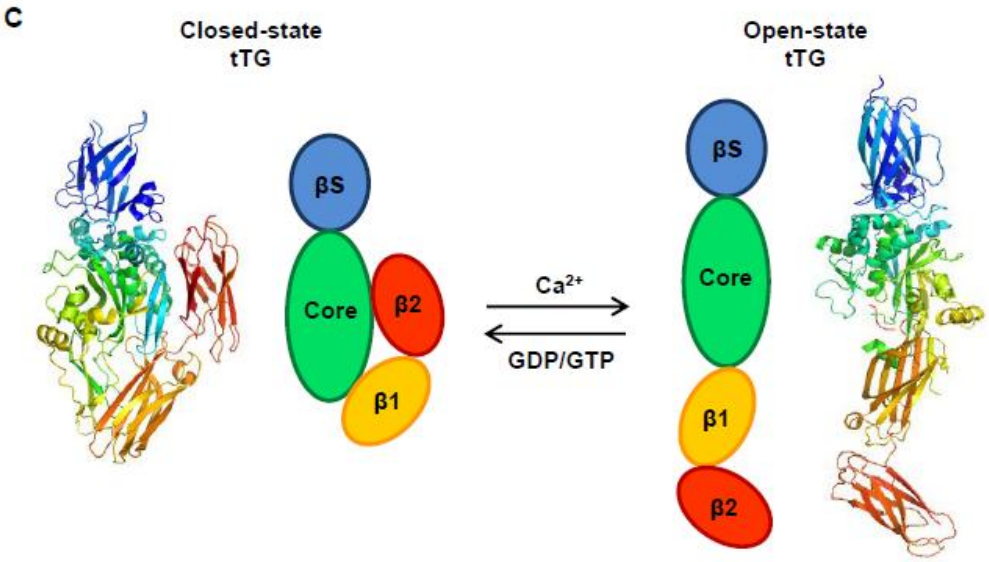
Closed-state
tTG
Open-state
tTG
βS
Core
β2
β1
Ca2+
GDP/GTP

Table 1.4. Human transglutaminase family.

The human family of transglutaminase genes and proteins are listed with their main functions, tissue distributions, and alternate names. {Adapted from (9)}

Gene	Protein	Chromosomal location	Molecular mass, kDa	Main function	Tissue distribution	Alternate names
TGM1	TG1	14q11.2	90	Cell envelope formation during keratinocyte differentiation	Membrane-bound keratinocytes	TG_k, keratinocyte TG, particulate TG
TGM2	TG2	20q11-12	80	Apoptosis, cell adhesion, matrix stabilization, signal transduction	Many tissues: cytosolic, nuclear, membrane, and extracellular	Tissue TG, TG_c, liver TG, endothelial TG, erythrocyte TG, Ghα
TGM3	TG3	20q11-12	77	Cell envelope formation during keratinocyte differentiation	Hair follicle, epidermis, brain	TG_E, callus TG, hair follicle TG, bovine snout TG
TGM4	TG4	3q21-22	77	Reproduction, especially in rodents as a result of semen coagulation	Prostate	TG_p androgen-regulated major secretory protein, vesiculase, dorsal prostate protein 1
TGM5	TG5	15q15.2	81	Cell envelope formation in keratinocytes	Foreskin keratinocytes, epithelial barrier lining, skeletal muscular striatum	TG_x
TGM6	TG6	20q11	78	Not known	Testis and lung	TG_y
TGM7	TG7	15q15.2	81	Not known	Ubiquitous but predominantly in testis and lung	TG_z
F13A1	FXIIIa	6q24-25	83	Blood clotting, wound healing, bone synthesis	Platelets, placenta, synovial fluid, chondrocytes, astrocytes, macrophages, osteoclasts and osteoblasts	Fibrin-stabilizing factor, fibrinoligase, plasma TG, Laki-Lorand factor
EPB42	Band4.2	15q15.2	72	Membrane integrity, cell attachment, signal transduction	Erythrocyte membranes, cone marrow, spleen	B4.2, ATP-binding erythrocyte membrane protein band 4.2

low levels are also detected in the nucleus, plasma membrane, and mitochondria (9, 10). Furthermore, it is secreted into the ECM through non-classical secretory pathways, such as microvesicles, though this process is not fully characterized (84, 85). In addition to its transamidation activity, tTG has GTP-binding activity and has been suggested to be capable of functioning as a protein disulfide isomerase (PDI) (82, 86-88). tTG has been reported to have a wide variety of targets, such as phospholipase $C\delta_1$, β-integrins, fibronectin, osteonectin, RhoA, multilineage kinases, retinoblastoma (Rb), PTEN, and IκBα (9, 10). But despite its many roles and targets, *TGM2* knockout mice have no phenotype apart from impaired wound healing and stress response (89, 90). However, up-regulated tTG expression has been linked to a number of diseases and pathologies, including celiac disease, neurodegenerative disorders, and cancer (91-93).

Regulation of tissue transglutaminase structure and activity

tTG is made up of 687 amino acids that are organized into four discrete domains (Figure 1.6B). The N-terminus adopts a β-sandwich fold, and contains binding sites for integrin and fibronectin; the catalytic core spans amino acids 140-454, and harbors the catalytic triad (Cys277, His335, Asp358); and the two C-terminal domains each adopt a β-barrel fold. There is a unique guanine-binding site between the catalytic core and β-barrel 1 that is distinct from those of heterotrimeric and monomeric G proteins (e.g. transducin and Cdc42, respectively), and three Ca^{2+} binding sites in the catalytic core (10, 82, 83, 94).

tTG can exist in two distinct conformations that are regulated by the binding of GTP/GDP and Ca^{2+}, as evidenced by their X-ray crystal structures (Figure 1.6C) (82, 83). When bound to guanine nucleotide, the C-terminal β-barrels interact with the catalytic core and cause

the protein to adopt what is referred to as the "closed" conformation. While tTG is in this state, it exhibits GTP-binding activity, but the transamidation active site is obscured and thus crosslinking activity is inhibited. However, high concentrations of Ca^{2+} allosterically activate tTG by inducing the β-barrels to dissociate from the core, allowing tTG to adopt a more extended conformation known as the "open" state. In this conformation, tTG exhibits transamidation activity, but is unable to bind GTP or GDP. Consistent with this finding, mutations that disturb the binding of the β-barrels to the core (e.g. R478L, R580L) result in constitutive transamidation activity and the loss of all GTP-binding capability (95, 96).

The transamidation reaction occurs through a two-step process: upon substrate binding, the nucleophilic Cys277 attacks the γ-carbon of glutamine in the donor protein, generating a thioester intermediate and releasing ammonia. In the second step, a primary amine, usually the ε-amino group of a protein-bound lysine residue, attacks the thioester intermediate to generate a stable isopeptide bond and release the product. If a primary amine acceptor is not present, a water molecule attacks the intermediate instead, resulting in a deamidation reaction in which glutamine is converted to glutamate (9, 10).

Like most enzymatic reactions, tTG-catalyzed transamidation is tightly regulated both inside and outside the cell. For intracellular tTG, this regulation is primarily accomplished through the cellular concentrations of GTP/GDP and Ca^{2+}. GTP is typically present at concentrations of ~150 μM in the cell, whereas the Ca^{2+} concentration is much lower at ~100 nM (10). Furthermore, the tTG dissociation constant for GTP/GDP is reported as 1.6 μM, but that of Ca^{2+} is 90 μM (9, 97). Thus, intracellular tTG is thought to be primarily bound to GTP/GDP in the closed and inactive conformation. Indeed, the de-regulation of tTG transamidation activity by mutations that promote the open conformation lead to cell death in NIH3T3 fibroblasts and HeLa

cells, suggesting that maintaining tTG predominantly in the closed state is critical for cell viability (95). Nevertheless, many tTG transamidation substrates have been identified, suggesting that specific physiological conditions, such as local increases in the Ca^{2+}concentration or unidentified binding partners, may open and activate tTG.

The cellular localization of tissue transglutaminase and accompanying functions

A number of tTG target proteins in the ECM, cytosol, plasma membrane, nucleus, and mitochondria have been proposed and suggested to have a variety of physiological effects (9, 10). Extracellular tTG has been shown to crosslink ECM proteins such as fibronectin and collagen, promoting the stability of the matrix and enhancing fibroblast and osteoblast adhesion (9, 98, 99). It can also support cell growth, survival, migration, and differentiation through the clustering of integrins and the formation of focal adhesions. The subsequent activation of integrin and focal-adhesion kinase (FAK) signaling promotes the activation of downstream effectors such as extracellular signal-regulated kinase (ERK) 1/2, Src, p190RhoGAP, RhoA, and ROCK. tTG has been further suggested to enhance integrin signaling by acting as an adaptor between integrins and either fibronectin or the platelet-derived growth factor receptor (PDGFR), which activates Akt signaling (9). Interestingly, extracellular tTG also catalyzes the deamidation of the wheat protein gliadin A, which has been shown to represent the molecular basis of celiac disease (91).

tTG also has been reported to have several targets in the cytosol that it regulates through both enzymatic and non-enzymatic means. The tTG-mediated transamidation of RhoA at Gln63 has been shown to constitutively activate this GTPase by blocking its GTP hydrolytic activity (100). Additionally, tTG can crosslink monoamines such as serotonin, histamine, dopamine, and

norepinephrine onto proteins to modulate their activity, and the serotonylation of RhoA and Rab4A GTPases has been suggested to be necessary for the exocytosis of platelet α-granules and platelet activation, adhesion, and aggregation (9, 101). tTG has also been suggested to promote the up-regulation of NF-κB signaling by inducing the degradation of IκBα, either by catalyzing its crosslinking and subsequent proteasomal degradation, or by directly binding to NF-κB, resulting in its non-proteasomal degradation (102, 103).

As a GTP-binding protein, tTG also has the potential to affect many different signaling pathways. It has been suggested to be a direct effector for many G protein-coupled receptors (GPCRs), including the α_1 adrenergic, thromboxane A2, oxytocin, and follicle-stimulating hormone receptors, and PLCδ_1 is one of its major downstream targets (9). Interestingly, PLCδ_1 has even been proposed to act as a guanine-nucleotide exchange factor (GEF) and GTP hydrolysis inhibitor factor for tTG, further stimulating its activity, which can promote the migration of fibroblasts (104, 105).

Although intracellular tTG is predominantly localized to the cytosol, it has been suggested to play important roles in the nucleus. A small pool (~5%) of tTG is localized to the nucleus, where it has been suggested to regulate gene expression (106). In the context of alcohol toxicity, tTG was reported to crosslink the Sp1 transcription factor, rendering it inactive and thus inhibiting the expression of growth factor receptors such as c-Met; in this manner, tTG activity can have a pro-apoptotic effect (107). Conversely, tTG has been suggested to interact with HIF-1β to prevent its dimerization with HIF-1α in cortical neurons, possibly protecting against neuronal cell death following ischemia or stroke (108). The cellular context likely plays a major role in determining whether tTG functions as a pro-apoptotic or anti-apoptotic factor.

Role of tissue transglutaminase in differentiation

Multiple members of the transglutaminase family, including tTG, appear to be involved in the differentiation of various cell types. In keratinocytes, TGs contribute to the cornification of the cell envelope by crosslinking involucrin, loricrin, filaggrin, and small proline-rich proteins, thereby providing the rigid structure and protective effects of the cornified layer of the epidermis. However, the precise role of tTG in this process is unknown (9). The role of tTG in neuronal differentiation is more well-characterized: in SH-SY5Y neuroblastoma cells, tTG promotes neurite outgrowth through its transamidation activity, potentially by stabilizing the tips of growing neurites (109). This may be accomplished through the tTG-mediated transamidation of RhoA, which leads to the activation of ERK1/2, JNK1, and p38γ MAP kinases (110, 111). tTG also appears to play a role in the differentiation of glial cells, mesenchymal SCs, osteoblasts, and many other cell types, as well (9).

Tissue transglutaminase in cancer progression

tTG has been the focus of a great deal of research regarding its roles in cancer progression. Although tTG cannot induce the transformation of fibroblasts on its own, it promotes their growth and survival in low serum conditions by activating the PI3K/Akt and mTOR complex 1 (mTORC1) signaling pathways, suggesting that it may support the transformed phenotype in certain cellular contexts (112). It has also been observed that tTG expression is enhanced in highly aggressive, metastatic, and drug-resistant tumors, indicating that it may be involved in tumor progression. This may be an outcome of the high degree of inflammation often associated with tumors, since inflammatory cytokines are known to induce tTG expression (113, 114). The crosslinking of fibronectin and collagen by extracellular tTG

subsequently promotes the stiffening of the ECM, which can support the migration of cancer cells (9, 98, 99). It can also lead to the activation of FAK, Akt, and NF-κB signaling, which in turn promote EMT and metastasis (9, 115, 116). Moreover, the tTG-mediated crosslinking of fibronectin in cancer cell-derived microvesicles promotes their docking onto recipient cells, and enhances the anchorage-independent growth and survival of these cells through the activation of FAK and ERK signaling (84). The up-regulation of tTG in lung cancer cells also promotes migration and invasion by increasing the expression of matrix metallopeptidase 9 (MMP-9), which in turn modifies the ECM (117).

Enhanced tTG expression and activity also result from the up-regulation of EGFR signaling in many types of cancer, including cervical carcinoma and breast cancer. These cells become dependent on tTG for EGF-induced migration, invasion, and anchorage-independent growth (96, 118-120). In particular, the treatment of HeLa cervical carcinoma cells with EGF was found to stimulate the transamidation activity of tTG, and induce it to localize to the leading edges of migrating cells. This was found to be dependent on the EGF-induced activation of c-Jun N-terminal kinase (JNK) (118). A later study expanded upon these findings, demonstrating that the EGF-induced accumulation of tTG at the leading edges of HeLa cells, and constitutive leading edge-localization of tTG in MDA-MB231 breast cancer cells, was dependent on the chaperonin activity of Hsp70 (120). Additionally, the treatment of SKBR3 and BT20 breast cancer cells with EGF was observed to significantly increase tTG protein levels, accompanied by the formation of ternary complexes containing tTG, Src, and keratin-19 that was dependent on the transamidation activity of tTG. The ensuing activation of Src led to a significant increase in the proliferation and anchorage-independent growth of these cells (119). Interestingly, tTG can also positively regulate the expression of the EGFR in GBM. Specifically, upon engaging the E3

ubiquitin ligase c-Cbl, tTG inhibits the down-regulation of the EGFR, thus enhancing its signaling lifetime (96). These results suggest that tTG and the EGFR may participate in a positive feedback loop that further promotes the oncogenesis of these cells.

Finally, there is evidence to suggest that tTG is involved in chemotherapy resistance and the self-renewal of CSCs (94, 121-124). In SKBR3 and BT-20 breast cancer cells, EGF was observed to inhibit the induction of apoptosis by the chemotherapeutic agent doxorubicin; this protective effect was dependent on the EGF-induced up-regulation of tTG expression, and the ability of tTG to bind Ca^{2+} and catalyze transamidation (94, 122). More recently, tTG has been implicated in the self-renewal and survival CSCs. It appears to function upstream of PI3K/Akt signaling in $CD44^{+}$ GSCs to promote the expression of inhibitor of DNA binding 1 (ID1), a transcription factor normally involved in maintaining the stemness of embryonic SCs and adult neural SCs. Thus, the knockdown or inhibition of tTG led to a significant attenuation of self-renewal, cell viability, and tumor formation *in vivo* (123). Similarly, tTG was required for the self-renewal and viability of CSCs derived from epidermal squamous cell carcinoma, and its ability to promote the CSC phenotype depended on the binding of guanine nucleotide, but not its transamidation activity (124). Together, these studies suggest that tTG may be an important therapeutic target in CSCs, as I will detail in Chapter 2.

As described above, a major role of tTG in cancer cells is to promote the up-regulation of growth factor signaling. Interestingly, advances in the study of de-regulated cellular energetics in cancer cells have found that metabolic reprogramming is an outcome of oncogenic signaling through growth factor receptors (e.g. the EGFR) and PI3K/Akt, potentially through the activity of tTG. This altered metabolic phenotype is critical for the enhanced proliferation commonly observed in cancer cells, and renders them highly dependent on both glucose and glutamine

metabolism (5, 6, 14). I therefore became interested in understanding the molecular mechanisms downstream of growth factor signaling that support the rapid proliferation of cancer cells, specifically the role of GLS in sustaining glutamine metabolism. As Chapter 3 of this thesis will discuss my studies of two alternatively spliced forms of this enzyme, I will provide an overview of cancer cell metabolism and our current understanding of GLS in normal and transformed cells in the remainder of this chapter.

Overview of cancer cell metabolism

Otto Warburg first observed in the early 20th century that rapidly proliferating tissues, including cancer cells, exhibit an altered metabolic phenotype relative to normal cells. They are characterized by the excess production of lactate, even under aerobic conditions, in a phenomenon that is now known as aerobic glycolysis, or the Warburg effect (125). Many decades passed before this alternative metabolic state became appreciated for its contributions to the development and progression of cancer, but it is now recognized as a major hallmark of neoplastic transformation, as described by Hanahan and Weinberg (1). The accumulation of genetic aberrations in oncogenes and tumor suppressors is now understood to play a major role in metabolic rewiring, and results in significant changes in the metabolism of glucose and glutamine that enhance cancer cell growth and proliferation (5-7).

Although cancer cells have been observed for many decades to take up elevated levels of glucose and metabolize it to lactate, the mechanism by which this altered metabolism promotes their rapid proliferation remained poorly understood until relatively recently. In non-proliferating cells, the complete oxidation of glucose to carbon dioxide through glycolysis and the tricarboxylic acid (TCA) cycle primarily supports the production of ATP through the generation

of reducing equivalents for oxidative phosphorylation. These metabolic pathways comprise a highly efficient means of generating the high energy bonds required to support countless cellular processes, with 36 molecules of ATP produced per molecule of glucose. Conversely, aerobic glycolysis results in the net production of ~4 molecules of ATP per molecule of glucose, and thus constitutes a very inefficient way of supporting cellular energetics (5). However, this seemingly counterintuitive metabolic process may actually generate ATP at a higher rate than oxidative phosphorylation, provided that glucose is present in excess quantities, and is now recognized as a key step in the accumulation of biomass to support cellular growth and division. For proliferating cells to successfully grow and divide, they must generate sufficient nucleic acids, proteins, and lipids to form a daughter cell, and this is primarily accomplished through the up-regulation of glucose and glutamine metabolism, and the diversion of glycolytic and TCA cycle intermediates into biosynthetic pathways (Figure 1.7). By modulating the flux of these metabolites, cancer cells harness glucose- and glutamine-derived carbon and nitrogen for the synthesis of nucleotides, amino acids, and fatty acids, thus allowing them to assemble the macromolecules required for proliferation (5, 6, 8).

The oncogenic activation of glycolysis

The metabolic phenotype exhibited by cancer cells is dependent on alterations in a multitude of signaling pathways and metabolic enzymes. The oncogenic activation of growth factor receptor signaling and the PI3K/Akt pathway (e.g. through the amplification of the EGFR, activating mutations in KRas, or the inactivation of PTEN) is responsible for many of these changes (8, 126). PI3K/Akt signaling results in the increased expression of glucose transporters

Figure 1.7. Overview of cancer cell metabolism.

The metabolic pathways that are commonly altered in cancer cells are shown. These include glycolysis, the TCA cycle, glutaminolysis, amino acid synthesis, lipid synthesis, and the pentose phosphate shunt. Oncogenic signaling that promotes this phenotype is shown in green; tumor suppressors are shown in red; enzymes that regulate key steps in these pathways are shown in blue. {Adapted from (5)}

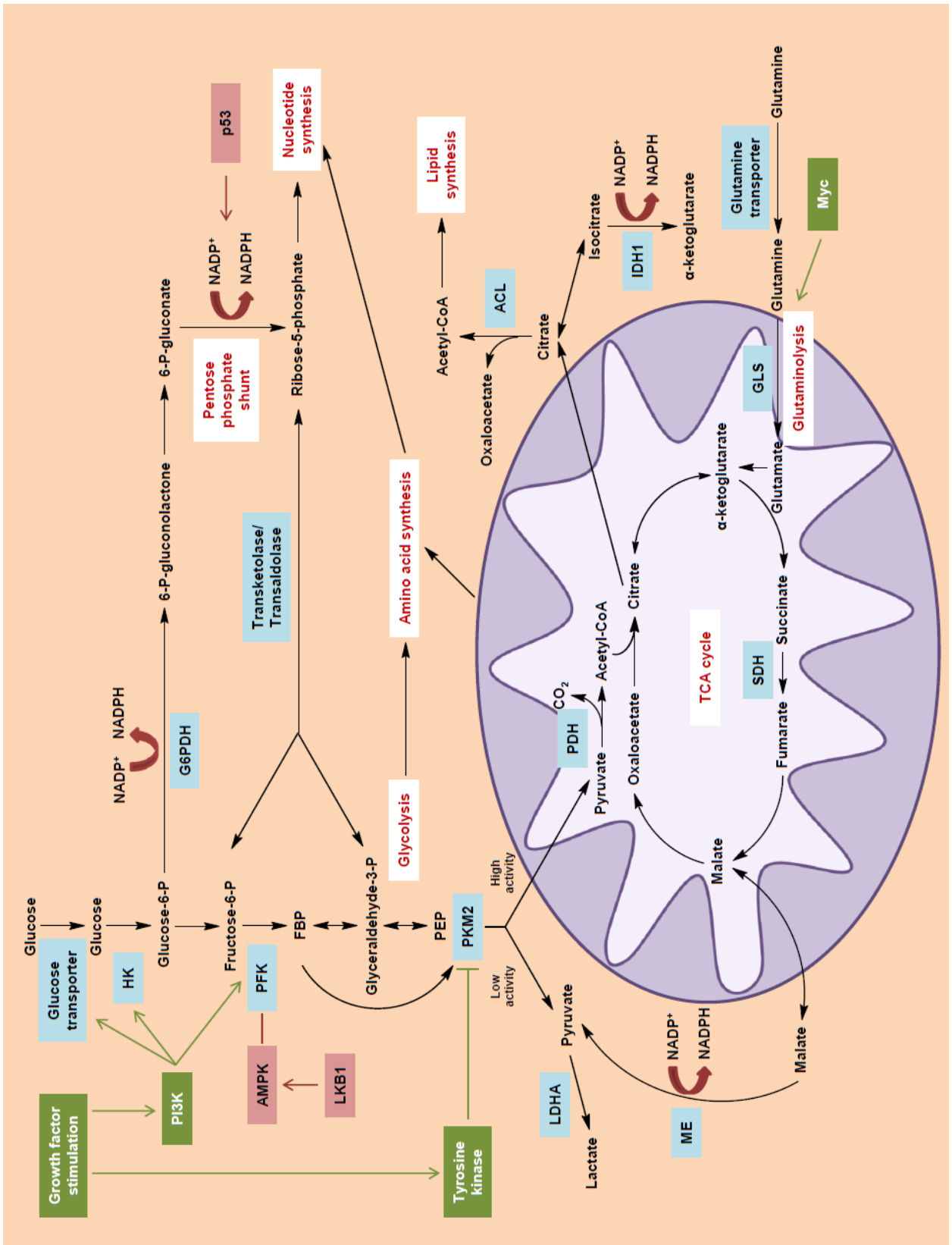
Glucose
Glucose transporter
Glucose
HK
Glucose-6-P
6-P-gluconolactone
6-P-gluconate
NADP+ NADPH
G6PDH
p53
NADP+ NADPH
Pentose phosphate shunt
Nucleotide synthesis
Ribose-5-phosphate
Transketolase/ Transaldolase
Fructose-6-P
PFK
FBP
Glyceraldehyde-3-P
Glycolysis
Amino acid synthesis
Lipid synthesis
Acetyl-CoA
ACL
Oxaloacetate
Citrate
Isocitrate
NADP+ NADPH
IDH1
α-ketoglutarate
Glutamine transporter
Glutamine
Myc
GLS
Glutaminolysis
Glutamate
α-ketoglutarate
PEP
PKM2
High activity
Low activity
PDH
CO2
Pyruvate
Acetyl-CoA
Citrate
TCA cycle
SDH
Succinate
Fumarate
Oxaloacetate
Malate
PI3K
AMPK
LKB1
Growth factor stimulation
Tyrosine kinase
LDHA
Pyruvate
Lactate
NADP+ NADPH
ME
Malate

that facilitate elevated glucose uptake, and Akt can phosphorylate key glycolytic enzymes, such as hexokinase (HK) and phosphofructokinase 2 (PFK2) to promote rapid flux through glycolysis (127, 128). Additionally, Akt phosphorylates the forkhead box protein O (FOXO) family transcription factors, resulting in the down-regulation of genes that promote cell cycle arrest, apoptosis, and DNA repair (8, 129). It can also stimulate protein synthesis by phosphorylating, and thus inactivating, tuberous sclerosis 2 (TSC2), a negative regulator of mTOR (128). The ensuing up-regulation of mTOR activity has been shown to induce the expression of hypoxia-inducible factor 1 (HIF1), a transcription factor that is normally expressed only under hypoxic conditions. The loss of the von Hippel-Lindau (VHL) tumor suppressor, which promotes HIF1 degradation during normoxia, can also contribute to the increased expression of HIF1 in cancer cells, even when oxygen is not limiting (8). Upon its induction, HIF1 enhances the glycolytic phenotype by stimulating the expression of glucose transporters, many glycolytic enzymes, and pyruvate dehydrogenase kinase 1 (PDK1), which inhibits the activity of pyruvate dehydrogenase (PDH), and thus limits the flux of pyruvate into the TCA cycle (130, 131). Pyruvate is subsequently converted to lactate by lactate dehydrogenase A (LDHA), whose expression is up-regulated by the oncogenic transcription factor Myc (132). This reaction is coupled to the oxidation of NADH to NAD^+, and therefore regenerates a critical electron acceptor that is required for continued glycolytic flux. In addition to inducing LDHA, Myc also promotes the glycolytic phenotype by inducing the expression of glucose transporters, glycolytic enzymes, and PDK1, and is essential for stimulating glutamine metabolism (see below) (8).

Regulation of glycolysis by tumor suppressors

In order for cancer cells to fully activate aerobic glycolysis, they must circumvent the actions of tumor suppressors such as VHL, PTEN, liver kinase B1 (LKB1), and p53, all of which are commonly mutated in cancer. As described above, VHL normally ensures the degradation of HIF1, and thus opposes glycolytic metabolism (8). PTEN is critical for turning off PI3K/Akt signaling, as it dephosphorylates PIP_3 (the product of PI3K), and thus its inactivation promotes the de-regulated signaling of Akt (126). Additionally, the LKB1-mediated stimulation of AMP-activated protein kinase (AMPK) is a crucial checkpoint for cell growth. AMPK functions as a cellular energy sensor by detecting the AMP/ATP ratio, and opposes Akt signaling to inhibit cell proliferation in times of energy stress. This growth control is accomplished in part through the AMPK-catalyzed phosphorylation of TSC2 and raptor, a component of mTORC1, resulting in the inhibition of mTORC1 activity and the suppression of protein synthesis. AMPK also stimulates the transcription factor FOXO3a (which is inhibited by Akt), leading to the induction of genes involved in apoptosis and metabolism. Additionally, AMPK activates p53, a tumor suppressor with pleiotropic roles in the regulation of the DNA damage response, cell growth, and metabolism (8, 133). Specifically, p53 induces the expression of HK, stimulating glycolysis for the production of ATP (134). However, p53 also antagonizes glycolytic metabolism by promoting the expression of TP53-induced glycolysis and apoptosis regulator (TIGAR), which reduces glycolytic flux by decreasing the concentration of fructose-2,6-bisphosphate, a glycolytic activator (135). The subsequent buildup of glycolytic intermediates results in their diversion into the pentose phosphate shunt, which supports the regeneration of the antioxidant NADPH. Finally, p53 promotes the expression of PTEN, thereby reducing signaling through PI3K/Akt (136). The inactivation of these various tumor suppressors can thus have significant

consequences for the regulation of cellular growth and metabolism, and contribute to the uncontrolled proliferation of cancer cells.

The diversion of metabolic intermediates into biosynthetic pathways

To support the maximal biosynthesis of nucleic acids, proteins, and lipids for cell proliferation, cancer cells must up-regulate glycolysis in conjunction with mechanisms for diverting glycolytic and TCA cycle intermediates into biosynthetic pathways (5, 6, 8). One of the most well-studied mechanisms for the regulation of glycolytic flux is the modulation of the final, rate-limiting step of this pathway, in which pyruvate kinase (PK) catalyzes the conversion of phosphoenolpyruvate (PEP) to pyruvate. Non-proliferating cells typically express an isoform of PK referred to as PKM1, which has high enzymatic activity, and promotes the flux of pyruvate into the mitochondria to support oxidative phosphorylation. However, many cancer cells instead express the PKM2 isoform, whose activity is significantly decreased upon phosphorylation by tyrosine kinases downstream of oncogenic growth factor signaling (see Figure 1.7) (137). The reduced rate of pyruvate production by PKM2 results in the buildup of glycolytic intermediates, which are then shuttled into the pentose phosphate shunt, nucleotide biosynthesis, and amino acid synthesis (5). In addition to PKM2, the suppression of PDH activity by PDK1 similarly reduces the flow of pyruvate into the TCA cycle, as described above (8).

TCA cycle intermediates are also crucial for the generation of biosynthetic precursors, particularly fatty acids for lipid synthesis. The export of citrate from the mitochondria into the cytosol is commonly up-regulated in cancer cells, and acetyl-CoA and oxaloacetate are then recaptured from cytosolic citrate through the enzymatic activity of ATP citrate lyase (ACL). Acetyl-CoA is then incorporated into fatty acids by fatty acid synthase (FAS), thus contributing

to the biosynthesis of lipids (6). However, the diversion of citrate into the cytosol constitutes a massive drain on TCA cycle carbon, which would be rapidly depleted without an anaplerotic carbon source. For this reason, among others, cancer cells become highly dependent on the up-regulation of glutamine metabolism, as described below (14, 138).

Pleiotropic roles of glutamine in cancer cell metabolism

In conjunction with the elevated glucose uptake and metabolism observed in nearly all cancer cells, glutamine metabolism is also highly up-regulated during neoplastic transformation (14, 138). This is largely an outcome of gene expression changes induced by oncogenic Myc: it facilitates the increased uptake of glutamine by directly stimulating the expression of the glutamine transporters SLC5A1 and SLC7A1, and indirectly stimulates the translation of GLS mRNA through the repression of two microRNAs, miR-23a and miR-23b (139). More recently, our laboratory has shown that the transcription factor c-Jun also promotes the expression of GLS by directly activating its transcription (MJ Lukey, et al., submitted). Upon translation, GLS localizes to the mitochondria, where it catalyzes the first step of glutaminolysis by converting glutamine to glutamate. Glutamate is subsequently metabolized to α-ketoglutarate (αKG), a TCA cycle intermediate, by glutamate dehydrogenase (GDH), or to alanine or aspartate by aminotransferases (ALT, AST). In this manner, glutaminolysis promotes the continued cycling of the TCA cycle, thus supporting the synthesis of fatty acids, and providing reducing equivalents in the form of NADH to support oxidative phosphorylation (6, 14).

In addition to its role as an anaplerotic source of carbon for the TCA cycle, glutamine has several other roles in cancer metabolism, as well. The glutamate derived from GLS catalysis contributes to the synthesis of non-essential amino acids by donating its α-nitrogen to alanine

and aspartate through the enzymatic activity of ALT and AST, and glutamine can support nucleotide synthesis by donating its γ-nitrogen to purine and pyrimidine rings (14). Moreover, glutamine is required for hexosamine biosynthesis and the glycosylation of secreted proteins and lipids in proliferating hematopoietic cells, and appears to contribute to the maturation of growth factor receptors (140). This process may potentially be harnessed by cancer cells as well, and depend on GLS activity.

Interestingly, glutamine also contributes to the production of glutathione, an antioxidant that is important for scavenging reactive oxygen species (ROS) generated by the increased metabolic flux of cancer cells (14, 138). When glutamine is metabolized by GLS2, an isozyme of GLS, the resulting glutamate is used for the synthesis of glutathione and the production of ATP through oxidative phosphorylation (141). Additionally, the export of glutamate through the X_c^- antiporter facilitates the uptake of cystine, which is subsequently converted to cysteine and incorporated into glutathione (142). However, cancer cells must carefully regulate the expression of GLS2, as it has been suggested to function as a tumor suppressor for reasons that are not fully understood.

Overview of the glutaminase family

Given the important contributions of GLS to glutamine metabolism in cancer cells, I became interested in understanding the molecular mechanisms that regulate the activity of this enzyme. As described above, GLS isozymes catalyze the hydrolysis of glutamine to glutamate, accompanied by the release of ammonia (Figure 1.8A) (143). They are encoded by two distinct genes, *GLS* and *GLS2*, and give rise to multiple isozymes. The alternative splicing of the *GLS* gene product gives rise to two distinct isoforms that are referred to as kidney-type glutaminase

Figure 1.8. Catalysis and structure of glutaminase.

(A) GLS isozymes catalyze the deamidation of glutamine to produce glutamate.

(B) The domain structures of GLS and GLS2 are shown. They each contain an N-terminal mitochondrial targeting sequence (MTS) that results in the cleavage of the N-terminus upon localization to the mitochondria, as well as a conserved glutaminase catalytic domain. However, each isoform possesses a unique C-terminus. The C-termini of KGA and LGA both include an ankyrin repeat domain (ANK), whereas that of LGA also contains a C-terminal PDZ-binding domain (PDB).

(C) The X-ray crystal structure of GAC in complex with phosphate (PDB: 3SS4) is shown. Each monomer of the GAC tetramer is individually colored, and phosphate is shown in red (150).

A

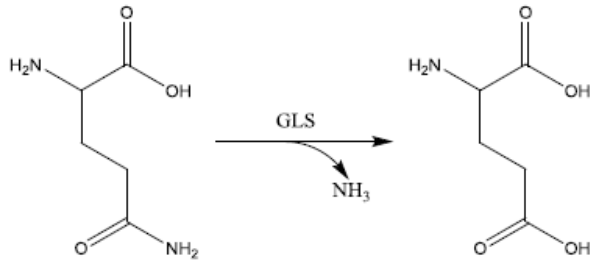

B

Encoded by *GLS*:

Kidney-type glutaminase (KGA): Exons 1-14, 16-19; 669 aa

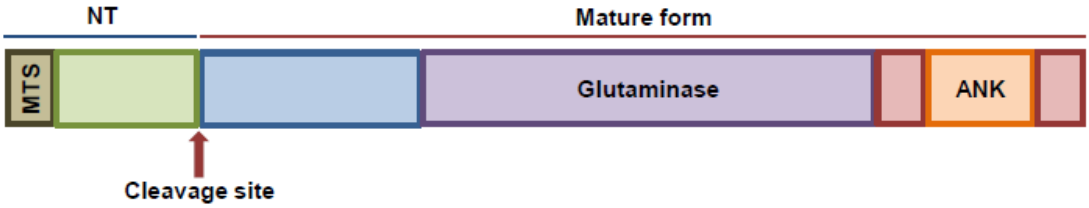

Glutaminase C (GAC): Exons 1-15; 598 aa

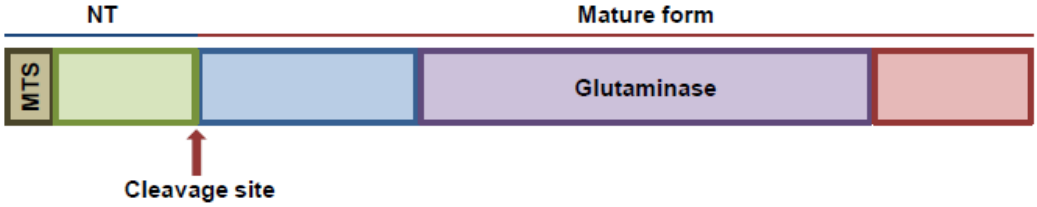

Encoded by *GLS2*:

Liver-type glutaminase (LGA): Exons 1-18; 602 aa

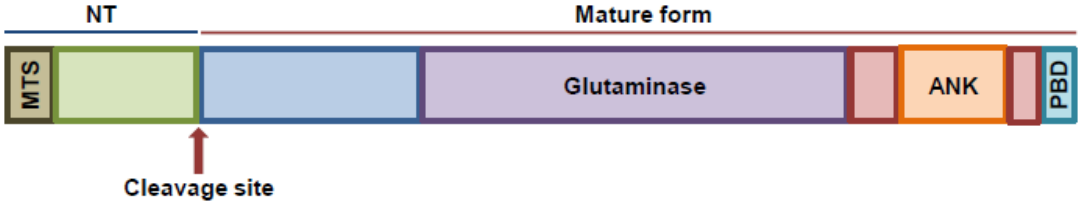

C

GAC tetramer

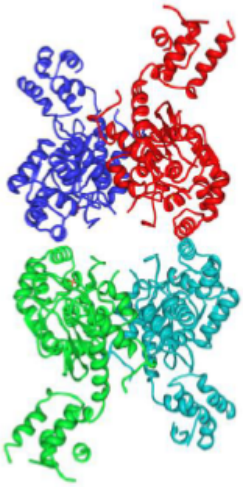

(KGA) and glutaminase C (GAC), while *GLS2* encodes liver-type glutaminase (LGA) (Figure 1.8B) (144-146). However, these isozymes were named after the tissues from which they were originally isolated, and it is now recognized that KGA is expressed fairly ubiquitously, while LGA is expressed in the liver, brain, and pancreas. The tissue distribution of GAC has not yet been fully determined (145).

Regulation of glutaminase structure and activity

As KGA and GAC are alternative splice variants, they exhibit a high degree of sequence identity: KGA is comprised of exons 1-14 and 16-19, while GAC is encoded by exons 1-15 (146). Thus, these two isoforms are distinguishable only by their unique C-termini. All three isozymes, including LGA, contain an N-terminal mitochondrial targeting sequence that directs their localization to the mitochondria, although their exact location within this organelle is still debated (147, 148). The N-terminus (72 amino acids, in the case of KGA and GAC) is subsequently cleaved to generate the mature form of each protein, which also contains a conserved catalytic domain and a unique C-terminus (149). As depicted in Figure 1.8B, the C-termini of KGA and LGA each include an ankyrin repeat domain, in addition to a PDZ-binding domain in LGA, which may facilitate protein-protein interactions (146).

Regarding their three-dimensional structure and enzymatic activation, each of these isozymes typically exists in an inactive dimeric state until stimulated by the binding of inorganic phosphate. *In vitro*, the presence of > 40 mM phosphate induces KGA and GAC to form catalytically active homotetramers, or potentially higher order oligomers (see Figure 1.8C) (150, 151). For this reason, these enzymes are sometimes referred to as "phosphate-activated glutaminases (PAGs)." However, the concentration of phosphate is relatively low *in vivo* (~1

mM in serum), suggesting that alternative mechanisms, such as post-translational modifications downstream of growth factor signaling, may also contribute to the formation of the active GLS species (152, 153). While each of these isozymes appears to be activated in a similar manner by phosphate, they exhibit different enzyme kinetics that may be important for their tissue-specific functions. KGA (and likely GAC) has a relatively low K_m for glutamine of ~2-5 mM, while that of LGA is 17 mM. Additionally, GAC and KGA activity can be inhibited by glutamate, which competes with glutamine binding in the active site, whereas LGA is unaffected by the buildup of this product (143).

Regulation of glutaminase expression

The regulation of KGA/GAC and LGA expression appears to be distinct, as well. One of the major physiological roles of KGA is the homeostatic regulation of plasma pH (see below). During the onset of metabolic acidosis, pH-response elements in the 3'UTR of the KGA transcript promote its stabilization in the kidney, leading to its increased expression (154). *GLS* expression is also indirectly up-regulated by Myc, which promotes the stability and translation of *GLS* transcripts by inhibiting the expression of miR-23a and miR-23b, as briefly described above (139). Furthermore, the transcription of *GLS* is directly stimulated by the transcription factor c-Jun in breast cancer cells (MJ Lukey, et al., submitted). Together, these transcription factors ensure that GLS isozymes are expressed at elevated levels in proliferating cells, including many cancer cells. Conversely, the expression of *GLS2* is directly up-regulated by the tumor suppressor p53, providing further evidence to suggest that LGA is a tumor suppressor (141).

Roles of glutaminase in normal tissues and cancer cells

Among the roles of GLS isozymes in normal tissues, perhaps the best-studied are its contributions to the renal response to metabolic acidosis, and its production of the neurotransmitter glutamate in the brain. The onset of metabolic acidosis results in a decrease in the plasma pH, triggering the up-regulation of KGA expression and glutamine transporters in the kidney. The ensuing increase in KGA activity augments the production of ammonia, which acts as a sponge for excess protons, and is then excreted as ammonium to restore pH levels to normal (154, 155). Alternatively, the production of glutamate by GLS isozymes is crucial in the brain, as this metabolite is a key neurotransmitter. Thus, it is not surprising that both KGA and LGA are widely expressed throughout the brain. However, the observed subcellular localization of LGA is unexpected: this isozyme is predominantly localized in neuronal nuclei, whereas KGA is observed in the mitochondria, as predicted (145). Thus, it is possible that KGA and LGA may have alternative roles in the brain, as appears to be the case in cancer cells.

In contrast to the physiological roles of GLS isozymes in normal tissues, cancer cells appear to depend primarily on GAC for TCA cycle anaplerosis (13). Recent studies have implicated GAC as an important target for therapeutic intervention in a variety of cancer cell types, including breast, glioma, B lymphoma, and prostate cancer cell lines, but have not addressed the role of KGA (139, 156-159). Specifically, GAC activity was observed to be up-regulated downstream of Rho GTPase and NF-κB signaling in breast cancer cells, and its inhibition by the small molecule inhibitor 968 significantly reduced cell proliferation, anchorage-independent growth, and the growth of tumors in mice (156). Similarly, a recently developed GLS inhibitor referred to as CB-839 was found to inhibit the growth of triple-negative breast cancer cells, and is currently in clinical trials for the treatment of a variety of solid tumors (159).

In contrast, studies of GLS2 have found that its expression is commonly down-regulated in cancer cells (160). Moreover, the ectopic expression of GLS2 in glioma and hepatocellular carcinoma cells significantly reduced their proliferation, anchorage-independent growth, and tumor formation *in vivo*, providing evidence for a tumor suppressor role for GLS2 (157, 161, 162). The varied roles of GAC and GLS2 isozymes in cancer cells have thus led us to ask what role KGA plays in cancer cells, and whether it functions to promote tumor growth, similar to GAC, or whether it is a tumor suppressor, like GLS2. Furthermore, it will be critical to understand whether GLS inhibitors can target the activity of KGA, and whether its inhibition will reduce the proliferation of cancer cells. My studies detailed in Chapter 3 of this thesis will aim to uncover the specific contributions of GAC and KGA to the transformed metabolic phenotype.

Overview of the thesis

Given that ALDH1A isozymes promote the self-renewal and therapy resistance of CSCs, I hypothesized that these effects may be mediated by their ability to regulate gene expression through the production of RA. I therefore investigated whether tTG, a protein with known contributions to cancer progression and whose expression is up-regulated by RA, may be induced downstream of ALDH1A isozymes in CSCs (9, 10). As detailed in Chapter 2, I used ALDH1A3^{+} MES GSCs to investigate a link between ALDH1A3 activity and tTG expression. I found that the expression of tTG is indeed dependent on the activity of ALDH1A3 in these cells, and makes them particularly vulnerable to small molecules that induce tTG to adopt an open conformation. Moreover, these tTG inhibitors sensitize MES GSCs to the cytotoxic effects of TMZ and radiation, and thus combination therapies including a tTG inhibitor may be

instrumental in eradicating the MES GSC population and preventing tumor recurrence in patients with HGG.

I was also very interested in understanding the specific roles of two GLS isoforms, namely KGA and GAC, in cancer cell metabolism and proliferation. This is the focus of Chapter 3. I found that GAC is expressed at much higher levels than KGA in a majority of cancer cell lines, which initially suggested that GAC may be better suited to support the transformed metabolic phenotype. However, I found that the relative contributions of KGA and GAC to cancer cell proliferation and anchorage-independent growth correlate with their expression levels. Moreover, I determined that both KGA and GAC are capable of inducing the transformation of fibroblasts when expressed in combination with an oncogene. Most notably, the GAC inhibitor 968 was able to block KGA-induced transformation, indicating that it will be an effective strategy for therapeutically targeting glutaminolysis in cells expressing either GAC or KGA.

REFERENCES

1. Hanahan D, Weinberg RA. Hallmarks of cancer: The next generation. Cell 2011;144(5):646-74.

2. Reya T, Morrison SJ, Clarke MF, Weissman IL. Stem cells, cancer, and cancer stem cells. Nature 2001;414(6859):105-11.

3. Pardal R, Clarke MF, Morrison SJ. Applying the principles of stem-cell biology to cancer. Nature Reviews Cancer 2003;3(12):895-902.

4. Visvader JE, Lindeman GJ. Cancer stem cells in solid tumours: Accumulating evidence and unresolved questions. Nature Reviews Cancer 2008;8(10):755-68.

5. Vander Heiden MG, Cantley LC, Thompson CB. Understanding the warburg effect: The metabolic requirements of cell proliferation. Science 2009;324(5930):1029-33.

6. DeBerardinis RJ, Lum JJ, Hatzivassiliou G, Thompson CB. The biology of cancer: Metabolic reprogramming fuels cell growth and proliferation. Cell metabolism 2008;7(1):11-20.

7. Levine AJ, Puzio-Kuter AM. The control of the metabolic switch in cancers by oncogenes and tumor suppressor genes. Science 2010;330(6009):1340-4.

8. Cairns RA, Harris IS, Mak TW. Regulation of cancer cell metabolism. Nature Reviews Cancer 2011;11(2):85-95.

9. Eckert RL, Kaartinen MT, Nurminskaya M, et al. Transglutaminase regulation of cell function. Physiol Rev 2014;94(2):383-417.

10. Gundemir S, Colak G, Tucholski J, Johnson GV. Transglutaminase 2: A molecular swiss army knife. Biochimica et Biophysica Acta (BBA)-Molecular Cell Research 2012;1823(2):406-19.

11. Ma I, Allan AL. The role of human aldehyde dehydrogenase in normal and cancer stem cells. Stem Cell Reviews and Reports 2011;7(2):292-306.

12. Vasiliou V, Thompson DC, Smith C, Fujita M, Chen Y. Aldehyde dehydrogenases: From eye crystallins to metabolic disease and cancer stem cells. Chem Biol Interact 2013;202(1):2-10.

13. Erickson JW, Cerione RA. Glutaminase: A hot spot for regulation of cancer cell metabolism? Oncotarget 2010;1(8):734-40.

14. DeBerardinis RJ, Cheng T. Q's next: The diverse functions of glutamine in metabolism, cell biology and cancer. Oncogene 2010;29(3):313-24.

15. Nguyen LV, Vanner R, Dirks P, Eaves CJ. Cancer stem cells: An evolving concept. Nature Reviews Cancer 2012;12(2):133-43.

16. Lapidot T, Sirard C, Vormoor J, et al. A cell initiating human acute myeloid leukaemia after transplantation into SCID mice. Nature 1994;367:17.

17. Bonnet D, Dick JE. Human acute myeloid leukemia is organized as a hierarchy that originates from a primitive hematopoietic cell. Nat Med 1997;3(7):730-7.

18. Reynolds BA, Rietze RL. Neural stem cells and neurospheres—re-evaluating the relationship. Nature methods 2005;2(5):333-6.

19. Ajani JA, Song S, Hochster HS, Steinberg IB. In: Cancer stem cells: The promise and the potential. Seminars in oncology; Elsevier; 2015. p. S3-S17.

20. Al-Hajj M, Wicha MS, Benito-Hernandez A, Morrison SJ, Clarke MF. Prospective identification of tumorigenic breast cancer cells. Proc Natl Acad Sci U S A 2003;100(7):3983-8.

21. Singh SK, Hawkins C, Clarke ID, et al. Identification of human brain tumour initiating cells. Nature 2004;432(7015):396-401.

22. O'Brien CA, Pollett A, Gallinger S, Dick JE. A human colon cancer cell capable of initiating tumour growth in immunodeficient mice. Nature 2007;445(7123):106-10.

23. Eramo A, Lotti F, Sette G, et al. Identification and expansion of the tumorigenic lung cancer stem cell population. Cell Death & Differentiation 2008;15(3):504-14.

24. Hermann PC, Huber SL, Herrler T, et al. Distinct populations of cancer stem cells determine tumor growth and metastatic activity in human pancreatic cancer. Cell stem cell 2007;1(3):313-23.

25. van den Hoogen C, van der Horst G, Cheung H, et al. High aldehyde dehydrogenase activity identifies tumor-initiating and metastasis-initiating cells in human prostate cancer. Cancer Res 2010;70(12):5163-73.

26. Dean M, Fojo T, Bates S. Tumour stem cells and drug resistance. Nature Reviews Cancer 2005;5(4):275-84.

27. Rich JN. Cancer stem cells in radiation resistance. Cancer Res 2007;67(19):8980-4.

28. Baumann M, Krause M, Hill R. Exploring the role of cancer stem cells in radioresistance. Nature Reviews Cancer 2008;8(7):545-54.

29. Bayin NS, Modrek AS, Placantonakis DG. Glioblastoma stem cells: Molecular characteristics and therapeutic implications. World journal of stem cells 2014;6(2):230.

30. Germano IM, Binello E. Stem cells and gliomas: Past, present, and future. J Neurooncol 2014;119(3):547-55.

31. Luo Y, Dallaglio K, Chen Y, et al. ALDH1A isozymes are markers of human melanoma stem cells and potential therapeutic targets. Stem Cells 2012;30(10):2100-13.

32. Smith C, Gasparetto M, Humphries K, Pollyea DA, Vasiliou V, Jordan CT. Aldehyde dehydrogenases in acute myeloid leukemia. Ann N Y Acad Sci 2014;1310(1):58-68.

33. Habib SJ, Chen BC, Tsai FC, et al. A localized wnt signal orients asymmetric stem cell division in vitro. Science 2013;339(6126):1445-8.

34. Vermeulen L, Felipe De Sousa, E Melo, van der Heijden M, et al. Wnt activity defines colon cancer stem cells and is regulated by the microenvironment. Nat Cell Biol 2010;12(5):468-76.

35. Kim Y, Kim KH, Lee J, et al. Wnt activation is implicated in glioblastoma radioresistance. Laboratory investigation 2012;92(3):466-73.

36. Hoffmeyer K, Raggioli A, Rudloff S, et al. Wnt/beta-catenin signaling regulates telomerase in stem cells and cancer cells. Science 2012;336(6088):1549-54.

37. Petrova R, Joyner AL. Roles for hedgehog signaling in adult organ homeostasis and repair. Development 2014;141(18):3445-57.

38. Coni S, Infante P, Gulino A. Control of stem cells and cancer stem cells by hedgehog signaling: Pharmacologic clues from pathway dissection. Biochem Pharmacol 2013;85(5):623-8.

39. Clement V, Sanchez P, De Tribolet N, Radovanovic I, i Altaba AR. HEDGEHOG-GLI1 signaling regulates human glioma growth, cancer stem cell self-renewal, and tumorigenicity. Current biology 2007;17(2):165-72.

40. Huang F, Zhuan-Sun Y, Zhuang Y, et al. Inhibition of hedgehog signaling depresses self-renewal of pancreatic cancer stem cells and reverses chemoresistance. Int J Oncol 2012;41(5):1707-14.

41. Sims-Mourtada J, Izzo JG, Apisarnthanarax S, et al. Hedgehog: An attribute to tumor regrowth after chemoradiotherapy and a target to improve radiation response. Clin Cancer Res 2006;12(21):6565-72.

42. Oskarsson T, Batlle E, Massagué J. Metastatic stem cells: Sources, niches, and vital pathways. Cell stem cell 2014;14(3):306-21.

43. Gottesman MM, Fojo T, Bates SE. Multidrug resistance in cancer: Role of ATP–dependent transporters. Nature Reviews Cancer 2002;2(1):48-58.

44. Mao P, Joshi K, Li J, et al. Mesenchymal glioma stem cells are maintained by activated glycolytic metabolism involving aldehyde dehydrogenase 1A3. Proc Natl Acad Sci U S A 2013;110(21):8644-9.

45. Bao S, Wu Q, McLendon RE, et al. Glioma stem cells promote radioresistance by preferential activation of the DNA damage response. Nature 2006;444(7120):756-60.

46. Vescovi AL, Galli R, Reynolds BA. Brain tumour stem cells. Nature Reviews Cancer 2006;6(6):425-36.

47. Nakano I. Stem cell signature in glioblastoma: Therapeutic development for a moving target. J Neurosurg 2015;122(2):324-30.

48. Sanai N, Alvarez-Buylla A, Berger MS. Neural stem cells and the origin of gliomas. N Engl J Med 2005;353(8):811-22.

49. Calabrese C, Poppleton H, Kocak M, et al. A perivascular niche for brain tumor stem cells. Cancer cell 2007;11(1):69-82.

50. Zhu TS, Costello MA, Talsma CE, et al. Endothelial cells create a stem cell niche in glioblastoma by providing NOTCH ligands that nurture self-renewal of cancer stem-like cells. Cancer Res 2011;71(18):6061-72.

51. Bao S, Wu Q, Sathornsumetee S, et al. Stem cell-like glioma cells promote tumor angiogenesis through vascular endothelial growth factor. Cancer Res 2006;66(16):7843-8.

52. Wang R, Chadalavada K, Wilshire J, et al. Glioblastoma stem-like cells give rise to tumour endothelium. Nature 2010;468(7325):829-33.

53. Cheng L, Huang Z, Zhou W, et al. Glioblastoma stem cells generate vascular pericytes to support vessel function and tumor growth. Cell 2013;153(1):139-52.

54. Sundar SJ, Hsieh JK, Manjila S, Lathia JD, Sloan A. The role of cancer stem cells in glioblastoma. Neurosurgical focus 2014;37(6):E6.

55. Gilbertson RJ, Rich JN. Making a tumour's bed: Glioblastoma stem cells and the vascular niche. Nature Reviews Cancer 2007;7(10):733-6.

56. Soeda A, Park M, Lee D, et al. Hypoxia promotes expansion of the CD133-positive glioma stem cells through activation of HIF-1α. Oncogene 2009;28(45):3949-59.

57. Li Z, Bao S, Wu Q, et al. Hypoxia-inducible factors regulate tumorigenic capacity of glioma stem cells. Cancer cell 2009;15(6):501-13.

58. Ye XZ, Xu SL, Xin YH, et al. Tumor-associated microglia/macrophages enhance the invasion of glioma stem-like cells via TGF-beta1 signaling pathway. J Immunol 2012;189(1):444-53.

59. Zagzag D, Lukyanov Y, Lan L, et al. Hypoxia-inducible factor 1 and VEGF upregulate CXCR4 in glioblastoma: Implications for angiogenesis and glioma cell invasion. Laboratory investigation 2006;86(12):1221-32.

60. Muzio G, Maggiora M, Paiuzzi E, Oraldi M, Canuto R. Aldehyde dehydrogenases and cell proliferation. Free Radical Biology and Medicine 2012;52(4):735-46.

61. Graham C, Brocklehurst K, Pickersgill R, Warren M. Characterization of retinaldehyde dehydrogenase 3. Biochem J 2006;394:67-75.

62. MacGibbon AK, Blackwell LF, Buckley PD. Kinetics of Sheep-Liver cytoplasmic aldehyde dehydrogenase. European Journal of Biochemistry 1977;77(1):93-100.

63. Liu Z, Sun Y, Rose J, et al. The first structure of an aldehyde dehydrogenase reveals novel interactions between NAD and the rossmann fold. Nature Structural & Molecular Biology 1997;4(4):317-26.

64. Lamb AL, Newcomer ME. The structure of retinal dehydrogenase type II at 2.7 Å resolution: Implications for retinal specificity. Biochemistry (N Y) 1999;38(19):6003-11.

65. Moore SA, Baker HM, Blythe TJ, Kitson KE, Kitson TM, Baker EN. Sheep liver cytosolic aldehyde dehydrogenase: The structure reveals the basis for the retinal specificity of class 1 aldehyde dehydrogenases. Structure 1998;6(12):1541-51.

66. Maden M. Retinoid signalling in the development of the central nervous system. Nature Reviews Neuroscience 2002;3(11):843-53.

67. Maden M. Retinoic acid in the development, regeneration and maintenance of the nervous system. Nature Reviews Neuroscience 2007;8(10):755-65.

68. Marletaz F, Holland LZ, Laudet V, Schubert M. Retinoic acid signaling and the evolution of chordates. Int J Biol Sci 2006;2(2):38-47.

69. Balmer JE, Blomhoff R. Gene expression regulation by retinoic acid. J Lipid Res 2002;43(11):1773-808.

70. Marcato P, Dean CA, Giacomantonio CA, Lee PW. Aldehyde dehydrogenase: Its role as a cancer stem cell marker comes down to the specific isoform. Cell Cycle 2011;10(9):1378-84.

71. Ginestier C, Hur MH, Charafe-Jauffret E, et al. ALDH1 is a marker of normal and malignant human mammary stem cells and a predictor of poor clinical outcome. Cell stem cell 2007;1(5):555-67.

72. Huang EH, Hynes MJ, Zhang T, et al. Aldehyde dehydrogenase 1 is a marker for normal and malignant human colonic stem cells (SC) and tracks SC overpopulation during colon tumorigenesis. Cancer Res 2009;69(8):3382-9.

73. Deng S, Yang X, Lassus H, et al. Distinct expression levels and patterns of stem cell marker, aldehyde dehydrogenase isoform 1 (ALDH1), in human epithelial cancers. PloS one 2010;5(4):e10277.

74. Rovira M, Scott SG, Liss AS, Jensen J, Thayer SP, Leach SD. Isolation and characterization of centroacinar/terminal ductal progenitor cells in adult mouse pancreas. Proc Natl Acad Sci U S A 2010;107(1):75-80.

75. Keller LH. Bone Marrow–Derived aldehyde Dehydrogenase–Bright stem and progenitor cells for ischemic repair. Congestive Heart Failure 2009;15(4):202-6.

76. Burger PE, Gupta R, Xiong X, et al. High aldehyde dehydrogenase activity: A novel functional marker of murine prostate stem/progenitor cells. Stem Cells 2009;27(9):2220-8.

77. Cheung A, Wan T, Leung J, et al. Aldehyde dehydrogenase activity in leukemic blasts defines a subgroup of acute myeloid leukemia with adverse prognosis and superior NOD/SCID engrafting potential. Leukemia 2007;21(7):1423-30.

78. Hilton J. Role of aldehyde dehydrogenase in cyclophosphamide-resistant L1210 leukemia. Cancer Res 1984;44(11):5156-60.

79. Sladek NE, Kollander R, Sreerama L, Kiang DT. Cellular levels of aldehyde dehydrogenases (ALDH1A1 and ALDH3A1) as predictors of therapeutic responses to cyclophosphamide-based chemotherapy of breast cancer: A retrospective study. Cancer Chemother Pharmacol 2002;49(4):309-21.

80. Dylla SJ, Beviglia L, Park I, et al. Colorectal cancer stem cells are enriched in xenogeneic tumors following chemotherapy. PloS one 2008;3(6):e2428.

81. Marcato P, Dean CA, Pan D, et al. Aldehyde dehydrogenase activity of breast cancer stem cells is primarily due to isoform ALDH1A3 and its expression is predictive of metastasis. Stem Cells 2011;29(1):32-45.

82. Liu S, Cerione RA, Clardy J. Structural basis for the guanine nucleotide-binding activity of tissue transglutaminase and its regulation of transamidation activity. Proc Natl Acad Sci U S A 2002;99(5):2743-7.

83. Pinkas DM, Strop P, Brunger AT, Khosla C. Transglutaminase 2 undergoes a large conformational change upon activation. PLoS Biol 2007;5(12):e327.

84. Antonyak MA, Li B, Boroughs LK, et al. Cancer cell-derived microvesicles induce transformation by transferring tissue transglutaminase and fibronectin to recipient cells. Proc Natl Acad Sci U S A 2011;108(12):4852-7.

85. Zemskov EA, Mikhailenko I, Hsia R, Zaritskaya L, Belkin AM. Unconventional secretion of tissue transglutaminase involves phospholipid-dependent delivery into recycling endosomes. PLoS One 2011;6(4):e19414.

86. Singh US, Erickson JW, Cerione RA. Identification and biochemical characterization of an 80 kilodalton GTP-binding/transglutaminase from rabbit liver nuclei. Biochemistry (N Y) 1995;34(48):15863-71.

87. Hasegawa G, Suwa M, Ichikawa Y, et al. A novel function of tissue-type transglutaminase: Protein disulphide isomerase. Biochem J 2003;373:793-803.

88. Mastroberardino PG, Farrace MG, Viti I, et al. "Tissue" transglutaminase contributes to the formation of disulphide bridges in proteins of mitochondrial respiratory complexes. Biochimica et Biophysica Acta (BBA)-Bioenergetics 2006;1757(9):1357-65.

89. Nanda N, Iismaa SE, Owens WA, Husain A, Mackay F, Graham RM. Targeted inactivation of Gh/tissue transglutaminase II. J Biol Chem 2001;276(23):20673-8.

90. De Laurenzi V, Melino G. Gene disruption of tissue transglutaminase. Mol Cell Biol 2001;21(1):148-55.

91. Klöck C, DiRaimondo TR, Khosla C. In: Role of transglutaminase 2 in celiac disease pathogenesis. Seminars in immunopathology; Springer; 2012. p. 513-22.

92. Lesort M, Tucholski J, Miller ML, Johnson GV. Tissue transglutaminase: A possible role in neurodegenerative diseases. Prog Neurobiol 2000;61(5):439-63.

93. Li B, Cerione RA, Antonyak M. Tissue transglutaminase and its role in human cancer progression. Adv Enzymol Relat Areas Mol Biol 2011;78:247.

94. Datta S, Antonyak MA, Cerione RA. Importance of Ca2 -dependent transamidation activity in the protection afforded by tissue transglutaminase against doxorubicin-induced apoptosis. Biochemistry (N Y) 2006;45(44):13163-74.

95. Datta S, Antonyak MA, Cerione RA. GTP-binding-defective forms of tissue transglutaminase trigger cell death. Biochemistry (N Y) 2007;46(51):14819-29.

96. Zhang J, Antonyak MA, Singh G, Cerione RA. A mechanism for the upregulation of EGF receptor levels in glioblastomas. Cell reports 2013;3(6):2008-20.

97. Bergamini CM. GTP modulates calcium binding and cation-induced conformational changes in erythrocyte transglutaminase. FEBS Lett 1988;239(2):255-8.

98. Shanmugasundaram S, Logan-Mauney S, Burgos K, Nurminskaya M. Tissue transglutaminase regulates chondrogenesis in mesenchymal stem cells on collagen type XI matrices. Amino Acids 2012;42(2-3):1045-53.

99. Nelea V, Nakano Y, Kaartinen MT. Size distribution and molecular associations of plasma fibronectin and fibronectin crosslinked by transglutaminase 2. The protein journal 2008;27(4):223-33.

100. Singh US, Kunar MT, Kao YL, Baker KM. Role of transglutaminase II in retinoic acid-induced activation of RhoA-associated kinase-2. EMBO J 2001;20(10):2413-23.

101. Walther DJ, Peter J, Winter S, et al. Serotonylation of small GTPases is a signal transduction pathway that triggers platelet α-granule release. Cell 2003;115(7):851-62.

102. Lee J, Kim YS, Choi DH, et al. Transglutaminase 2 induces nuclear factor-kappaB activation via a novel pathway in BV-2 microglia. J Biol Chem 2004;279(51):53725-35.

103. Kumar S, Mehta K. Tissue transglutaminase constitutively activates HIF-1α promoter and nuclear factor-κB via a non-canonical pathway. 2012.

104. Baek KJ, Kang S, Damron D, Im M. Phospholipase Cdelta1 is a guanine nucleotide exchanging factor for transglutaminase II (galpha h) and promotes alpha 1B-adrenoreceptor-mediated GTP binding and intracellular calcium release. J Biol Chem 2001;276(8):5591-7.

105. Stephens P, Grenard P, Aeschlimann P, et al. Crosslinking and G-protein functions of transglutaminase 2 contribute differentially to fibroblast wound healing responses. J Cell Sci 2004;117(Pt 15):3389-403.

106. Park D, Choi SS, Ha K. Transglutaminase 2: A multi-functional protein in multiple subcellular compartments. Amino Acids 2010;39(3):619-31.

107. Tatsukawa H, Fukaya Y, Frampton G, et al. Role of transglutaminase 2 in liver injury via cross-linking and silencing of transcription factor Sp1. Gastroenterology 2009;136(5):1783,1795. e10.

108. Filiano AJ, Bailey CD, Tucholski J, Gundemir S, Johnson GV. Transglutaminase 2 protects against ischemic insult, interacts with HIF1beta, and attenuates HIF1 signaling. FASEB J 2008;22(8):2662-75.

109. Tucholski J, Lesort M, Johnson G. Tissue transglutaminase is essential for neurite outgrowth in human neuroblastoma SH-SY5Y cells. Neuroscience 2001;102(2):481-91.

110. Tucholski J, Johnson GV. Tissue transglutaminase directly regulates adenylyl cyclase resulting in enhanced cAMP-response element-binding protein (CREB) activation. J Biol Chem 2003;278(29):26838-43.

111. Singh US, Pan J, Kao YL, Joshi S, Young KL, Baker KM. Tissue transglutaminase mediates activation of RhoA and MAP kinase pathways during retinoic acid-induced neuronal differentiation of SH-SY5Y cells. J Biol Chem 2003;278(1):391-9.

112. Boroughs LK, Antonyak MA, Cerione RA. A novel mechanism by which tissue transglutaminase activates signaling events that promote cell survival. J Biol Chem 2014;289(14):10115-25.

113. Quan G, Choi J, Lee D, Lee S. TGF-β1 up-regulates transglutaminase two and fibronectin in dermal fibroblasts: A possible mechanism for the stabilization of tissue inflammation. Arch Dermatol Res 2005;297(2):84-90.

114. Suto N, Ikura K, Sasaki R. Expression induced by interleukin-6 of tissue-type transglutaminase in human hepatoblastoma HepG2 cells. J Biol Chem 1993;268(10):7469-73.

115. Verma A, Guha S, Wang H, et al. Tissue transglutaminase regulates focal adhesion kinase/AKT activation by modulating PTEN expression in pancreatic cancer cells. Clin Cancer Res 2008;14(7):1997-2005.

116. Verma A, Mehta K. Transglutaminase-mediated activation of nuclear transcription factor-κB in cancer cells: A new therapeutic opportunity. Current cancer drug targets 2007;7(6):559-65.

117. Li Z, Xu X, Bai L, Chen W, Lin Y. Epidermal growth factor receptor-mediated tissue transglutaminase overexpression couples acquired tumor necrosis factor-related apoptosis-inducing ligand resistance and migration through c-FLIP and MMP-9 proteins in lung cancer cells. J Biol Chem 2011;286(24):21164-72.

118. Antonyak MA, Li B, Regan AD, Feng Q, Dusaban SS, Cerione RA. Tissue transglutaminase is an essential participant in the epidermal growth factor-stimulated signaling pathway leading to cancer cell migration and invasion. J Biol Chem 2009;284(27):17914-25.

119. Li B, Antonyak MA, Druso JE, Cheng L, Nikitin AY, Cerione RA. EGF potentiated oncogenesis requires a tissue transglutaminase-dependent signaling pathway leading to src activation. Proc Natl Acad Sci U S A 2010;107(4):1408-13.

120. Boroughs LK, Antonyak MA, Johnson JL, Cerione RA. A unique role for heat shock protein 70 and its binding partner tissue transglutaminase in cancer cell migration. J Biol Chem 2011;286(43):37094-107.

121. Antonyak MA, Singh US, Lee DA, et al. Effects of tissue transglutaminase on retinoic acid-induced cellular differentiation and protection against apoptosis. J Biol Chem 2001;276(36):33582-7.

122. Antonyak MA, Miller AM, Jansen JM, et al. Augmentation of tissue transglutaminase expression and activation by epidermal growth factor inhibit doxorubicin-induced apoptosis in human breast cancer cells. J Biol Chem 2004;279(40):41461-7.

123. Fu J, Yang QY, Sai K, et al. TGM2 inhibition attenuates ID1 expression in CD44-high glioma-initiating cells. Neuro Oncol 2013;15(10):1353-65.

124. Fisher ML, Keillor JW, Xu W, Eckert RL, Kerr C. Transglutaminase is required for epidermal squamous cell carcinoma stem cell survival. Mol Cancer Res 2015.

125. Koppenol WH, Bounds PL, Dang CV. Otto warburg's contributions to current concepts of cancer metabolism. Nature Reviews Cancer 2011;11(5):325-37.

126. Wong K, Engelman JA, Cantley LC. Targeting the PI3K signaling pathway in cancer. Curr Opin Genet Dev 2010;20(1):87-90.

127. Elstrom RL, Bauer DE, Buzzai M, et al. Akt stimulates aerobic glycolysis in cancer cells. Cancer Res 2004;64(11):3892-9.

128. Robey RB, Hay N. In: Is akt the "Warburg kinase"?—Akt-energy metabolism interactions and oncogenesis. Seminars in cancer biology; Elsevier; 2009. p. 25-31.

129. Khatri S, Yepiskoposyan H, Gallo CA, Tandon P, Plas DR. FOXO3a regulates glycolysis via transcriptional control of tumor suppressor TSC1. J Biol Chem 2010;285(21):15960-5.

130. Semenza GL. HIF-1: Upstream and downstream of cancer metabolism. Curr Opin Genet Dev 2010;20(1):51-6.

131. Papandreou I, Cairns RA, Fontana L, Lim AL, Denko NC. HIF-1 mediates adaptation to hypoxia by actively downregulating mitochondrial oxygen consumption. Cell metabolism 2006;3(3):187-97.

132. Dang CV, Kim J, Gao P, Yustein J. The interplay between MYC and HIF in cancer. Nature Reviews Cancer 2008;8(1):51-6.

133. Shackelford DB, Shaw RJ. The LKB1–AMPK pathway: Metabolism and growth control in tumour suppression. Nature Reviews Cancer 2009;9(8):563-75.

134. Mathupala SP, Heese C, Pedersen PL. Glucose catabolism in cancer cells: THE TYPE II HEXOKINASE PROMOTER CONTAINS FUNCTIONALLY ACTIVE RESPONSE ELEMENTS FOR THE TUMOR SUPPRESSOR p53. J Biol Chem 1997;272(36):22776-80.

135. Bensaad K, Tsuruta A, Selak MA, et al. TIGAR, a p53-inducible regulator of glycolysis and apoptosis. Cell 2006;126(1):107-20.

136. Stambolic V, MacPherson D, Sas D, et al. Regulation of PTEN transcription by p53. Mol Cell 2001;8(2):317-25.

137. Christofk HR, Vander Heiden MG, Harris MH, et al. The M2 splice isoform of pyruvate kinase is important for cancer metabolism and tumour growth. Nature 2008;452(7184):230-3.

138. Shanware NP, Mullen AR, DeBerardinis RJ, Abraham RT. Glutamine: Pleiotropic roles in tumor growth and stress resistance. Journal of molecular medicine 2011;89(3):229-36.

139. Gao P, Tchernyshyov I, Chang T, et al. c-myc suppression of miR-23a/b enhances mitochondrial glutaminase expression and glutamine metabolism. Nature 2009;458(7239):762-5.

140. Wellen KE, Lu C, Mancuso A, et al. The hexosamine biosynthetic pathway couples growth factor-induced glutamine uptake to glucose metabolism. Genes Dev 2010;24(24):2784-99.

141. Hu W, Zhang C, Wu R, Sun Y, Levine A, Feng Z. Glutaminase 2, a novel p53 target gene regulating energy metabolism and antioxidant function. Proc Natl Acad Sci U S A 2010;107(16):7455-60.

142. Lo M, Wang Y, Gout PW. The x c− cystine/glutamate antiporter: A potential target for therapy of cancer and other diseases. J Cell Physiol 2008;215(3):593-602.

143. Curthoys NP, Watford M. Regulation of glutaminase activity and glutamine metabolism. Annu Rev Nutr 1995;15(1):133-59.

144. Elgadi KM, Meguid RA, Qian M, Souba WW, Abcouwer SF. Cloning and analysis of unique human glutaminase isoforms generated by tissue-specific alternative splicing. Physiol Genomics 1999;1(2):51-62.

145. Márquez J, de la Oliva, Amada R López, Matés JM, Segura JA, Alonso FJ. Glutaminase: A multifaceted protein not only involved in generating glutamate. Neurochem Int 2006;48(6):465-71.

146. Porter LD, Ibrahim H, Taylor L, Curthoys NP. Complexity and species variation of the kidney-type glutaminase gene. Physiol Genomics 2002;9(3):157-66.

147. Kalra J, Brosnan JT. The subcellular localization of glutaminase isoenzymes in rat kidney cortex. J Biol Chem 1974;249(10):3255-60.

148. Aledo JC, de Pedro E, Gomez-Fabre PM, de Castro IN, Marquez J. Submitochondrial localization and membrane topography of ehrlich ascitic tumour cell glutaminase. Biochimica et Biophysica Acta (BBA)-Biomembranes 1997;1323(2):173-84.

149. Srinivasan M, Kalousek F, Farrell L, Curthoys NP. Role of the N-terminal 118 amino acids in the processing of the rat renal mitochondrial glutaminase precursor. J Biol Chem 1995;270(3):1191-7.

150. Cassago A, Ferreira AP, Ferreira IM, et al. Mitochondrial localization and structure-based phosphate activation mechanism of glutaminase C with implications for cancer metabolism. Proc Natl Acad Sci U S A 2012;109(4):1092-7.

151. Katt WP, Cerione RA. Glutaminase regulation in cancer cells: A druggable chain of events. Drug Discov Today 2014;19(4):450-7.

152. Almaden Y, Hernandez A, Torregrosa V, et al. High phosphate level directly stimulates parathyroid hormone secretion and synthesis by human parathyroid tissue in vitro. J Am Soc Nephrol 1998;9(10):1845-52.

153. Turner A, McGivan J. Glutaminase isoform expression in cell lines derived from human colorectal adenomas and carcinomas. Biochem J 2003;370:403-8.

154. Curthoys NP, Gstraunthaler G. Mechanism of increased renal gene expression during metabolic acidosis. Am J Physiol Renal Physiol 2001;281(3):F381-90.

155. Gstraunthaler G, Holcomb T, Feifel E, Liu W, Spitaler N, Curthoys NP. Differential expression and acid-base regulation of glutaminase mRNAs in gluconeogenic LLC-PK(1)-FBPase(+) cells. Am J Physiol Renal Physiol 2000;278(2):F227-37.

156. Wang J, Erickson JW, Fuji R, et al. Targeting mitochondrial glutaminase activity inhibits oncogenic transformation. Cancer cell 2010;18(3):207-19.

157. Martín-Rufián M, Nascimento-Gomes R, Higuero A, et al. Both GLS silencing and GLS2 overexpression synergize with oxidative stress against proliferation of glioma cells. Journal of molecular medicine 2014;92(3):277-90.

158. Katt WP, Ramachandran S, Erickson JW, Cerione RA. Dibenzophenanthridines as inhibitors of glutaminase C and cancer cell proliferation. Mol Cancer Ther 2012;11(6):1269-78.

159. Gross MI, Demo SD, Dennison JB, et al. Antitumor activity of the glutaminase inhibitor CB-839 in triple-negative breast cancer. Mol Cancer Ther 2014;13(4):890-901.

160. Szeliga M, Obara-Michlewska M. Glutamine in neoplastic cells: Focus on the expression and roles of glutaminases. Neurochem Int 2009;55(1):71-5.

161. Liu J, Zhang C, Lin M, et al. Glutaminase 2 negatively regulates the PI3K/AKT signaling and shows tumor suppression activity in human hepatocellular carcinoma. Oncotarget 2014;5(9):2635.

162. Szeliga M, Obara-Michlewska M, Matyja E, et al. Transfection with liver-type glutaminase cDNA alters gene expression and reduces survival, migration and proliferation of T98G glioma cells. Glia 2009;57(9):1014-23.

CHAPTER 2

The up-regulation of tissue transglutaminase by aldehyde dehydrogenase 1A3 makes glioma stem cells susceptible to therapeutic intervention

Abstract

Aldehyde dehydrogenase 1 (ALDH1) family proteins, notably ALDH1A1 and ALDH1A3, are common markers for cancer stem cells (CSCs) of several tissue origins. However, very little is known regarding the mechanism by which ALDH1 enzymes contribute to the tumor-initiating properties of CSCs, or how these cells can be targeted therapeutically. Here, we investigate the enzymatic function of ALDH1A3 in glioma stem cells (GSCs), and propose a role for this enzyme as a master regulator of gene expression via the production of retinoic acid (RA), a well-known activator of transcription. Specifically, we demonstrate that RA generated by ALDH1A3 in GSCs induces the expression of tissue transglutaminase (tTG), a dual-function enzyme with both GTP-binding and transamidation activities that has been implicated in the survival and chemotherapy resistance of cancer cells. We further show that the ALDH1A3-dependent up-regulation of tTG offers a potentially novel strategy for the therapeutic targeting of cancer stem cells, through the use of inhibitors that drive tTG to an "open" conformational state that is cytotoxic. Indeed, inhibitors which induce the open state of tTG significantly compromise the self-renewal and proliferation of $ALDH1A3^{+}$ GSCs. Moreover, we demonstrate that combination therapies including a tTG inhibitor and temozolomide or radiation are markedly effective inhibiting GSCs, thus highlighting the potential for tTG inhibitors to be used in combination therapies for patients with high grade glioma.

Introduction

Members of the ALDH1 family of proteins, particularly ALDH1A1 and ALDH1A3, have been found to be markers of cancer stem cells (CSCs) of various tissue origins, including tumors of the brain, head and neck, breast, liver, lung, ovaries, pancreas, prostate, colon, bladder, and skin, as well as leukemia (1-13). While a growing body of evidence suggests that ALDH1 family proteins are critical for maintaining the stem cell-like properties of CSCs, very little is known regarding the mechanisms by which ALDH1 isozymes support self-renewal and tumor initiation. Furthermore, $ALDH1^+$ CSCs are not readily susceptible to therapeutic intervention, as they exhibit resistance to most standard therapies, including chemotherapy and radiation (14-16). As ALDH1 proteins function as retinaldehyde dehydrogenases that catalyze the conversion of retinal to retinoic acid (RA), an activator of transcription, these enzymes play an important role in the regulation of gene expression, and when de-regulated, may help drive the CSC phenotype (1, 17, 18). However, the genes whose expression is increased by RA in CSCs have only just begun to be identified (12).

To investigate the role of RA signaling downstream of ALDH1 proteins in CSCs, we used glioma stem cells (GSCs) previously derived from high grade gliomas (HGGs) as a model system. These GSCs were classified as either mesenchymal (MES) or proneural (PN) based on their gene expression signatures, and exhibit distinct phenotypes. MES GSCs display a highly aggressive phenotype characterized by an elevated capacity for self-renewal, proliferation, and tumorigenicity in an orthotopic mouse model of HGG, whereas PN GSCs exhibit a much lower rate of proliferation and self-renewal, and generate much less aggressive tumors in mice. Importantly, ALDH1A3 is expressed specifically in MES, but not PN, GSCs, and is required to maintain their CSC phenotype (2). As such, we chose to investigate the downstream targets of

ALDH1A3-induced RA signaling in MES GSCs to better understand how ALDH1A3 influences gene expression, and to potentially identify new therapeutic targets in ALDH1A3^{+} cells.

Of particular interest as a putative candidate for regulation by ALDH1A3 in MES GSCs is tissue transglutaminase (tTG), a dual-function GTP-binding protein/crosslinking enzyme encoded by *TGM2*, a well-known transcriptional target of RA which has been previously linked to the development of aggressive cancers. The promoter region of *TGM2* contains an RA-response element (RARE), which is bound by a heterodimer comprised of the retinoic acid receptor (RAR) and the retinoid X receptor (RXR) (19, 20). In the absence of RA, the RAR/RXR heterodimer recruits co-repressors that lead to histone deacetylation and the subsequent repression of transcription. However, in the presence of RA, the RAR/RXR heterodimer releases the co-repressor complexes from the *TGM2* promoter, and instead recruits co-activator complexes that promote histone acetylation and gene transcription (18, 21, 22).

We and others have implicated tTG in the survival, chemotherapy resistance, migration, and regulation of EGF receptor signaling in different cancer cell types, including glioblastoma (23-29). We have also previously shown that tTG can exist in two discrete conformations which are associated with distinct functional properties. The binding of guanine nucleotide induces tTG to adopt a "closed" state, in which the two C-terminal β-barrels fold back on and interact with the core domain, effectively making the protein crosslinking (acyl transferase) active site inaccessible. However, upon exposure to high concentrations of Ca^{2+}, which causes a weakening of the affinity for guanine nucleotide and the subsequent loss of interactions between the core and C-terminus, tTG adopts a more extended conformation known as the "open" state (29-31). The induction of this conformation of tTG, either by treating cells with small molecules that bind

to the protein crosslinking active site of tTG or by expressing tTG mutants that are defective in binding guanine nucleotides, causes a severe cytotoxic effect (29, 31).

Here, we show that tTG expression is induced by ALDH1A3 in MES GSCs. Although we have not been able to directly implicate tTG in contributing to the enhanced survival of MES GSCs, its specific up-regulated expression offered a potentially unique strategy for the therapeutic targeting of these highly aggressive tumor initiator cells. Specifically, we have taken advantage of our previous findings that induction of the open state of tTG causes cytotoxicity (23, 24, 29, 31), and demonstrate that targeting tTG with inhibitors which cause tTG to adopt an open state markedly attenuates the self-renewal and proliferation of MES GSCs. Moreover, we go on to show that combining a tTG inhibitor with either radiation or temozolomide (TMZ) significantly impairs self-renewal and proliferation, as well as induces cell death in MES GSCs. Taken together, our results suggest that tTG may represent a novel therapeutic target for aggressive GSCs, as well as a variety of other $ALDH1^{+}$ cancer cells.

Results

ALDH1A3 induces tTG expression in glioma stem cells

To investigate the induction of tTG expression by ALDH1A3, we began by examining the expression levels of these two proteins in a panel of GSCs composed of four PN and four MES GSC cell lines. We confirmed, by qPCR and Western blotting analysis, that ALDH1A3 is expressed at high levels in MES GSCs, whereas it is nearly undetectable in PN GSCs, as previously reported (2). Interestingly, we found that tTG is also expressed exclusively in MES GSCs, and its expression is correlated with that of ALDH1A3 in a panel of patient-derived GSC cell lines, glioblastoma cell lines, and astrocytes (Figure 2.1A-C) (Figure 2.1C kindly provided

Figure 2.1. ALDH1A3 regulates tTG expression in MES GSCs.

(A) RNA was isolated from PN and MES GSCs, and cDNA was generated as described in "Materials and Methods." qPCR was then performed with primer sets that amplify ALDH1A3 and tTG transcripts, and the results of three independent experiments were averaged and plotted with the PN GSC 19 cell line normalized to one. *p* values are represented as follows: ****, $p < 0.0001$.

(B) Whole cell lysates from PN and MES GSCs were immunoblotted with ALDH1A3, tTG, and Vinculin antibodies.

(C) ALDH1A3 and tTG mRNA levels are correlated in GSC, GBM, and astrocyte cell lines.

(D) tTG transamidation activity in PN and MES GSCs was analyzed by the incorporation of a biotinylated-pentylamine (BPA) onto cell lysates, and detected with a Streptavidin antibody.

(E) MES GSC cell line 326 was treated with the indicated compounds for seven days, followed by RNA isolation and qRT-PCR analysis of tTG transcript levels. The results of independent experiments ($n \geq 3$) were averaged and plotted. *p* values are represented as follows: *, $p < 0.05$; ***, $p < 0.001$.

(F) MES GSC cell lines 13 and 326 were infected with a control lentivirus or lentiviruses containing two distinct ALDH1A3 shRNAs. The cells were split after 24 hours, and treated with either DMSO or RA and selected with puromycin for six days. The cells were then collected for RNA isolation and qRT-PCR analysis of ALDH1A3 and tTG expression. The results of three independent experiments were averaged and plotted. *p* values are represented as follows: *, $p < 0.05$; **, $p < 0.01$; ***, $p < 0.001$.

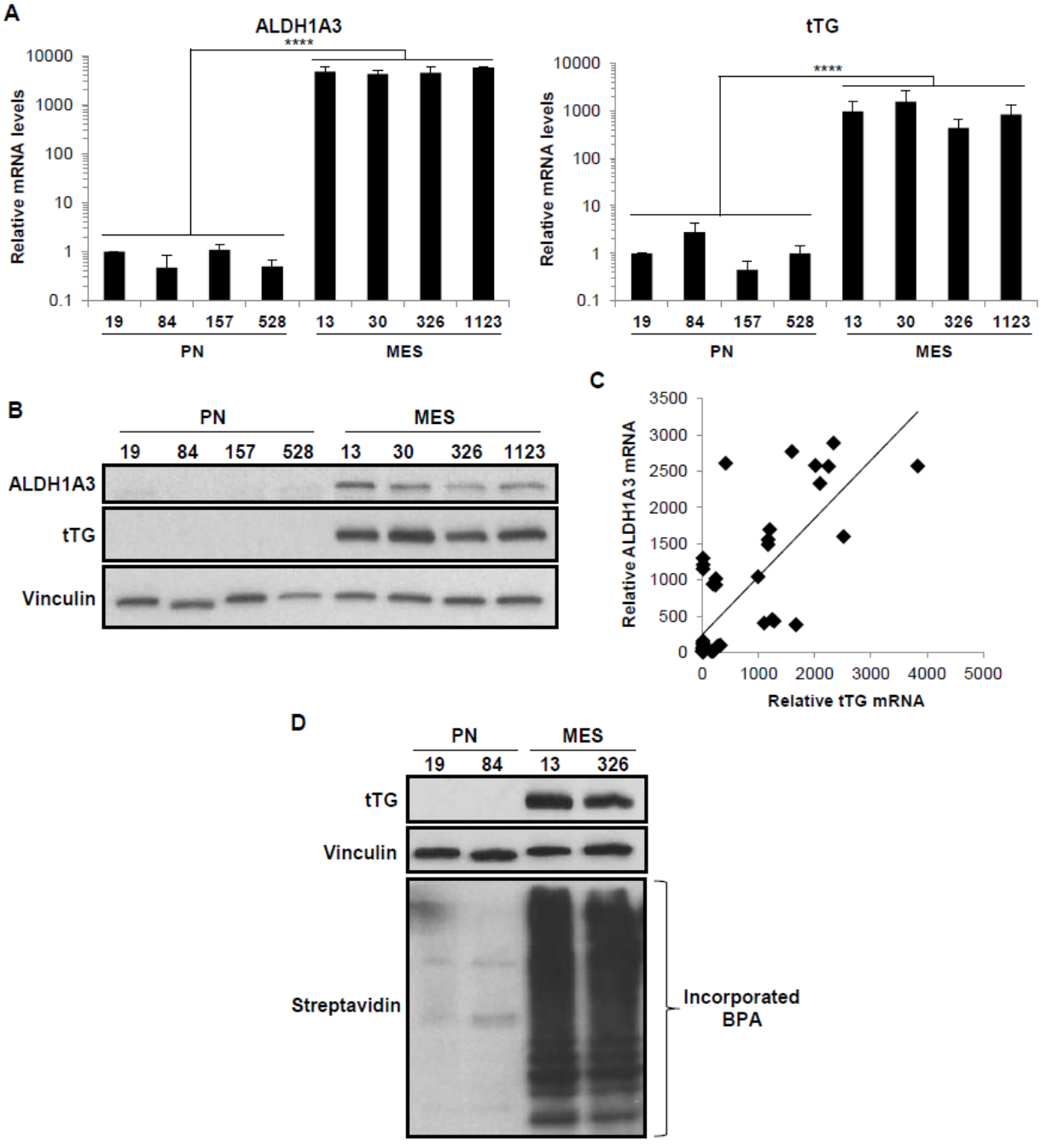
A
ALDH1A3
****
Relative mRNA levels
10000
1000
100
10
1
0.1
19
84
157
528
13
30
326
1123
PN
MES
tTG
****
Relative mRNA levels
10000
1000
100
10
1
0.1
19
84
157
528
13
30
326
1123
PN
MES
B
PN
MES
19
84
157
528
13
30
326
1123
ALDH1A3
tTG
Vinculin
C
Relative ALDH1A3 mRNA
3500
3000
2500
2000
1500
1000
500
0
0
1000
2000
3000
4000
5000
Relative tTG mRNA
D
PN
MES
19
84
13
326
tTG
Vinculin
Streptavidin
Incorporated
BPA

Figure 2.1 Continued

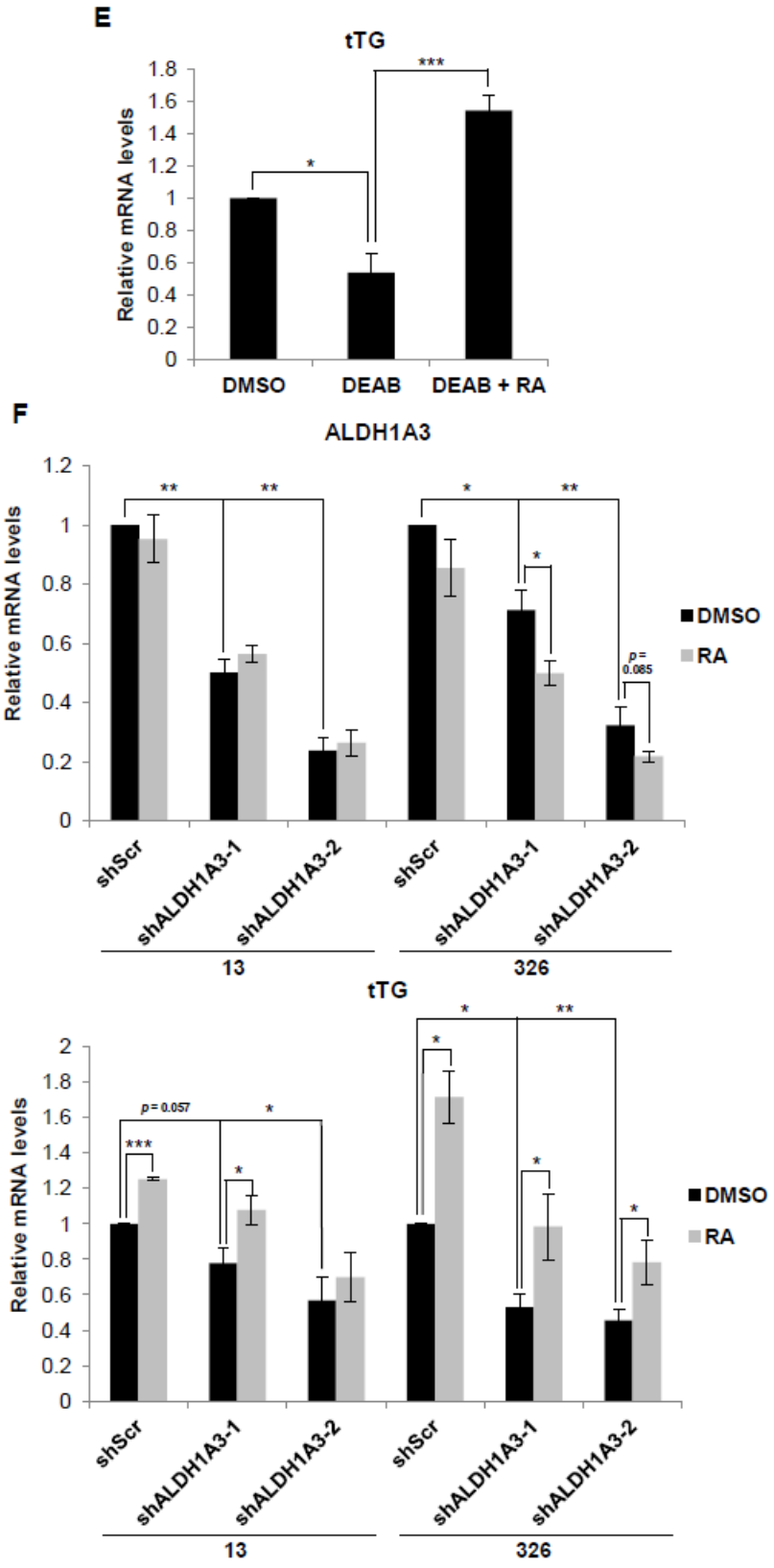

by Dr. Ichiro Nakano, Ohio State University). Consistent with this finding, tTG enzymatic transamidation activity is detected in MES GSCs, but is absent in PN GSCs, as measured by the incorporation of a biotinylated pentylamine (BPA) onto cell lysate proteins (Figure 2.1D). These results, combined with the previously elucidated mechanism of tTG induction by RA, suggested that tTG expression could be induced downstream of ALDH1A3.

Next, we examined whether tTG expression is dependent on the ability of ALDH1A3 to generate RA. After treating the MES GSC cell line 326 for seven days with DEAB, an inhibitor of the enzymatic activity of ALDH1 family proteins, we observed a reduction in tTG mRNA levels that could be rescued upon treatment with RA (Figure 2.1E). We complemented this study by knocking down ALDH1A3 expression in MES GSC cell lines 13 and 326, which caused a significant reduction in tTG mRNA levels that was again rescued by the addition of RA (Figure 2.1F, bottom panel). We also observed a down-regulation of ALDH1A3 expression in response to RA in the MES GSC 326 cell line, in agreement with previous reports describing the negative regulation of ALDH1A3 transcription by RA (Figure 2.1F, top panel) (1). Taken together, these data show that the production of RA by ALDH1A3 induces the expression of tTG in MES GSCs.

We then set out to determine whether ALDH1A3 is sufficient to induce tTG expression in GSCs that do not normally express these proteins, specifically, by taking advantage of the ALDH1A3$^-$/tTG$^-$ PN GSC cell lines 19 and 84. As a preliminary experiment, we treated these cells with RA for three days, and then determined the levels of tTG by qPCR and Western blotting. Figures 2.2A and 2.2B show that tTG transcript and protein levels can indeed be induced by RA in PN GSCs, although the PN GSC 84 cell line appears to be more sensitive to this treatment than the PN GSC 19 cell line.

Figure 2.2. Retinoic acid and ALDH1A3 induce tTG expression in PN GSCs.

(A) PN GSC cell lines 19 and 84 were treated with 0.5 μM RA for 72 hours, then collected for RNA isolation and qRT-PCR analysis of tTG expression. The results of three independent experiments were averaged and plotted. *p* values are represented as follows: **, $p < 0.01$; ****, $p < 0.0001$.

(B) PN GSC cells lines 19 and 84 were treated as in A, and whole cell lysates were collected and immunoblotted with tTG and Vinculin antibodies.

(C) PN GSC cell lines 19 and 84 were infected with a control lentivirus or lentiviruses containing either a wild-type or catalytically-inactive form of ALDH1A3. The cells were split 24 hours later and selected with puromycin for six days, followed by RNA isolation and qRT-PCR analysis of ALDH1A3 and tTG expression. The results of independent experiments ($n \geq 3$) were averaged and graphed. *p* values are represented as follows: *, $p < 0.05$; **, $p < 0.01$; ***, $p < 0.001$, ****, $p < 0.0001$.

(D) PN GSC cell lines 19 and 84 were treated as in C, and whole cell lysates were collected and immunoblotted with V5, tTG, and Vinculin antibodies.

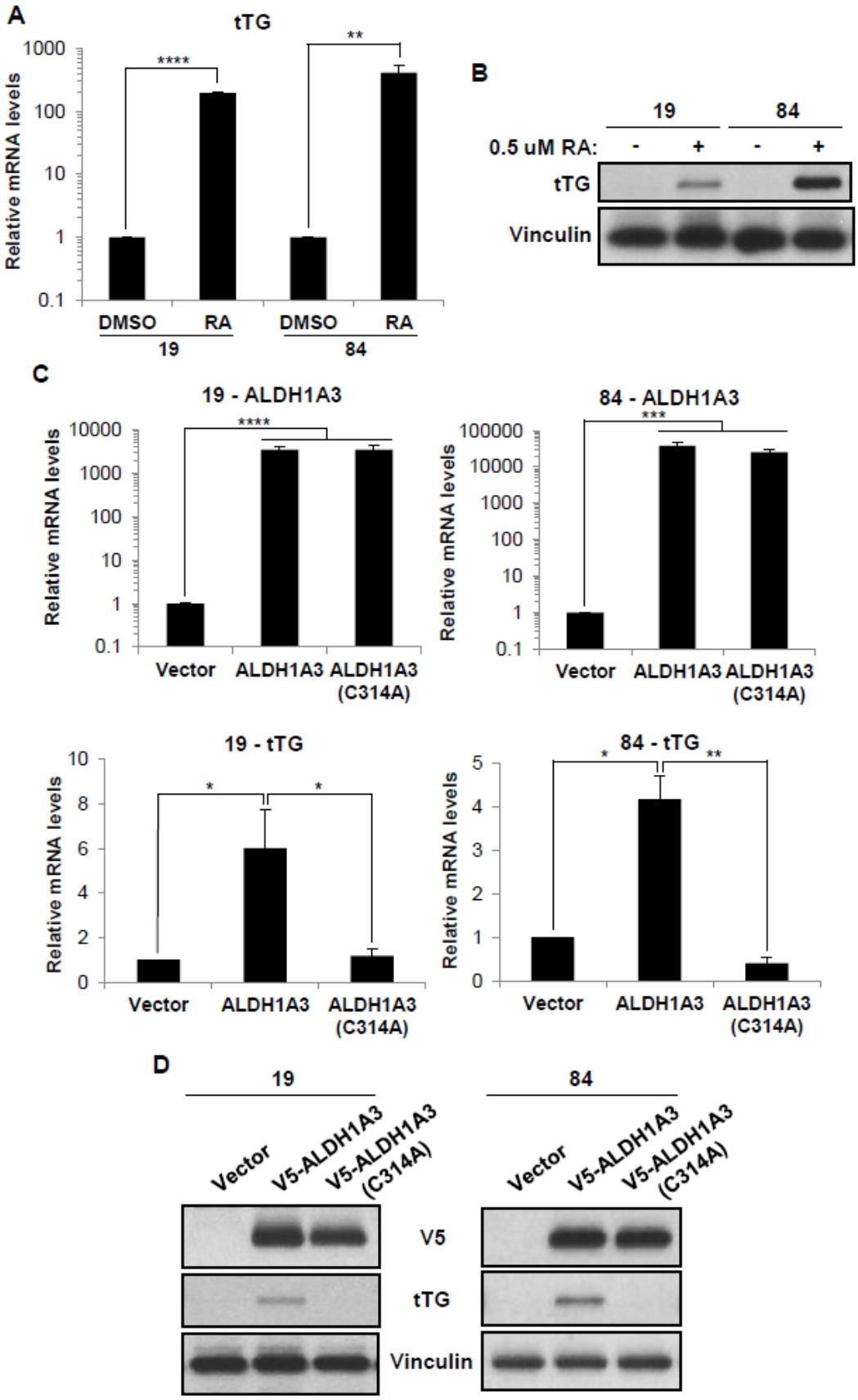
A
tTG
Relative mRNA levels
1000
100
10
1
0.1
****
**
DMSO
RA
DMSO
RA
19
84
B
19
84
0.5 uM RA:
-
+
-
+
tTG
Vinculin
C
19 - ALDH1A3
Relative mRNA levels
10000
1000
100
10
1
0.1
****
Vector
ALDH1A3
ALDH1A3 (C314A)
84 - ALDH1A3
Relative mRNA levels
100000
10000
1000
100
10
1
0.1
***
Vector
ALDH1A3
ALDH1A3 (C314A)
19 - tTG
Relative mRNA levels
10
8
6
4
2
0
*
*
Vector
ALDH1A3
ALDH1A3 (C314A)
84 - tTG
Relative mRNA levels
5
4
3
2
1
0
*
**
Vector
ALDH1A3
ALDH1A3 (C314A)
D
19
84
Vector
V5-ALDH1A3
V5-ALDH1A3 (C314A)
Vector
V5-ALDH1A3
V5-ALDH1A3 (C314A)
V5
tTG
Vinculin

To look specifically at the role of ALDH1A3 in regulating tTG expression levels, we next generated a V5-tagged wild-type ALDH1A3 expression construct, as well as a V5-tagged catalytically inactive mutant of the enzyme (ALDH1A3(C314A)) that cannot produce RA. These constructs, or an empty vector as a control, were introduced into the PN GSC cell lines 19 and 84 using a lentiviral system, and cells stably expressing each construct were generated. Seven days post-infection, we observed a significant increase in the expression of each ALDH1A3 construct (Figure 2.2C, upper panel). Additionally, we found that the ectopic expression of wild-type ALDH1A3 induces tTG expression, whereas the catalytically inactive ALDH1A3 does not, as read out by qPCR and Western blotting (Figure 2.2C, lower panel, D). Thus, ALDH1A3 is sufficient to induce tTG expression in PN GSCs, and this induction is dependent on the production of RA through ALDH1A3 catalysis.

Based on these results, we next asked whether ALDH1 isozymes induce tTG expression in other cancer cell types aside from MES GSCs. To do so, we treated several cancer cell lines with or without the ALDH1 inhibitor DEAB, followed by flow cytometry analysis to identify $ALDH1^{high}$ and $ALDH1^{low}$ populations. The untreated cells exhibiting the highest 15% and lowest 15% ALDH1 activity were then sorted and collected, followed by qRT-PCR analysis for tTG expression (Figure 2.3A, B). As expected, we observed that in the MES GSC 326 cell line, tTG transcript levels are significantly lower in the $ALDH1^{low}$ cells compared with the $ALDH1^{high}$ population, exhibiting a 50% decrease in tTG expression. Interestingly, we found that this relationship between ALDH1 activity and tTG expression is conserved in the more differentiated glioblastoma cell line U87, as well as in HeLa cervical carcinoma cells, A549 lung carcinoma cells, and MIA PaCa-2 pancreatic carcinoma cells. These data demonstrate that the induction of

Figure 2.3. tTG expression is correlated with ALDH1 activity.

(A) Cancer cells were collected and stained using the ALDEFLUOR kit as described in "Materials and Methods." The untreated cells ("- DEAB") with the top 15% and bottom 15% ALDH1 activity (shown in gray) were gated as indicated and collected.

(B) RNA was isolated from the cells collected in A for qRT-PCR analysis of tTG expression. The results of independent experiments ($n \geq 3$) were averaged and graphed. *p* values are represented as follows: *, $p < 0.05$; **, $p < 0.01$; ***, $p < 0.001$.

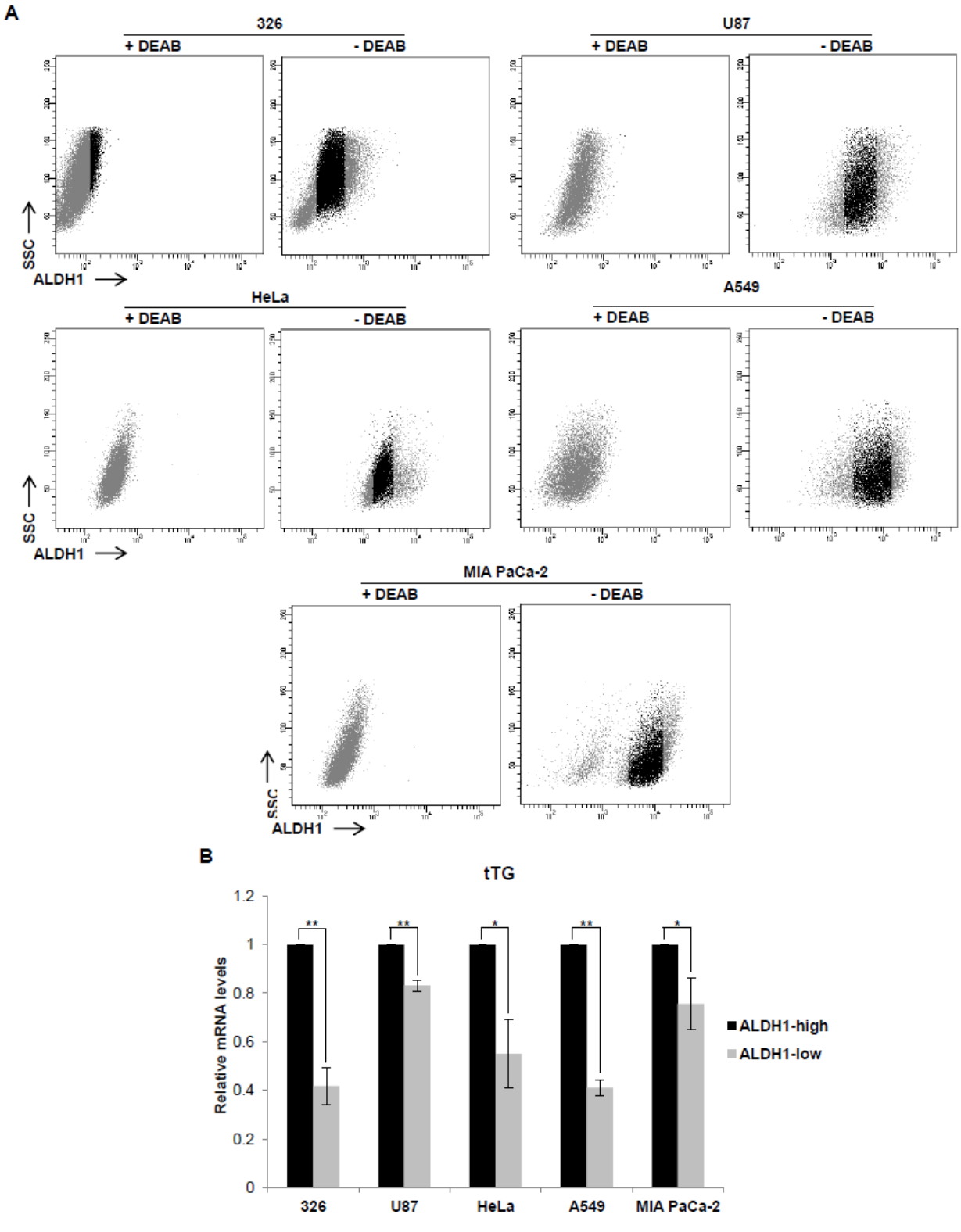
A
326
+ DEAB
- DEAB
U87
+ DEAB
- DEAB
SSC
ALDH1
HeLa
+ DEAB
- DEAB
A549
+ DEAB
- DEAB
SSC
ALDH1
MIA PaCa-2
+ DEAB
- DEAB
SSC
ALDH1
B
tTG
Relative mRNA levels
1.2
1
0.8
0.6
0.4
0.2
0
**
**
*
**
*
326
U87
HeLa
A549
MIA PaCa-2
ALDH1-high
ALDH1-low

tTG expression by ALDH1A3 in MES GSCs is maintained in other cell types expressing ALDH1 isozymes, thus raising the possibility that tTG may be used as a marker and/or therapeutic target in MES GSCs and HGG, as well as in many other cancers containing $ALDH1^+$ cells.

Targeting of tTG blocks the self-renewal and proliferation of MES GSCs

tTG has been implicated in multiple aspects of the transformed phenotype in various cancer cells, including $CD44^+$ GSCs and epidermal CSCs (32, 33). As such, we were surprised to find that the genetic silencing of tTG in MES GSCs had little observable impact on the ability of MES GSCs to self-renew, proliferate or survive various insults such as nutrient deprivation, and challenges with chemotherapeutic agents (data not shown). Nonetheless, given the abundant expression of tTG in MES GSCs, we hypothesized that if we could induce a cytotoxic conformation of tTG (i.e., the "open state"), we could strategically target ALDH1A3-expressing MES GSCs regardless of whatever biological role tTG is playing in these cells. Previously, we demonstrated that the open conformation of tTG can be achieved either through the use of transamidation inhibitors (eg. MDC, Z-Don) or by the introduction of a point mutation into the GTP-binding domain of tTG (eg. R580L, R580K, see Figure 2.4A). Once driven into a persistent open state, we have found that tTG is highly toxic to a number of different cell types, including leukemia cells, breast cancer cells, NIH3T3 fibroblasts, and HeLa cervical carcinoma cells (23, 24, 29, 31).

As a first step to investigate the potential effects of the open conformation of tTG in MES GSCs, we wanted to compare the effects of expressing an HA-tagged wild-type form of tTG with those of HA-tagged tTG (C277S,R580L), a transamidation-defective, open-state mutant, in the

Figure 2.4. Open-state tTG inhibits MES GSC self-renewal and proliferation.

(A) tTG exists in two distinct conformations referred to as the "closed" and "open" states, accompanied by GTPase and transamidation activity, respectively. Ca^{2+} and the tTG inhibitors MDC and Z-Don induce tTG to adopt an open conformation, whereas the binding of GTP/GDP allows tTG to assume a closed conformation.

(B) MES GSC cell lines 13 and 326 were infected with either a control lentivirus, or lentiviruses containing either an HA-tagged wild-type form of tTG, or an HA-tagged transamidation-defective, open-state tTG mutant (HA-tTG(C277S,R580L)). Whole cell lysates were collected at the indicated time points following infection, and immunoblotted with HA and Vinculin antibodies.

(C) Whole cell lysates collected from MES GSC cell lines 13 and 326 were immunoblotted with tTG and Vinculin antibodies (left panel), or incubated with or without MDC and Z-Don. tTG transamidation activity was read-out by the incorporation of a biotinylated-pentylamine (BPA) onto cell lysates, and detected with a Streptavidin antibody.

(D) and **(E)** MES GSC cell lines 13 and 326 were dissociated into single cells and seeded at 5 x 10^3 cells/well in 12-well plates.

(D) Neurospheres were counted after 72 hours. Each experiment was performed in triplicate, and the results were averaged and graphed. *p* values are represented as follows: ****, $p < 0.0001$.

(E) The cells were counted at the indicated time points to determine cell proliferation. Each experiment was performed in triplicate, and the results were averaged and graphed. *p* values are represented as follows: ****, $p < 0.0001$.

Figure 2.4 continued

(F) tTG inhibitors induce cell death following nutrient deprivation. MES GSC cell lines 13 and 326 were dissociated into single cells, and seeded at 2 x 10^4 cells/well in 12-well plates in either GSC medium or DMEM/F12 with the indicated compounds. The cells were collected after 48 hours, stained with Trypan Blue Solution, and the viable and dead cells were counted. Each experiment was performed in triplicate, and the results were averaged and graphed. *p* values are represented as follows: **, $p < 0.01$; ***, $p < 0.001$; ****, $p < 0.0001$.

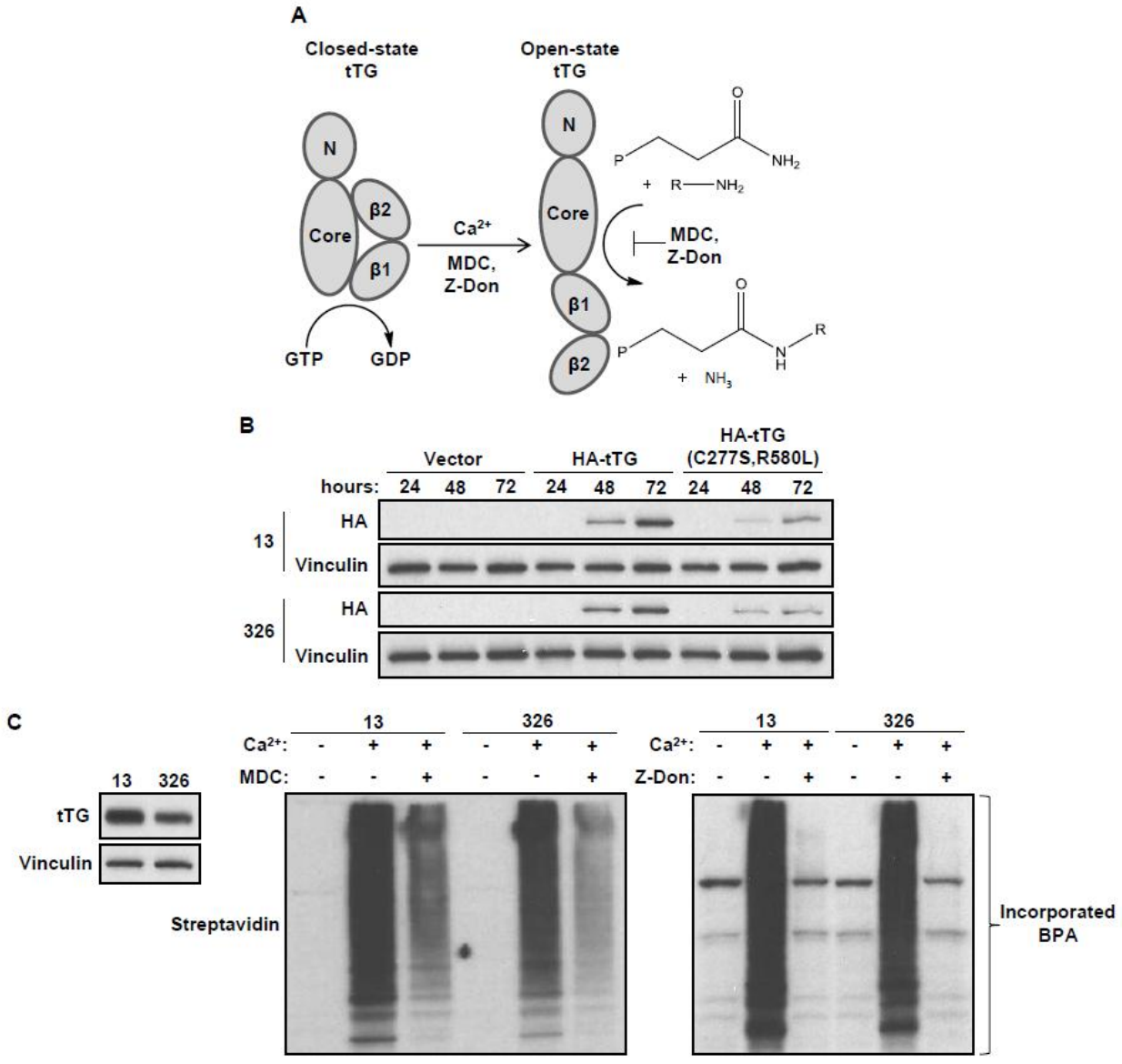
A
Closed-state tTG
Open-state tTG
N
Core
β2
β1
GTP
GDP
Ca2+
MDC,
Z-Don
MDC,
Z-Don
B
Vector
HA-tTG
HA-tTG (C277S,R580L)
hours: 24 48 72 24 48 72 24 48 72
13
326
HA
Vinculin
C
13 326
tTG
Vinculin
Ca2+: - + + - + +
MDC: - - + - - +
Streptavidin
Z-Don: - - + - - +
Incorporated BPA

Figure 2.4 Continued

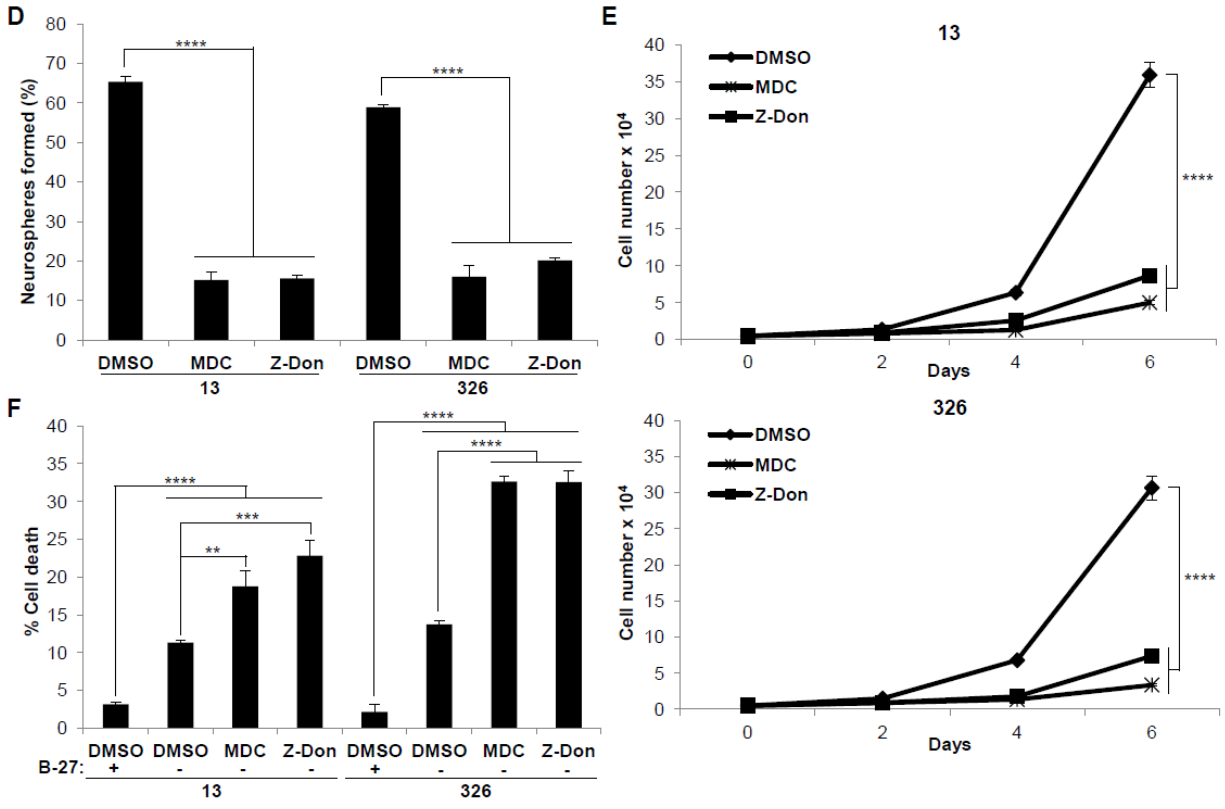

MES GSC cell lines 13 and 326 (31). However, while performing these experiments we found that although the expression of the wild-type tTG increases significantly over the course of 72 hours, the expression of the tTG mutant is very low (Figure 2.4B). Thus, it appears that this cytotoxic tTG mutant is selected against in the MES GSCs, consistent with our previous findings for open-state forms of tTG in NIH3T3 and HeLa cells, making further studies with this mutant untenable (31).

We then went on to probe the effects of open-state tTG on the self-renewal, proliferation and survival of MES GSCs with two commonly used tTG inhibitors, MDC and Z-Don. MDC functions as a competitive inhibitor of tTG by acting as an alternative amine donor for the transamidase activity of tTG, whereas Z-Don binds irreversibly to the transamidation active site cysteine, shutting off transamidation activity and restricting tTG to the open state (i.e. for example, see Figure 2.4C) (34-36). Upon treatment of the MES GSC cell lines 13 and 326 with these inhibitors, we observed a dramatic reduction in their abilities to form neurospheres, suggesting that targeting tTG can indeed block the self-renewal of these cells (Figure 2.4D). Correspondingly, the proliferation of these cells is significantly reduced when treated with MDC and Z-Don as well (Figure 2.4E). To test the effects of tTG inhibitors on the survival of the MES GSC cell lines 13 and 326, we challenged these cells by starving them of heparin and B-27, a serum replacement, in the presence or absence of MDC and Z-Don. Upon carrying out cell viability assays, we observed that nutrient starvation slightly induced cell death, but this effect was significantly enhanced by targeting tTG (Figure 2.4F). Together, these data suggest that the induction of the open state of tTG by tTG inhibitors can provide a therapeutic benefit in MES GSCs and HGG.

tTG inhibitors synergize with chemotherapy and radiation to induce cell death

As GSCs exhibit tumor-initiating properties as well as enhanced evasion of chemo- and radiotherapy relative to non-GSCs, they are thought to be the primary drivers of tumor recurrence (14, 16, 37-39). Thus, combination therapies that target and kill GSCs may be a promising way of treating HGG, and so we examined the benefits of combining tTG inhibitors with the current standard of care for HGG, namely radiation and TMZ (16). Upon obtaining dose curves for Z-Don, radiation, and TMZ in proliferation assays (Figure 2.5A-C), we determined the IC_{50} values for each treatment for their subsequent use in combination therapies. We then radiated MES GSC cell lines 13 and 326 in combination with Z-Don, and found a significant decrease in neurosphere formation and proliferation, and an increase in cell death (Figure 2.6A-C). Likewise, we treated MES GSCs with a combination of TMZ and Z-Don, and again observed a strong inhibition of self-renewal and proliferation (Figure 2.6D and E). Strikingly, cell viability assays show that while sub-lethal doses of TMZ and Z-Don individually have little impact on cell survival, the combination therapy leads to a synthetic lethality in MES GSCs (Figure 2.6F).

Discussion

In this study, we set out to better understand the role of ALDH1 isozymes in CSCs, and potentially identify therapeutic targets in $ALDH1^+$ cells. Although numerous studies have classified both ALDH1A1 and ALDH1A3 as markers of CSCs derived from several distinct tumor types, the functional roles of these enzymes in CSCs have not been well-defined (1). Limited studies have suggested that ALDH1A3 supports stemness in GSCs by promoting glycolysis/gluconeogenesis, and is associated with higher Stat3 signaling in $ALDH1^+$ CSCs derived from non-small cell lung cancer (2, 6). A report examining melanoma CSCs described a

Figure 2.5. Z-Don, radiation, and TMZ dose curves.

Dose curves were generated for Z-Don **(A)**, radiation **(B)**, and TMZ **(C)** in MES GSC cell lines 13 and 326. Spheres were dissociated into single cells, seeded at 5 x 10^3 cells/well in 12-well plates, and treated with the indicated therapies. The cells were counted after 6 days to determine cell proliferation. Each experiment was performed in triplicate, and the results were averaged and graphed to reflect percent inhibition by the indicated treatment.

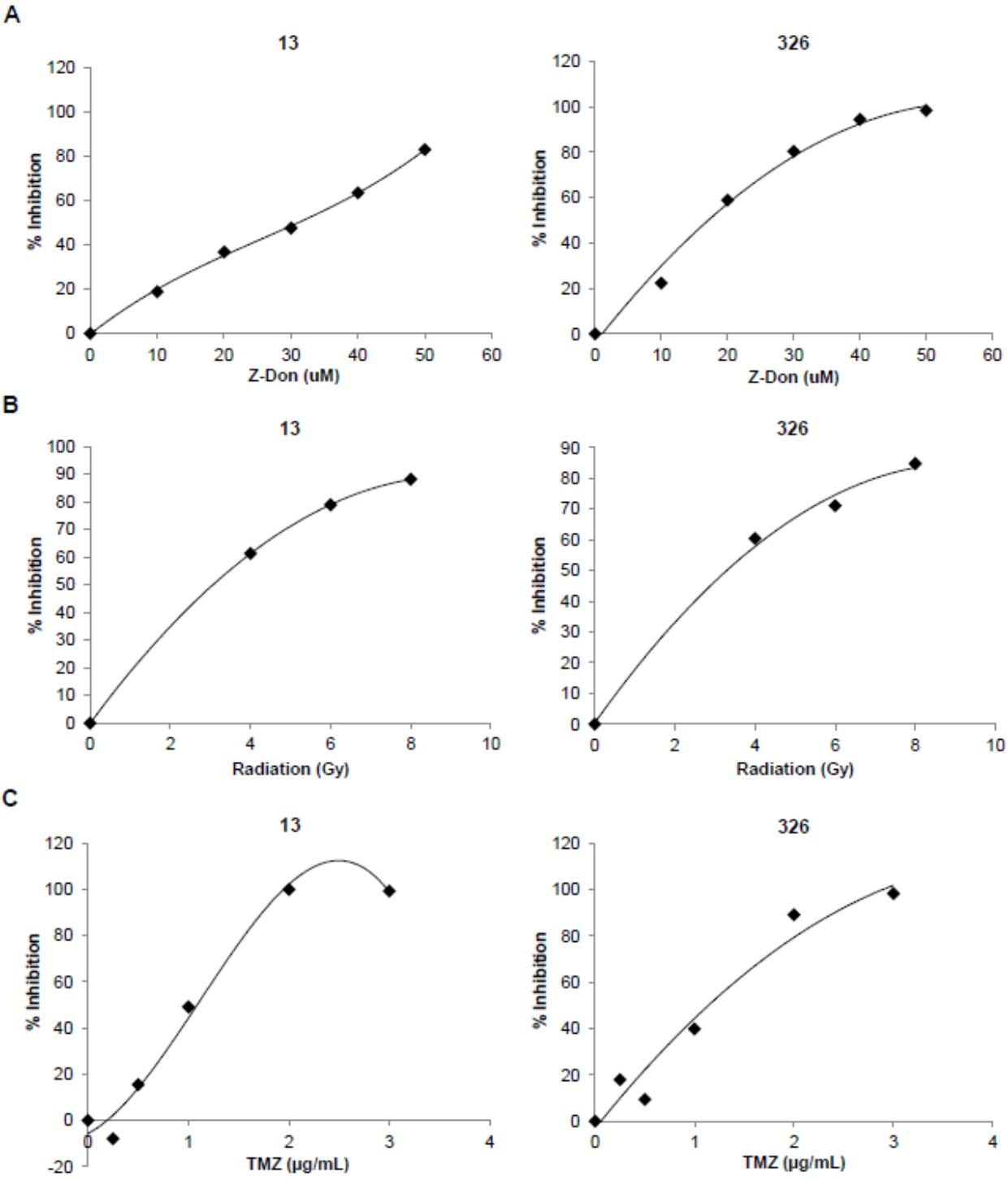
A
13
% Inhibition
Z-Don (uM)
326
% Inhibition
Z-Don (uM)
B
13
% Inhibition
Radiation (Gy)
326
% Inhibition
Radiation (Gy)
C
13
% Inhibition
TMZ (µg/mL)
326
% Inhibition
TMZ (µg/mL)

Figure 2.6. Combination therapies including the tTG inhibitor Z-Don inhibit MES GSC self-renewal and proliferation, and induce cell death.

(A-C) MES GSC cell lines 13 and 326 were dissociated into single cells, seeded at 5 x 10^3 cells/well in 12-well plates with or without Z-Don, and radiated after 2-4 hours.

(A) Neurosphere formation was counted after 72 hours. Each experiment was performed in triplicate, and the results were averaged and graphed. *p* values are represented as follows: ****, $p < 0.0001$.

(B) The cells were counted at the indicated time points to determine cell proliferation. Each experiment was performed in triplicate, and the results were averaged and graphed. *p* values are represented as follows: ****, $p < 0.0001$.

(C) The cells were collected after six days and stained with Trypan Blue Solution, and the viable and dead cells were counted. Each experiment was performed in triplicate, and the results were averaged and graphed. *p* values are represented as follows: ****, $p < 0.0001$.

Figure 2.6 continued.

(D-F) MES GSC cell lines 13 and 326 were dissociated into single cells, and seeded at 5 x 10^3 cells/well in 12-well plates with or without the indicated compounds.

(D) Neurosphere formation was counted after 72 hours. Each experiment was performed in triplicate, and the results were averaged and graphed. *p* values are represented as follows: *, $p < 0.05$; **, $p < 0.01$; ****, $p < 0.0001$.

(E) The cells were counted at the indicated time points to determine cell proliferation. Each experiment was performed in triplicate, and the results were averaged and graphed. *p* values are represented as follows: ****, $p < 0.0001$.

(F) The cells were collected after six days and stained with Trypan Blue Solution, and the viable and dead cells were counted. Each experiment was performed in triplicate, and the results were averaged and graphed. *p* values are represented as follows: ****, $p < 0.0001$.

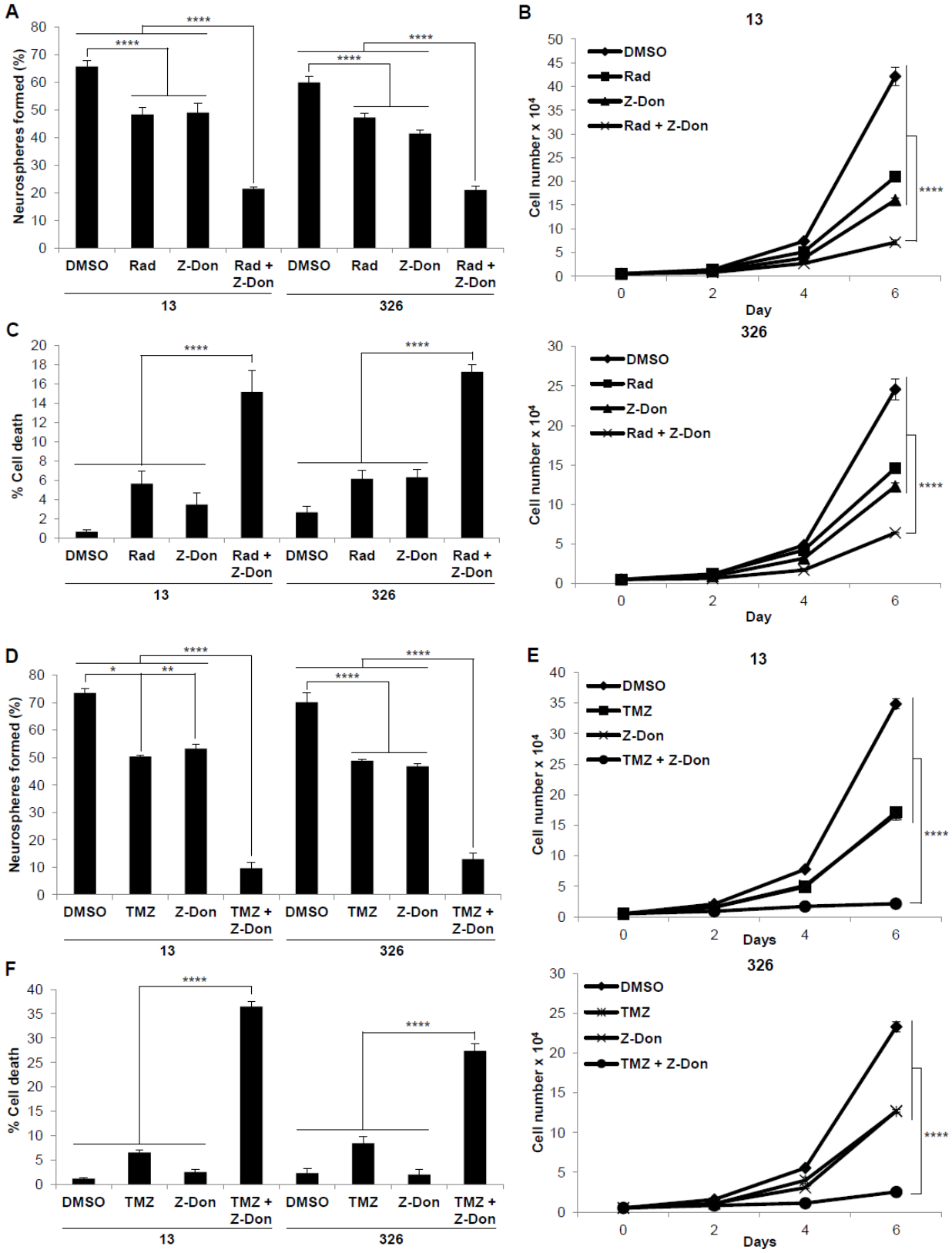
A
Neurospheres formed (%)
DMSO
Rad
Z-Don
Rad + Z-Don
13
326
B
13
Cell number x 10⁴
Day
C
% Cell death
D
TMZ
TMZ + Z-Don
E
Days
F

number of genes that appear to be regulated by ALDH1A1 and/or ALDH1A3, including *CDC42*, a gene containing RAREs (12). Here, we have investigated the role of ALDH1A3 in cancer progression using ALDH1A3^{+} and ALDH1A3^{-} GSCs as a model system. We show that ALDH1A3 regulates the expression of the RARE-containing gene, *TGM2*, in MES GSCs, through its enzymatic conversion of retinaldehyde to RA. Using ALDH1A3 knockdowns and an inhibitor of ALDH1 enzymatic activity, we have found that ALDH1A3 mediates the transcriptional regulation of *TGM2* in MES GSCs. Moreover, the over-expression of ALDH1A3 in PN GSCs is sufficient to induce tTG expression, whereas a catalytically inactive form of this enzyme (ALDH1A3(C314A)) is ineffective. Given that ALDH1A family isozymes each function as retinaldehyde dehydrogenases, this mechanism for the induction of tTG expression, as well as that of several other RA-regulated genes, may potentially be broadly expanded to include several other types of ALDH1^{+} CSCs and cancer cells (1, 17, 18).

Interestingly, the cellular concentration of RA appears to have a strong impact on the outcome of RA-induced gene expression. RA signaling plays a critical role during development, especially in the differentiation of stem cells into neural progenitors and neurons (40, 41). *In vitro* experiments aimed at inducing the differentiation of embryonic stem cells into neural progenitor cells typically involve RA concentrations ranging from 5 μM to 5 mM (42). However, in the case of MES GSCs, the endogenous RA concentration is likely much lower so as to promote the stemness of these cells, rather than inducing their differentiation. Indeed, our unpublished observations have suggested that a relatively low concentration of RA (0.5 μM) induces MES GSCs to become adherent rather than grow as neurospheres in suspension, suggesting that they are transitioning toward a more differentiated state. In treating PN GSCs with 0.5 μM RA, or when over-expressing the wild-type ALDH1A3, we have noted that some of

these cells also begin to attach to tissue culture flasks, as well as exhibit slower growth kinetics relative to their untreated counterparts (data not shown). These results suggest that ALDH1A3 and RA alone cannot induce the highly aggressive phenotype of MES GSCs, and likely work together with other tumor suppressors or oncogenes (e.g. the EGFRvIII) in MES GSCs to promote their rapid proliferation and tumorigenicity.

The observed sensitivity of PN and MES GSCs to low levels of RA suggests that the concentration of this compound must be carefully regulated in order to maintain the CSC phenotype. In part, this regulation is accomplished through a negative feedback loop that down-regulates the expression of ALDH1 isozymes. Thus, rather than being induced by RA, as genes with RAREs are, the transcription of ALDH1 genes is instead inhibited by RA, leading to an eventual reduction in the RA concentration (1). This feedback loop can be observed in Figure 2.1F, particularly in the MES GSC 326 cell line, in which ALDH1A3 transcript levels are decreased following treatment with RA. Therefore, it appears that nanomolar levels of RA are capable of promoting the CSC phenotype in MES GSCs, whereas higher concentrations of RA seem to induce the differentiation of these cells. Indeed, RA therapy is commonly used for the treatment of acute promyelocytic leukemia, leading to the differentiation of leukemic cells and often resulting in a complete remission (43-45). These results indicate that proteins in the RA signaling pathway, including ALDH1 isozymes and RAR/RXR heterodimers, have the potential to be further exploited in the treatment of various types of cancer.

In exploring the regulation of gene expression by ALDH1A3 in GSCs, we also sought to understand a potential role for tTG in these cells. Interestingly, tTG has been reported to play an important part in the differentiation of normal stem and progenitor cells during development, such as the differentiation of neural progenitors into neurons and osteoblasts into osteocytes (19,

46, 47). Notably, ALDH1 proteins are also expressed in many normal stem and progenitor cells, including neural stem cells and hematopoietic stem cells (48). Thus, the mechanism of tTG induction by ALDH1A3 that we have observed in MES GSCs may be a reflection of a normal stem cell process. However, critical differences in the gene expression profiles of MES GSCs versus normal stem cells likely determine the extent to which tTG promotes differentiation versus tumor progression. In the context of MES GSCs, the high degree of growth factor signaling (e.g. through the EGFRvIII or MET), in combination with stem cell factors such as WNT and BMI1, may overwhelm any differentiation-promoting effects of tTG (38, 49-51).

In addition to the well-established roles of tTG in development, our laboratory and others have previously demonstrated critical roles for tTG in various aspects of the cancer cell phenotype. These functions include the up-regulation of EGFR levels in glioblastoma through the binding of tTG to c-Cbl, the migration of HeLa cervical carcinoma cells and MDA-MB231 breast cancer cells through an interaction with Hsp70, and the docking of cancer cell-derived microvesicles onto recipient cells through the tTG-mediated cross-linking of fibronectin (27-29). Furthermore, Fu and colleagues demonstrated that tTG regulates the expression of inhibitor of DNA binding 1 (ID1) in $CD44^+$ GSCs, and is essential for their survival and proliferation, and recently, tTG was shown to be necessary for the survival, self-renewal, and migration of epidermal CSCs (32, 33). We thus anticipated a similar role for tTG in the highly aggressive phenotype of MES GSCs, and it was quite unexpected when we found that this was not the case, at least in any of the transformation assays that we performed. These results likely are due to the enhanced ability of MES GSCs to adapt to and overcome cellular stresses to which other cancer cells normally succumb. Moreover, tTG may work in parallel with other proteins and signaling pathways to promote the growth and survival of MES GSCs, and thus the loss of one component

may be compensated for by other proteins and signaling pathways. Indeed, the high degree of CSC resistance to conventional therapies suggests that these cells exhibit redundant pathways to maintain their stemness, proliferation, and survival.

Given what appears to be a dispensable role for tTG in the highly adaptive MES GSCs, therapeutically targeting these cells with tTG inhibitors would not seem to be a viable strategy. However, we report here that the use of tTG inhibitors significantly attenuates neurosphere formation, proliferation, and survival of MES GSCs, and this is attributed to the ability of these inhibitors to induce a cytotoxic, open state of tTG, in addition to inhibiting transamidation activity. The open-state conformation of tTG has been shown to inhibit cancer cell survival (23, 24, 29, 31). Although this conformation is naturally-occurring and required for the transglutaminase activity of tTG, the open and closed states are strictly regulated in cells by both guanine nucleotide and Ca^{2+} concentrations. The binding of GTP/GDP induces tTG to adopt a closed conformation, accompanied by GTPase activity, whereas the release of guanine nucleotide and high concentrations of Ca^{2+} allow tTG to adopt the more extended open conformation, leading to the exposure of the transamidation catalytic site. Based on the high cellular levels of GTP and the carefully regulated secretion of Ca^{2+}, it is likely that tTG primarily exists in the closed-state in cells (19, 20).

As noted, the tTG inhibitors MDC and Z-Don both shift tTG into the open-state conformation (34-36). With the balance between the open and closed states of tTG thus shifted, the impact of these inhibitors may be potentiated through a loss of GTP-binding activity and the associated binding partners of the closed-state tTG (e.g. c-Cbl, phospholipase C-δ1), as well as de-regulated transamidase activity and potentially alternative binding partners of the open-state (19, 29). Therefore, the genetic knockdown of tTG may not recapitulate the effects of the open-

state tTG, which may be thought of as a gain-of-function mutant. Indeed, our laboratory has previously shown that tTG mutants that cannot bind GTP and are thus forced to adopt an open conformation (e.g. tTG(R580K), tTG(R580L)) are selected against and rapidly induce cell death in NIH3T3 and HeLa cells. Furthermore, tTG double mutants that are both GTPase- and transamidase-defective show similar effects, suggesting that these mutants trigger cell death through aberrant protein-protein interactions, potentially by inhibiting proteins necessary for cell viability or promoting the activity of pro-apoptotic proteins (31). While binding partners that exclusively interact with the open-state tTG have yet to be determined, it seems plausible that MDC and Z-Don could be inducing inappropriate interactions between tTG and other proteins in MES GSCs, resulting in the observed inhibition of self-renewal and proliferation.

As such, targeting tTG with drugs that induce the open conformation may be a powerful method for eliminating tTG-expressing cancer cells, including $ALDH1^{+}$ GSCs. The synthetic lethality that we have observed with a combination therapy of Z-Don and TMZ, and the additive effects of Z-Don and radiation, further indicate that tTG inhibitors have the potential to halt the growth of HGG, and lead to the reduction and possible elimination of GSCs when used in combination with the standard of care for this disease. Moreover, these combination therapies may allow lower doses of TMZ and radiation to be used in HGG patients, potentially reducing the side effects commonly experienced with these treatments. Finally, our finding that tTG expression is significantly higher in $ALDH1^{high}$ versus $ALDH1^{low}$ cancer cells suggests that tTG may be a common target for therapeutic intervention across many different types of cancer. New combination therapies involving the use of tTG inhibitors that induce the tTG open-state may therefore show promise for the treatment of $ALDH1^{+}$ cancers, potentially leading to the elimination of CSCs and the prevention of tumor recurrence.

Materials and methods

Cell culture

GSCs were cultured as described previously (2). Briefly, the cells were maintained in DMEM/F12 supplemented with B-27 (2%), heparin (5 mg/mL), glutamine (4.5 mM), penicillin-streptomycin (100 U/mL), basic FGF (bFGF) (20 ng/mL), and EGF (20 ng/mL). Growth factors (bFGF and EGF) were added every 3-4 days. MES GSCs were dissociated into single cells via gentle pipetting, and PN GSCs were dissociated with TrypLE Express Enzyme and gentle pipetting. Where indicated, MES and PN GSCs were cultured in 0.5 μM RA, and MES GSCs were cultured in 100 μM diethylaminobenzaldehyde (DEAB). Unless otherwise noted, the MES GSC 13 cell line was treated with 50 μM monodansylcadaverine (MDC) and 40 μM Z-DON-Val-Pro-Leu-OMe (Z-Don), and the MES GSC 326 cell line was treated with 60 μM MDC and 30 μM Z-Don. HEK293T and A549 cells were maintained in DMEM containing 10% FBS; U87 and HeLa cells were cultured in RPMI containing 10% FBS; and MIA PaCa-2 cells were maintained in DMEM supplemented with 10% FBS and 2.5% HS. All cells were incubated in a humidified atmosphere with 5% CO_2 at 37°C.

Reagents and antibodies

DMEM/F12, DMEM, RPMI, TrypLE Express, trypsin, FBS, HS, N2, Trypan Blue Solution, and puromycin were purchased from Gibco; B-27, penicillin-streptomycin, and EGF were from Invitrogen; heparin, glutamine, DEAB, RA, MDC, dimethyl sulfoxide (DMSO), TMZ, and polybrene (hexadimethrine bromide) were from Sigma; bFGF was from Peprotech; polyethylenimine (PEI) was from Polysciences, Inc.; biotinylated pentylamine (BPA) was from Pierce; and Z-Don was from Zedira. The ALDEFLUOR kit was from STEMCELL

Technologies; QIAshredder and RNeasy Mini Kit were from Qiagen; Superscript III First-Strand Synthesis System was from Invitrogen; and iTaq Universal SYBR Green Supermix was from Bio-Rad. Primary antibodies used in this study were anti-ALDH1A3 (abcam), anti-tissue Transglutaminase II (Cocktail) (Neomarkers), anti-V5 (Invitrogen), anti-HA (Cell Signaling), anti-Vinculin (Sigma), and horseradish-peroxidase-conjugated streptavidin (Pierce).

Cloning and DNA constructs

ALDH1A3 was amplified from cDNA isolated from the MES GSC 1123 cells. The PCR product was then purified and ligated into the pcDNA3.1D/V5-His-TOPO vector (Invitrogen) according to the manufacturer's instructions. The V5-tagged ALDH1A3 was then cloned into a lentivirus overexpression construct (pCDH-CMV-MCS-EF1-Puro, System Biosciences). The ALDH1A3(C314A) construct was generated using the following primers: ALDH1A3(C314A) forward: AAGGCCAGTGTGCCACGGCAGCCT; ALDH1A3(C314A) reverse: AGGCTGCCGTGGCACACTGGCCTT. The tTG wild-type and tTG (C277S,R580L) constructs were previously cloned into the pSIN vector by Dr. Jingwen Zhang (formerly of Cornell University). The following shRNA constructs were purchased from Sigma: ALDH1A3 clone 1: TRCN0000027144; ALDH1A3 clone 2: TRCN0000027160; tTG clone 1: TRCN0000000239; tTG clone 2: TRCN0000272816.

Lentivirus generation and transduction

Viruses were generated by co-transfecting HEK293T cells with the lentiviral expression construct of interest and the packaging plasmids pMD-G and pCMV.d8.2, using PEI in DMEM containing 10% FBS. The cells were allowed to grow overnight, and the medium was changed to

serum-free DMEM the following day. The medium containing viral particles was then collected after 24 hours and 48 hours, combined, centrifuged at 1800 rpm for 5 minutes, then aliquoted and stored at -80°C. Viral transduction was carried out by dissociating GSCs into single cells, and incubating them with viral particles and polybrene (10 µg/mL). 24 hours later, the cells were washed and incubated in fresh GSC medium, and selected with puromycin (MES GSCS: 4 µg/mL; PN GSCS: 0.5 µg/mL).

RNA isolation and quantitative real-time PCR

Cells were washed 2 times in cold phosphate-buffered saline (PBS), and RNA was isolated using Qiagen QIAshredder columns and the Qiagen RNeasy Mini Kit according to the manufacturer's instructions. The Superscript III First-Strand Synthesis System was used to synthesize cDNA from equal amounts of RNA according to the manufacturer's instructions. For quantitative Real-Time PCR (qRT-PCR), each master mix contained cDNA, primers (0.3125 µM each), water, and iTaq Universal SYBR Green Supermix. Each master mix was divided into triplicate reactions containing 23 µL each. qRT-PCR was carried out using the 7500 Fast Real-Time PCR System (Applied Biosystems) with the following amplification program: 50°C for 2 minutes, 95°C for 10 minutes, and 40 cycles of 95°C for 15 seconds followed by 60°C for 1 minute. Dissociation curves were carried out to analyze amplicon quality, and GAPDH was used as an internal control. Primer sequences used in this study are: ALDH1A3 forward: TGGATCAACTGCTACAACGC; ALDH1A3 reverse: CACTTCTGTGTATTCGGCCA; tTG forward: CTTTGTCTTTGCGGAGGTC; tTG reverse: CAGTTTGTTCAGGTGGTTCG; GAPDH forward: GAAGGTGAAGGTCGGAGTCA; GAPDH reverse: TTGAGGTCAATGAAGGGGTC.

Western blot analysis

Cells were washed 2 times in cold PBS, then lysed in cell lysis buffer (50 mM HEPES, 200 mM NaCl, 25 mM NaF, 50 mM β-Glycerophosphate, 1 mM $MgCl_2$, 1% Triton X-100, 1 mM DTT, 1 mM Na_3VO_4, 1 µg/mL aprotinin, and 1 µg/mL leupeptin). The lysates were centrifuged at 13,000 rpm for 15 minutes at 4°C, and equal amounts of protein were diluted with Laemmli sample buffer, boiled, and subjected to SDS-PAGE. The proteins were transferred onto PVDF membranes, and the membranes were blocked with 5% nonfat dry milk in TBST (20 mM Tris, 137 mM NaCl, pH 7.4, 0.05% Tween-20). The membranes were incubated with the primary antibodies either overnight at 4°C or for 1 hour at room temperature, then washed 3 times with TBST. Anti-mouse and anti-rabbit secondary antibodies conjugated to HRP (Cell Signaling) were diluted in TBST and incubated with the membranes for 1 hour at room temperature. Membranes were washed 3 times in TBST, and visualized on x-ray film using Western Lightning *Plus*-ECL (PerkinElmer).

Transamidation assay

15 µg of cell lysates were incubated in a buffer containing 10 mM DTT, 10 mM $CaCl_2$, and 62.5 µM BPA for 15 minutes at room temperature. For assays analyzing the inhibition of tTG by Z-Don, cell lysates were incubated with Z-Don for 30 minutes prior to the addition of the transamidation buffer. For analysis of MDC inhibition of transamidation, cell lysates were incubated with 200 µM MDC. The reactions were quenched by the addition of Laemmli sample buffer, and the samples were boiled for 5 minutes. The proteins were separated by SDS-PAGE, transferred onto a PVDF membrane, and blocked overnight in BBST (100 mM boric acid, 20 mM sodium borate, 0.01% SDS, 0.15% Tween-20, 80 mM NaCl) containing 10% BSA. The

membranes were then incubated in BBST containing 5% BSA and 1:5000 HRP-conjugated streptavidin for 1 hour at 4°C, washed thoroughly in BBST, and visualized on x-ray film using Western Lightning *Plus*-ECL.

FACS analysis

For cell sorting based on ALDH1 activity, cells were collected, dissociated into single cells, and counted on a hemocytometer. They were then incubated with or without the ALDH1 inhibitor DEAB (150 μM), and stained using the ALDEFLUOR Kit according to the manufacturer's protocol. The cells were then sorted on a BD FACSAria (BD Biosciences), and those cells in the top 15 percent and bottom 15 percent of ALDH1 activity were collected for RNA isolation and qRT-PCR, as described above.

Neurosphere forming assay

MES GSCs were dissociated into single cells, and seeded at 5×10^3 cells/well in 12-well plates. Spheres were counted after 3 days on an inverted microscope. MES GSC aggregates containing > 4 cells were defined as neurospheres.

Proliferation assay

MES GSCs were dissociated into single cells, and 12-well plates were seeded with 5×10^3 cells/well. After 3 days, each well was supplemented with 2 mL GSC medium containing growth factors and inhibitors. Viable cells were quantified after 2, 4, and 6 days by staining with Trypan Blue Solution and counting cells on a hemocytometer. Those cells that excluded the dye were considered viable cells.

Cell viability assay

For assays carried out in supplement-free medium, MES GSCs were seeded at 2 x 10^4 cells/well in 12-well plates in either GSC medium or DMEM/F12, with or without inhibitors. 48 hours later, the cells were collected, stained with Trypan Blue Solution, and the viable and dead cells were counted on a hemocytometer. ≥ 200 cells were counted for each sample. For assays carried out in complete GSC medium with a combination of Z-Don and TMZ or radiation, the cells were seeded at 5 x 10^3 cells/well in 12-well plates, and treated with IC_{50} doses for each treatment (MES GSC 13 cell line: 30 µM Z-Don, 1 µg/mL TMZ, 3 Gy; MES GSC 326 cell line: 20 µM Z-Don, 1 µg/mL TMZ, and 3 Gy). Radiation was carried out 2-4 hours after seeding the cells. Fresh medium containing growth factors and inhibitors was added to each well after 3 days. After 6 days, the viable and dead cells were counted as described above.

Statistical analysis

Each experiment was carried out a minimum of three times. For data presented as bar or line graphs, error bars represent the standard error of the mean (SEM). Statistical significance was calculated in Excel using F-tests for sample variance and Student's t tests for significance. *p* values < 0.05 were considered statistically significant, and were indicated with asterisks.

Acknowledgments

We gratefully acknowledge Dr. Ichiro Nakano (Ohio State University, Columbus, Ohio) for providing the glioma stem cells used in this work, as well as Figure 2.1C and helpful discussions. We also acknowledge Dr. Jingwen Zhang (formerly of Cornell University, Ithaca, NY) for providing the tTG lentiviral vectors, and Christian Abratte and Rob Munroe for radiating cells.

We gratefully acknowledge Cindy Westmiller for expert secretarial assistance, and Dorian LaTocha (Cornell Biomedical Sciences Flow Cytometry Core Lab, Cornell University, Ithaca, NY) for flow cytometry operation. Cytometry core supported in part by the ESSCF, NYS-DOH, Contract #C026718. Opinions expressed are solely of the author; they do not necessarily reflect the view of ESSCB, the NYS-DOH, or NYS.

REFERENCES

1. Ma I, Allan AL. The role of human aldehyde dehydrogenase in normal and cancer stem cells. Stem Cell Reviews and Reports 2011;7(2):292-306.

2. Mao P, Joshi K, Li J, et al. Mesenchymal glioma stem cells are maintained by activated glycolytic metabolism involving aldehyde dehydrogenase 1A3. Proc Natl Acad Sci U S A 2013;110(21):8644-9.

3. Clay MR, Tabor M, Owen JH, et al. Single-marker identification of head and neck squamous cell carcinoma cancer stem cells with aldehyde dehydrogenase. Head Neck 2010;32(9):1195-201.

4. Marcato P, Dean CA, Pan D, et al. Aldehyde dehydrogenase activity of breast cancer stem cells is primarily due to isoform ALDH1A3 and its expression is predictive of metastasis. Stem Cells 2011;29(1):32-45.

5. Lingala S, Cui Y, Chen X, et al. Immunohistochemical staining of cancer stem cell markers in hepatocellular carcinoma. Exp Mol Pathol 2010;89(1):27-35.

6. Shao C, Sullivan JP, Girard L, et al. Essential role of aldehyde dehydrogenase 1A3 for the maintenance of non-small cell lung cancer stem cells is associated with the STAT3 pathway. Clin Cancer Res 2014;20(15):4154-66.

7. Saw YT, Yang J, Ng SK, et al. Characterization of aldehyde dehydrogenase isozymes in ovarian cancer tissues and sphere cultures. BMC Cancer 2012;12:329.

8. Rasheed ZA, Yang J, Wang Q, et al. Prognostic significance of tumorigenic cells with mesenchymal features in pancreatic adenocarcinoma. J Natl Cancer Inst 2010;102(5):340-51.

9. van den Hoogen C, van der Horst G, Cheung H, et al. High aldehyde dehydrogenase activity identifies tumor-initiating and metastasis-initiating cells in human prostate cancer. Cancer Res 2010;70(12):5163-73.

10. Huang EH, Hynes MJ, Zhang T, et al. Aldehyde dehydrogenase 1 is a marker for normal and malignant human colonic stem cells (SC) and tracks SC overpopulation during colon tumorigenesis. Cancer Res 2009;69(8):3382-9.

11. Keymoosi H, Gheytanchi E, Asgari M, Shariftabrizi A, Madjd Z. ALDH1 in combination with CD44 as putative cancer stem cell markers are correlated with poor prognosis in urothelial carcinoma of the urinary bladder. Asian Pac J Cancer Prev 2014;15:2013-20.

12. Luo Y, Dallaglio K, Chen Y, et al. ALDH1A isozymes are markers of human melanoma stem cells and potential therapeutic targets. Stem Cells 2012;30(10):2100-13.

13. Smith C, Gasparetto M, Humphries K, Pollyea DA, Vasiliou V, Jordan CT. Aldehyde dehydrogenases in acute myeloid leukemia. Ann N Y Acad Sci 2014;1310(1):58-68.

14. Dean M, Fojo T, Bates S. Tumour stem cells and drug resistance. Nature Reviews Cancer 2005;5(4):275-84.

15. Baumann M, Krause M, Hill R. Exploring the role of cancer stem cells in radioresistance. Nature Reviews Cancer 2008;8(7):545-54.

16. Bayin NS, Modrek AS, Placantonakis DG. Glioblastoma stem cells: Molecular characteristics and therapeutic implications. World journal of stem cells 2014;6(2):230.

17. Vasiliou V, Thompson DC, Smith C, Fujita M, Chen Y. Aldehyde dehydrogenases: From eye crystallins to metabolic disease and cancer stem cells. Chem Biol Interact 2013;202(1):2-10.

18. Marletaz F, Holland LZ, Laudet V, Schubert M. Retinoic acid signaling and the evolution of chordates. Int J Biol Sci 2006;2(2):38-47.

19. Eckert RL, Kaartinen MT, Nurminskaya M, et al. Transglutaminase regulation of cell function. Physiol Rev 2014;94(2):383-417.

20. Gundemir S, Colak G, Tucholski J, Johnson GV. Transglutaminase 2: A molecular swiss army knife. Biochimica et Biophysica Acta (BBA)-Molecular Cell Research 2012;1823(2):406-19.

21. Bastien J, Rochette-Egly C. Nuclear retinoid receptors and the transcription of retinoid-target genes. Gene 2004;328:1-16.

22. Soprano DR, Qin P, Soprano KJ. Retinoic acid receptors and cancers. Annu Rev Nutr 2004;24:201-21.

23. Antonyak MA, Singh US, Lee DA, et al. Effects of tissue transglutaminase on retinoic acid-induced cellular differentiation and protection against apoptosis. J Biol Chem 2001;276(36):33582-7.

24. Antonyak MA, Miller AM, Jansen JM, et al. Augmentation of tissue transglutaminase expression and activation by epidermal growth factor inhibit doxorubicin-induced apoptosis in human breast cancer cells. J Biol Chem 2004;279(40):41461-7.

25. Antonyak MA, Li B, Regan AD, Feng Q, Dusaban SS, Cerione RA. Tissue transglutaminase is an essential participant in the epidermal growth factor-stimulated signaling pathway leading to cancer cell migration and invasion. J Biol Chem 2009;284(27):17914-25.

26. Li B, Antonyak MA, Druso JE, Cheng L, Nikitin AY, Cerione RA. EGF potentiated oncogenesis requires a tissue transglutaminase-dependent signaling pathway leading to src activation. Proc Natl Acad Sci U S A 2010;107(4):1408-13.

27. Boroughs LK, Antonyak MA, Johnson JL, Cerione RA. A unique role for heat shock protein 70 and its binding partner tissue transglutaminase in cancer cell migration. J Biol Chem 2011;286(43):37094-107.

28. Antonyak MA, Li B, Boroughs LK, et al. Cancer cell-derived microvesicles induce transformation by transferring tissue transglutaminase and fibronectin to recipient cells. Proc Natl Acad Sci U S A 2011;108(12):4852-7.

29. Zhang J, Antonyak MA, Singh G, Cerione RA. A mechanism for the upregulation of EGF receptor levels in glioblastomas. Cell reports 2013;3(6):2008-20.

30. Liu S, Cerione RA, Clardy J. Structural basis for the guanine nucleotide-binding activity of tissue transglutaminase and its regulation of transamidation activity. Proc Natl Acad Sci U S A 2002;99(5):2743-7.

31. Datta S, Antonyak MA, Cerione RA. GTP-binding-defective forms of tissue transglutaminase trigger cell death. Biochemistry (N Y) 2007;46(51):14819-29.

32. Fu J, Yang QY, Sai K, et al. TGM2 inhibition attenuates ID1 expression in CD44-high glioma-initiating cells. Neuro Oncol 2013;15(10):1353-65.

33. Fisher ML, Keillor JW, Xu W, Eckert RL, Kerr C. Transglutaminase is required for epidermal squamous cell carcinoma stem cell survival. Mol Cancer Res 2015.

34. Badarau E, Collighan RJ, Griffin M. Recent advances in the development of tissue transglutaminase (TG2) inhibitors. Amino Acids 2013;44(1):119-27.

35. Lindemann I, Boettcher J, Oertel K, Weber J, Hils M, Pasternack R, et al. Transglutaminase 2 in complex with a novel inhibitor. PDB code: 3S3P 2012.

36. Schaertl S, Prime M, Wityak J, et al. A profiling platform for the characterization of transglutaminase 2 (TG2) inhibitors. J Biomol Screen 2010;15(5):478-87.

37. Rich JN. Cancer stem cells in radiation resistance. Cancer Res 2007;67(19):8980-4.

38. Reya T, Morrison SJ, Clarke MF, Weissman IL. Stem cells, cancer, and cancer stem cells. Nature 2001;414(6859):105-11.

39. Visvader JE, Lindeman GJ. Cancer stem cells in solid tumours: Accumulating evidence and unresolved questions. Nature Reviews Cancer 2008;8(10):755-68.

40. Maden M. Retinoid signalling in the development of the central nervous system. Nature Reviews Neuroscience 2002;3(11):843-53.

41. Maden M. Retinoic acid in the development, regeneration and maintenance of the nervous system. Nature Reviews Neuroscience 2007;8(10):755-65.

42. Chuang J, Tung L, Lin Y. Neural differentiation from embryonic stem cells in vitro: An overview of the signaling pathways. World journal of stem cells 2015;7(2):437.

43. Altucci L, Gronemeyer H. The promise of retinoids to fight against cancer. Nature Reviews Cancer 2001;1(3):181-93.

44. Brown G, Hughes P. Retinoid differentiation therapy for common types of acute myeloid leukemia. Leukemia research and treatment 2012;2012.

45. Lengfelder E, Saussele S, Weisser A, Büchner T, Hehlmann R. Treatment concepts of acute promyelocytic leukemia. Crit Rev Oncol 2005;56(2):261-74.

46. Tucholski J, Lesort M, Johnson G. Tissue transglutaminase is essential for neurite outgrowth in human neuroblastoma SH-SY5Y cells. Neuroscience 2001;102(2):481-91.

47. Singh US, Pan J, Kao YL, Joshi S, Young KL, Baker KM. Tissue transglutaminase mediates activation of RhoA and MAP kinase pathways during retinoic acid-induced neuronal differentiation of SH-SY5Y cells. J Biol Chem 2003;278(1):391-9.

48. Muzio G, Maggiora M, Paiuzzi E, Oraldi M, Canuto R. Aldehyde dehydrogenases and cell proliferation. Free Radical Biology and Medicine 2012;52(4):735-46.

49. Mimeault M, Batra SK. Complex oncogenic signaling networks regulate brain Tumor-Initiating cells and their progenies: Pivotal roles of Wild-Type EGFR, EGFRvIII mutant and hedgehog cascades and novel multitargeted therapies. Brain Pathology 2011;21(5):479-500.

50. Vescovi AL, Galli R, Reynolds BA. Brain tumour stem cells. Nature Reviews Cancer 2006;6(6):425-36.

51. Pardal R, Clarke MF, Morrison SJ. Applying the principles of stem-cell biology to cancer. Nature Reviews Cancer 2003;3(12):895-902.

CHAPTER 3

A comparative analysis of two glutaminase isoforms in cancer cell metabolism

Abstract

The rapid proliferation observed in many tumors and cancer cell lines is highly dependent on their ability to take up nutrients and incorporate them into macromolecules and biomass. To support their high rates of proliferation, cancer cells undergo key changes in their metabolic wiring to promote the biosynthesis of nucleic acids, proteins, and lipids. In contrast to the metabolic profile of quiescent cells, characterized by the oxidation of glucose for the production of ATP, oncogenic transformation often leads to the up-regulation of signaling activities through growth factor receptors and the PI3K/Akt pathway, resulting in an alternative metabolic phenotype referred to as "the Warburg effect." This metabolic reprogramming promotes the utilization of glycolytic and tricarboxylic acid (TCA) cycle intermediates for the production of nucleotides, amino acids, and fatty acids, but can lead to the depletion of these critical metabolites without another carbon source to replenish them. For this reason, cancer cells up-regulate glutamine metabolism to help drive the TCA cycle, notably through the increased expression and activation of mitochondrial glutaminase (GLS). While our laboratory has previously suggested that the GLS isoform glutaminase C (GAC) serves a critical role in catalyzing glutamine metabolism in cancer cells, it remains unknown whether the other major splice variant of GLS, referred to as kidney-type glutaminase (KGA), contributes to cancer cell metabolism. Understanding the specific contributions of each isoform will be critical for designing therapeutic strategies for targeting glutamine metabolism in cancer cells. Here, we show that GAC and KGA appear to have redundant roles in glutamine metabolism and

transformation, with their relative contributions to cancer cell proliferation being primarily dependent on their expression levels.

Introduction

Cancer cells are highly dependent on elevated levels of the biosynthetic precursors of proteins, lipids, and nucleic acids to support their rapid growth and proliferation. The accumulation of biomass is critical for cellular growth, and is accomplished primarily through the rewiring of metabolic pathways to induce a more proliferative phenotype (1, 2). Genetic aberrations leading to the over-expression of growth factor receptors (e.g. the epidermal growth factor receptor (EGFR)), or to mutations in key signaling proteins such as KRas, often result in broad transcriptional changes that lead to the reprogramming of several key metabolic pathways, including glycolysis and the tricarboxylic acid (TCA) cycle. The corresponding shift from a resting state metabolic phenotype, characterized predominantly by the oxidation of glucose via glycolysis and the TCA cycle for the production of ATP, to a state in which enhanced levels of glucose are taken up and excreted in the form of lactate, has become widely recognized as a hallmark of cancer, and is commonly referred to as aerobic glycolysis or "the Warburg effect" (3, 4). Although glycolysis is a highly inefficient means of producing ATP as compared with oxidative phosphorylation in the mitochondrial electron transport chain, several key changes manifested in the Warburg effect are now understood to be critical for the rapid growth of cancer cells (1). Among these is the diversion of glycolytic and TCA cycle intermediates into nucleotide, amino acid, and fatty acid biosynthetic pathways to generate the necessary macromolecules for cell growth and division. However, the depletion of these critical

intermediates, particularly in the mitochondria, would swiftly bring the TCA cycle to a halt without an anaplerotic source of carbon and nitrogen to replenish them (1-4).

In response to the demanding biosynthetic requirements imposed by the Warburg effect, cancer cells adapt by up-regulating pathways involved in glutamine metabolism (4-6). Activation of the transcription factor Myc and signaling through the Rho GTPases lead to increased expression of glutamine transporters and glutaminase (GLS), which catalyzes the conversion of glutamine to glutamate in the mitochondria (7, 8). The subsequent conversion of glutamate to the TCA cycle intermediate α-ketoglutarate (αKG) by glutamate dehydrogenase (GDH) or aminotransferases provides a direct feed-in to this pathway, and ensures its continued cycling. This metabolic rewiring often results in a significantly elevated demand for glutamine, and has led to the classification of many cancer cell lines as "glutamine-addicted" (5, 6). For this reason, GLS has gained a great deal of attention for its role as a gateway enzyme in glutamine metabolism, and is a potential therapeutic target in a wide variety of cancer cells (9-11).

Studies from our laboratory of a small molecule inhibitor, referred to as compound 968, led to the discovery that GLS activity is up-regulated via Rho GTPase-dependent signaling events, and is necessary for the proliferation of several cancer cell lines (8, 10). Recent studies have further delineated the signaling pathway downstream of the Rho GTPases that leads to enhanced GLS expression in breast cancer cell lines, identifying the transcription factor c-Jun as a direct activator of *GLS* transcription (MJ Lukey, et al., submitted). However, these studies have focused primarily on an isoform of GLS known as glutaminase C (GAC), without addressing the role of the other major GLS splice variant, known as kidney-type glutaminase (KGA), in cancer cell metabolism. Understanding the potential differences in the regulation and activity of these isoforms will be especially important when designing therapeutic strategies for inhibiting

glutamine metabolism in cancer cells. Additionally, several key investigations have uncovered a major role of alternative splicing in promoting the Warburg effect, such as through the selective expression of the phosphofructokinase 2 isoform FB3 (PFKFB3) and pyruvate kinase M2 (PKM2), in cancer cells (12, 13). Moreover, the GLS isozyme encoded by *GLS2* has been suggested to function as a tumor suppressor (14, 15). Thus, we became interested in understanding whether KGA promotes cancer cell growth, like GAC, or if it antagonizes transformation, similar to GLS2. As such, we have undertaken a comparative analysis of these two GLS isoforms in cancer cells in order to more fully understand the specific contributions of each enzyme in mediating the Warburg effect and Rho GTPase-driven transformation. We have determined that GAC is the predominant GLS isoform expressed in a variety of cancer cell lines, despite its exhibiting indistinguishable enzyme activity and transforming capabilities from KGA. Thus, the two major isoforms of GLS appear to play redundant roles in glutamine metabolism, and their relative contributions to the cancer cell metabolic phenotype are likely determined by their relative expression levels.

Results

GAC is the predominant GLS isoform expressed in cancer cells

To understand the relative roles of GAC and KGA in cancer cell metabolism, we began by carrying out a comparative sequence analysis of these two isoforms. Alternative splicing of the *GLS* gene product results in two highly similar transcripts that encode KGA and GAC; each mRNA is composed of exons 1-14, but contains a unique 3' tail including either exons 16-19 (KGA) or exon 15 (GAC) (16-18). The enzymes encoded by these transcripts exhibit approximately 80-90% sequence identity, with the first 550 amino acids being identical in KGA

and GAC. Each isoform contains a 16-amino acid N-terminal mitochondrial targeting sequence, and the resulting localization to the mitochondria leads to the cleavage of the first 72 amino acids of each protein (19, 20). The mature form of each enzyme is comprised of an N-terminus, a conserved enzymatic active site (glutaminase domain) that is responsible for the catalytic conversion of glutamine to glutamate, and a distinct C-terminus that distinguishes KGA from GAC. Although the C-terminus of GAC does not contain any notable sequence motifs, the C-terminus of KGA includes an ankyrin repeat domain that may regulate protein-protein interactions (Figure 3.1A) (21). The discrete C-termini of these two isoforms led us to hypothesize that they may result in distinct modes of regulation for these enzymes in cancer cells, and that perhaps one isoform was better suited to support glutamine metabolism and TCA cycle anaplerosis.

To determine if either isoform was preferentially expressed by cancer cells, we carried out a Western blot analysis of a panel of cancer cell lines comprised of breast cancer cells (SKBR3, MDA-MB468, BT474), cervical carcinoma cells (HeLa), glioblastoma and glioma stem cells (U87, GSC 83, GSC 1123), pancreatic carcinoma cells (MIA PaCa-2), and transformed human embryonic kidney cells (HEK293T). Using a GLS antibody that recognizes an epitope common to GAC and KGA, we compared the relative expression levels of these two isoforms. A majority of the cancer cells were found to express significantly higher levels of GAC than KGA, with only one cell line (BT474) showing appreciable levels of KGA expression (Figure 3.1B). These results suggested that GAC may be more effective at supporting glutamine metabolism in cancer cells, or that KGA may oppose this metabolic phenotype.

Figure 3.1. Two splice variants are encoded by *GLS*.

(A) Two splice variants of glutaminase, referred to as kidney-type glutaminase (KGA) and glutaminase C (GAC), are encoded by *GLS*. Each transcript includes exons 1-14 and a 3' terminus comprised of either exons 16-19 (KGA) or exon 15 (GAC). The resulting enzymes encoded by these transcripts are identical for amino acid residues 1-550, and are distinguished by their unique C-terminal tails. KGA and GAC each contain an N-terminal mitochondrial targeting sequence (MTS), and the 72 amino acid N-terminus (NT) is cleaved upon localization to the mitochondria. The mature form of each isoform contains a conserved glutaminase domain and distinct C-terminal tail, with that of KGA including an ankyrin repeat domain (ANK).

(B) A panel of cancer cell lines was examined for GAC and KGA expression by Western blot analysis with GLS and Vinculin antibodies.

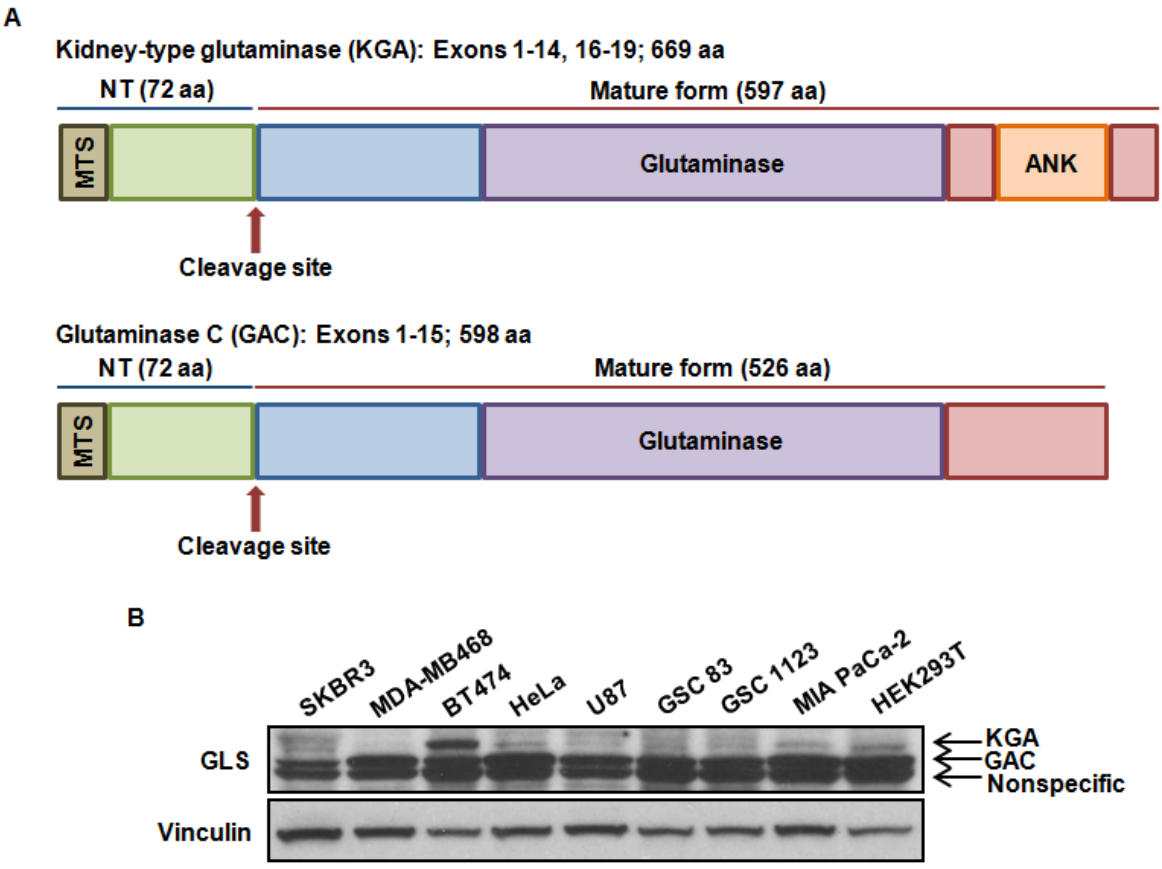
A
Kidney-type glutaminase (KGA): Exons 1-14, 16-19; 669 aa
NT (72 aa)
Mature form (597 aa)
MTS
Glutaminase
ANK
Cleavage site
Glutaminase C (GAC): Exons 1-15; 598 aa
NT (72 aa)
Mature form (526 aa)
MTS
Glutaminase
Cleavage site
B
SKBR3
MDA-MB468
BT474
HeLa
U87
GSC 83
GSC 1123
MIA PaCa-2
HEK293T
GLS
Vinculin
KGA
GAC
Nonspecific

GAC and KGA exhibit comparable enzymatic activity and transforming capabilities

To better understand why GAC is expressed at higher levels than KGA in cancer cells, we next examined the enzymatic activity of each isoform in MDA-MB231 breast cancer cells and HEK293T cells. To do so, we generated constructs encoding a V5-tagged form of either GAC or KGA, and ectopically expressed them in the aforementioned cell lines. The whole cell lysates were collected 48 hours post-transfection, immunoprecipitated with a V5 antibody, and analyzed by Western blot analysis (Figure 3.2A). The immunoprecipitates were also subjected to glutaminase activity assays, which were carried out in the presence or absence of inorganic phosphate, an *in vitro* allosteric activator of GLS, in order to compare the "basal" activity of each isoform (i.e. without the addition of phosphate) to that of the fully activated enzyme (following phosphate addition) (22). As expected, we observed that phosphate caused a significant increase in GAC and KGA activity. However, there was no significant difference in the basal activity of GAC and KGA in either cell line, or in the percent activation of each isoform (Figure 3.2B, C).

We next examined whether KGA can contribute to the transformation of NIH 3T3 fibroblasts. This phenotype is read out through focus formation assays, in which transformation is manifested by the loss of cell-cell contact inhibition, and the acquired propensity of fibroblasts to form foci that can be visualized with crystal violet. Although GAC is unable to induce the transformation of fibroblasts on its own, the co-expression of GAC with an activated Rho GTPase (e.g. Cdc42(F28L)) leads to the robust transformation of these cells (8). Likewise, we found that neither GAC nor KGA is sufficient to induce the transformation of fibroblasts, whereas oncogenic Dbl, a de-regulated guanine nucleotide exchange factor (GEF) and activator of the Rho GTPases, is highly transforming in these cells (Figure 3.3A, top panel) (23). However, the co-expression of either GAC or KGA with suboptimal levels of Dbl results in a

Figure 3.2. GAC and KGA exhibit comparable glutaminase activity.

(A) MDA-MB231 and HEK293T cells were either mock transfected, or transfected with V5-tagged GAC or V5-tagged KGA constructs. Whole cell lysates were collected 48 hours post-transfection, and immunoprecipitated with a V5 antibody as described in "Materials and Methods." The whole cell lysates and 10% of the immunoprecipitated proteins were then subjected to Western blot analysis with V5 and Vinculin antibodies. WCL, whole cell lysate; IP, immunoprecipitation.

(B) MDA-MB231 and HEK293T immunoprecipitates from A were analyzed for their glutaminase activity. Assays were carried out with or without the addition of inorganic phosphate (Pi). The results of three independent experiments were averaged and graphed with the activity of "V5-GAC + Pi" normalized to 1, and statistical significance was determined. *, $p < 0.05$; **, $p < 0.01$.

(C) The results of the glutaminase activity assay in B were plotted with basal activity represented as a percentage of phosphate-stimulated activity, and statistical significance was determined. ns, not significant.

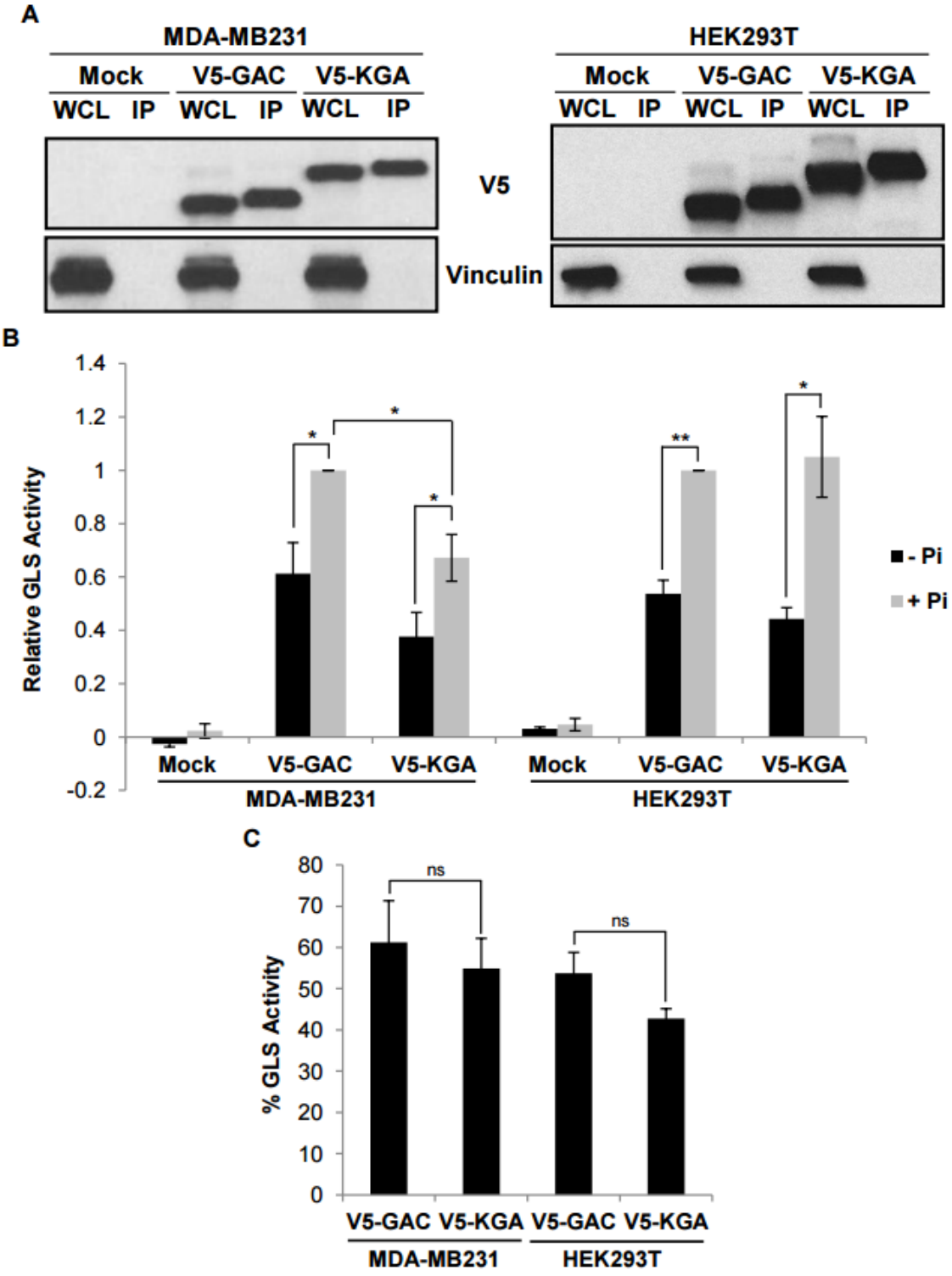
A
MDA-MB231
HEK293T
Mock
V5-GAC
V5-KGA
WCL IP WCL IP WCL IP
V5
Vinculin
B
Relative GLS Activity
1.4
1.2
1
0.8
0.6
0.4
0.2
0
-0.2
*
*
*
**
*
Mock V5-GAC V5-KGA Mock V5-GAC V5-KGA
MDA-MB231
HEK293T
- Pi
+ Pi
C
% GLS Activity
80
70
60
50
40
30
20
10
0
ns
ns
V5-GAC V5-KGA V5-GAC V5-KGA
MDA-MB231
HEK293T

Figure 3.3. GAC and KGA synergize with oncogenic Dbl to induce transformation.

(A) GAC and KGA were analyzed for their ability to synergize with Dbl and transform NIH 3T3 fibroblasts using the focus formation assay, as outlined in "Materials and Methods." Briefly, NIH 3T3 cells were either mock transfected, transfected with 1 µg Dbl, V5-GAC, or V5-KGA, or transfected with a combination of 1 µg V5-GAC or V5-KGA together with the indicated amounts of Dbl. The cells were cultured in DMEM + 5% CS and allowed to grow for 12-14 days, followed by fixing with 3.7% formaldehyde and staining with 0.4% crystal violet.

(B) Focus formation assays were conducted as in A, and NIH 3T3 cells were treated with either DMSO or 10 µM 968 where indicated.

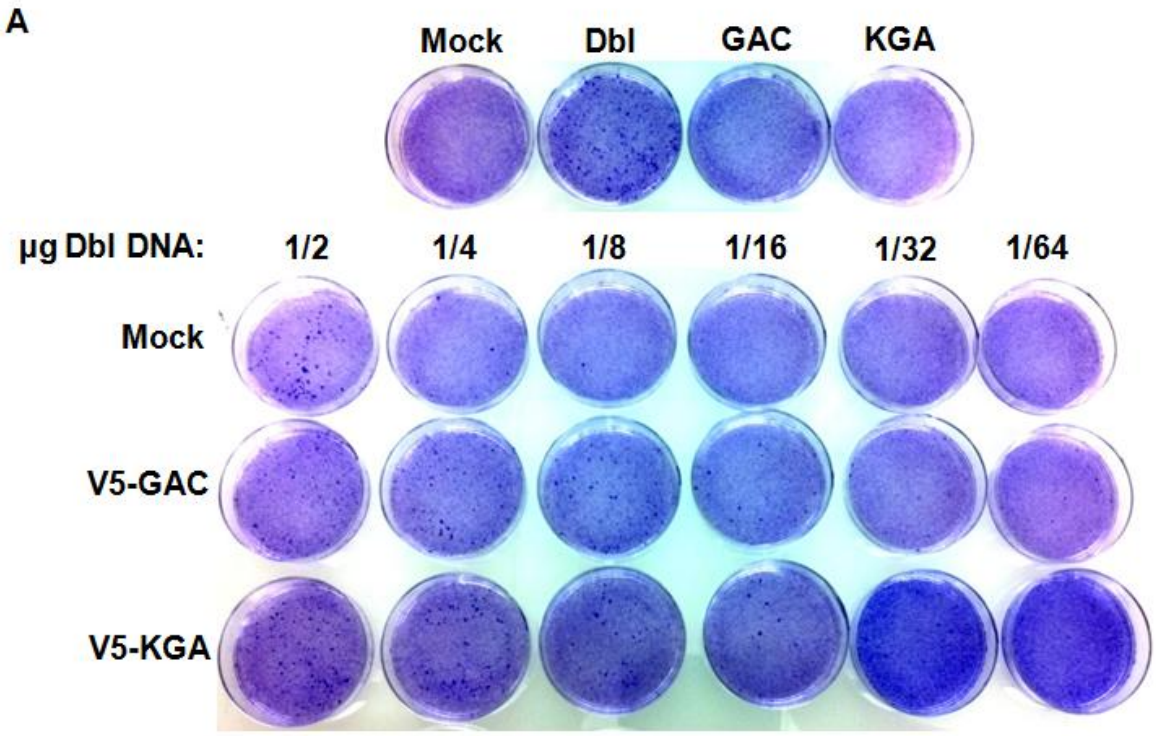
A
Mock
Dbl
GAC
KGA
µg Dbl DNA:
1/2
1/4
1/8
1/16
1/32
1/64
Mock
V5-GAC
V5-KGA

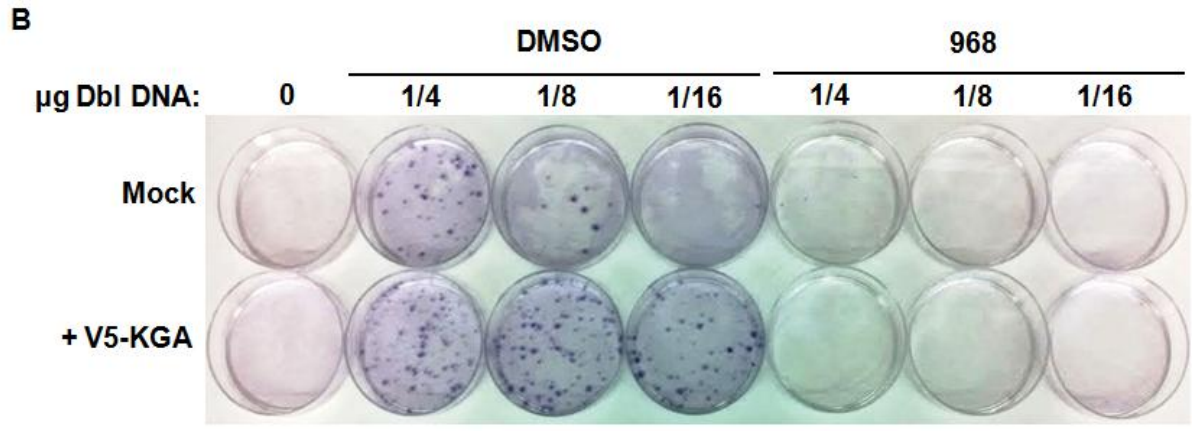
B
DMSO
968
µg Dbl DNA:
0
1/4
1/8
1/16
1/4
1/8
1/16
Mock
+ V5-KGA

synergistic induction of focus formation (Figure 3.3A, bottom panel). This marked synergy is especially apparent at the lowest levels of Dbl expression, where Dbl is unable to induce focus formation, but leads to robust transformation when co-expressed with either GAC or KGA. In addition to the synergy we have observed between Dbl and either GAC or KGA, we have found that Dbl- and KGA-induced focus formation can be inhibited by the small molecule GLS inhibitor 968, as we have previously shown for GAC (Figure 3.3B) (8). This suggests that KGA plays a role in transformation analogous to that of GAC, most likely by supporting glutamine metabolism and TCA cycle anaplerosis. Together, the comparable enzymatic activity and abilities of GAC and KGA to synergize with oncogenic Dbl suggest that both GLS isoforms are capable of contributing to cellular transformation and glutamine metabolism in cancer cells.

The roles of GAC and KGA in proliferation and anchorage-independent growth depend on their relative expression levels

Given that GAC and KGA exhibit similar enzymatic activity and transforming capabilities, we investigated their relative roles in the proliferation of cancer cells. To do so, we knocked down their expression in MDA-MB231 and MIA PaCa-2 cells using siRNAs that either target both GLS isoforms, or specifically target GAC or KGA (Figure 3.4A). For Western blotting analyses, we used antibodies that specifically recognize either GAC or KGA so as to better detect the knockdown levels of each isoform. However, the relative abundance of GAC versus KGA cannot be compared using these antibodies. 48 hours post-transfection, the cells were seeded for proliferation assays, and counted after four days of growth. We observed that the total GLS knockdowns led to a reduction in proliferation in both cell lines, whereas the individual knockdowns of GAC or KGA were somewhat harder to interpret (Figure 3.4B).

Figure 3.4. Glutaminase contributes to the proliferation of cancer cells.

(A) MDA-MB231 and MIA PaCa-2 cells were transfected with either a negative control siRNA (siScr), siRNAs targeted toward both GLS isoforms, or siRNAs specifically targeting either GAC or KGA. 48 hours post-transfection, whole cell lysates were collected and analyzed by Western blot analysis with GAC, KGA, and Vinculin antibodies.

(B) The MDA-MB231 and MIA PaCa-2 cells described in A were seeded in 6-well plates at a density of 2.5×10^4 cells/well in complete growth medium. The medium was replenished after 2 days, and the cells were counted after 4 days. Each experiment was performed in triplicate, and the results were averaged and graphed.

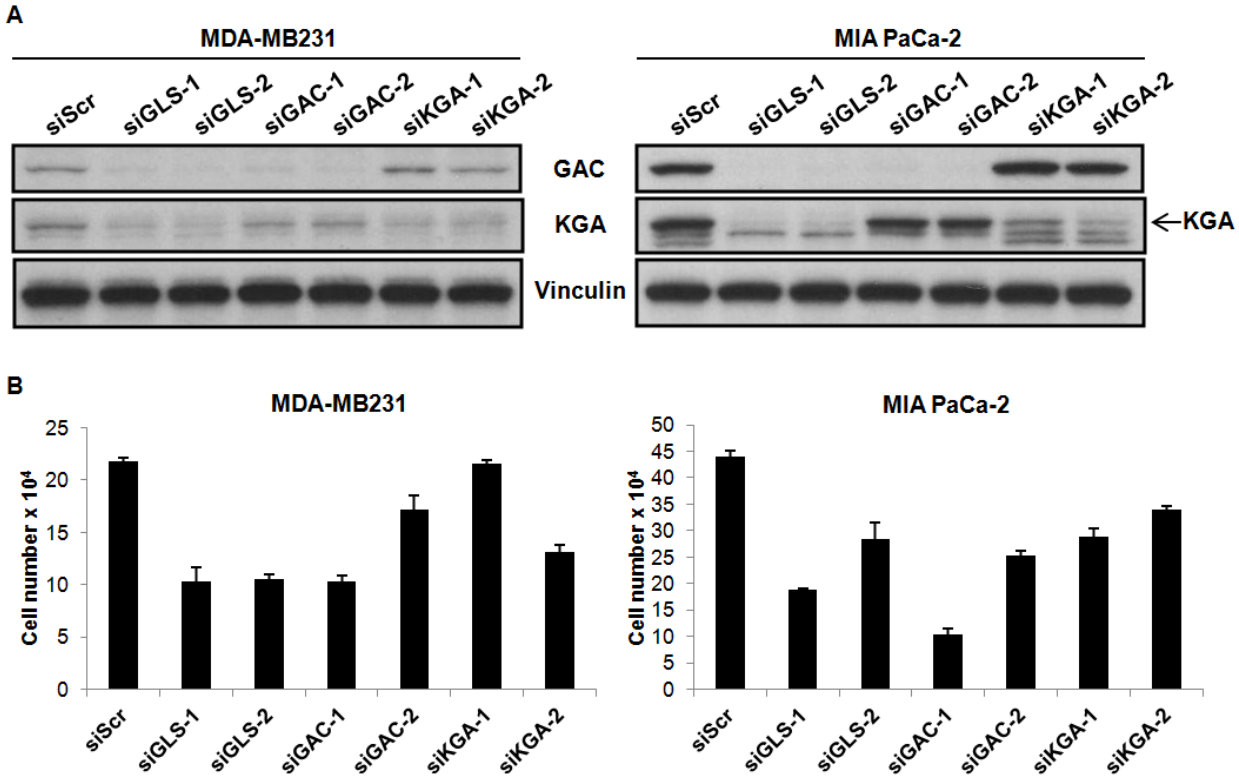
A
MDA-MB231
MIA PaCa-2
siScr
siGLS-1
siGLS-2
siGAC-1
siGAC-2
siKGA-1
siKGA-2
GAC
KGA
Vinculin
←KGA
B
MDA-MB231
MIA PaCa-2
Cell number x 10⁴
0
5
10
15
20
25
30
35
40
45
50

To further characterize the contributions of each isoform to the transformed cancer cell phenotype, we next examined the importance of GAC and KGA for anchorage-independent growth. These assays challenge the cells' ability to survive and form colonies while suspended in agarose, which mimics the stressful conditions of the tumor microenvironment. As a preliminary test of the importance of GLS and glutamine metabolism in anchorage-independent growth, we carried out GLS knockdowns in MIA PaCa-2 cells, and examined their ability to form colonies in soft agar (Figure 3.5A, B). We found that the knockdowns strongly compromised colony formation in these cells, implying that GLS is critical for the survival and growth of these cells under stressful conditions. To ensure that these growth defects were specific to the down-regulation of glutamine metabolism, we also treated the cells with or without dimethyl-αKG (dm-αKG), a cell permeable analog of the TCA cycle intermediate αKG. We observed ~75% rescue of growth under these conditions, suggesting that the GLS knockdowns primarily inhibit colony formation through a loss of TCA cycle anaplerosis. Furthermore, we found that treating MIA PaCa-2 cells with BPTES, a highly specific inhibitor of GLS, also results in a dramatic reduction in anchorage-independent growth, and can be rescued upon treatment with dm-αKG (Figure 3.5C) (9, 24). Together, these data suggest that GLS-derived glutamate and αKG are crucial for the anchorage-independent growth of MIA PaCa-2 cells, and the soft agar assay is a valid means of studying GLS and glutamine metabolism.

With these data in hand, we chose to move forward with our comparative analysis of GAC and KGA by comparing their relative roles in anchorage-independent growth in MIA PaCa-2 cells and A549 lung carcinoma cells. In addition to readily giving rise to colony formation in soft agar, A549 cells express detectable levels of KGA as well as GAC, allowing for a more direct analysis of the importance of each isoform than in cell lines with low KGA

Figure 3.5. Glutaminase is required for anchorage-independent growth in soft agar.

(A) MIA PaCa-2 cells were transfected with either a negative control siRNA (siScr), or siRNAs that target both GLS isoforms. Whole cell lysates were collected 48 hours post-transfection, and were analyzed by Western blot analysis with GLS and Vinculin antibodies.

(B) The MIA PaCa-2 cells described in A were analyzed for anchorage-independent growth in soft agar as outlined in "Materials and Methods." Briefly, cells were seeded at a density of 5 x 10^3 cells/well in 6 well plates 48 hours post-siRNA transfection. The cells were supplemented with complete growth medium every 5-6 days, and colonies were counted after 14 days. Each experiment was performed in triplicate, and the results were averaged and graphed.

(C) MIA PaCa-2 cells were analyzed for anchorage-independent growth in soft agar. The cells were seeded at a density of 5 x 10^3 cells/well in 6 well plates in complete growth medium containing DMSO, 25 μM BPTES, and 4 mM dm-αKG, alone or in the indicated combinations. Fresh growth medium containing inhibitors was added every 5-6 days, and the colonies were counted after 14 days. Each experiment was performed in triplicate, and the results were averaged and graphed.

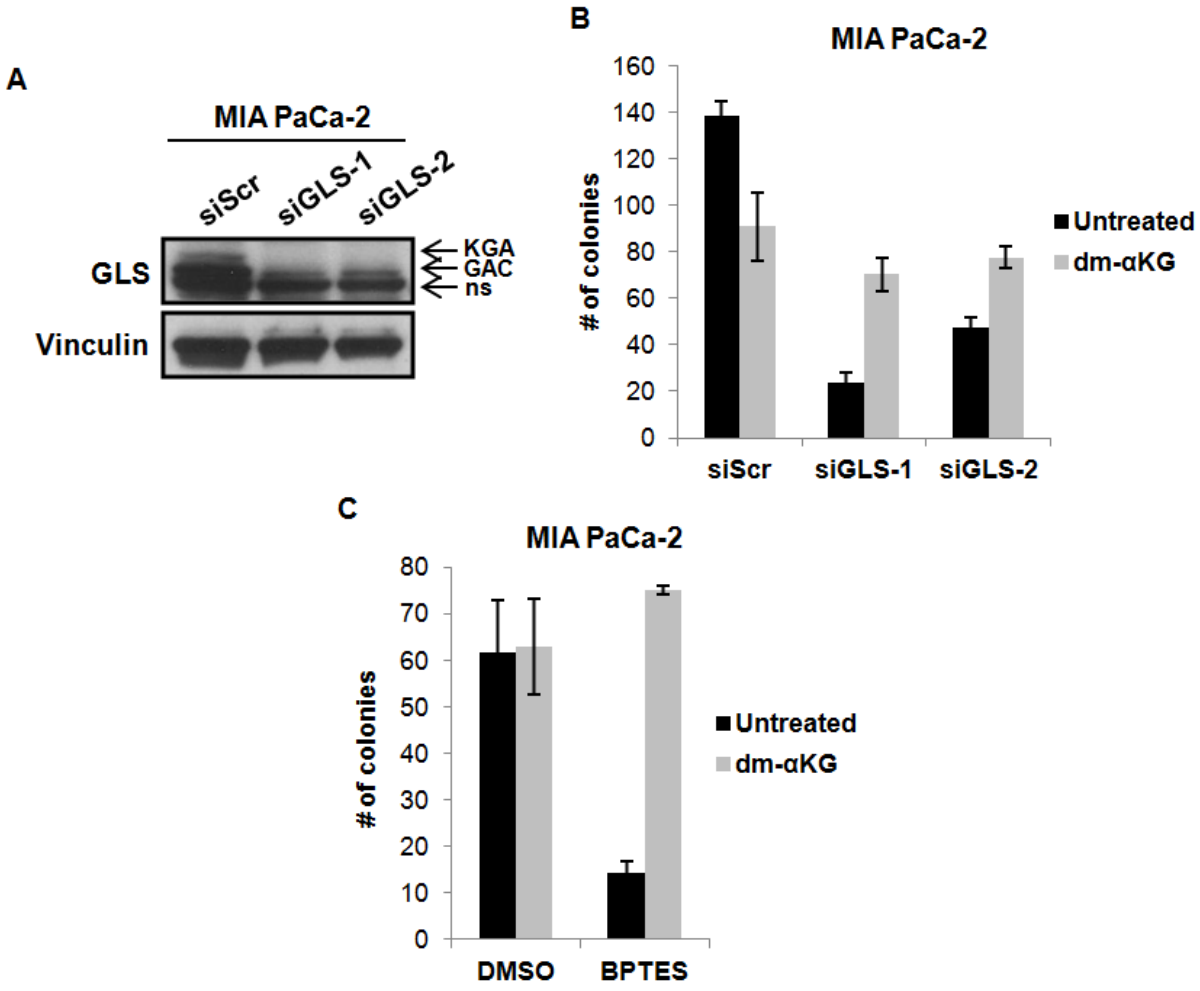
A
MIA PaCa-2
siScr
siGLS-1
siGLS-2
GLS
KGA
GAC
ns
Vinculin
B
MIA PaCa-2
# of colonies
160
140
120
100
80
60
40
20
0
siScr
siGLS-1
siGLS-2
Untreated
dm-αKG
C
MIA PaCa-2
# of colonies
80
70
60
50
40
30
20
10
0
DMSO
BPTES
Untreated
dm-αKG

expression. We again performed siRNA knockdowns targeting either GAC, KGA, or both isoforms, and carried out soft agar assays to analyze anchorage-independent growth (Figure 3.6A, B). In each cell line, we observed a striking inhibition of colony formation following the total GLS knockdowns. MIA PaCa-2 cells, which predominantly express GAC, were also highly sensitive to the knockdown of this isoform, but were insensitive to the loss of KGA. In contrast with this result, A549 cells were susceptible to the knockdown of both GAC and KGA, and none of the individual isoform knockdowns fully recapitulated the growth inhibition observed with the total GLS knockdowns. These results are consistent with the notion that the relative expression levels of GAC and KGA are responsible for their contributions to proliferation and anchorage-independent growth. Thus, it appears that both isoforms are competent to support glutamine metabolism and are functionally redundant in cancer cells.

Discussion

In this study, we set out to determine the specific contributions of two GLS isoforms, GAC and KGA, to cellular transformation and cancer cell metabolism and growth. The crucial function of GLS in glutamine consumption and TCA cycle anaplerosis has been well-documented, yet very limited studies distinguish between the relative roles of GAC and KGA (8, 25). We were especially interested in uncovering any potential differences between these two isoforms given that GLS2 has been suggested to function as a tumor suppressor, in stark contrast to the role of GLS in promoting the transformed metabolic phenotype. While GLS expression is induced by Myc and c-Jun, GLS2 expression is instead stimulated by the tumor suppressor p53 (MJ Lukey, et al., submitted) (7, 15). Functionally, these isozymes each convert glutamine to glutamate, but the fate of glutamate can differ depending on its production by GLS or GLS2.

Figure 3.6. The relative contributions of GAC and KGA to anchorage-independent growth depend on their expression levels.

(A) MIA PaCa-2 and A549 cells were transfected with either a negative control siRNA (siScr), siRNAs targeted toward both GLS isoforms, or siRNAs specifically targeting either GAC or KGA. 48 hours post-transfection, whole cell lysates were collected and analyzed by Western blot analysis with GAC, KGA, GLS, and Vinculin antibodies.

(B) The MIA PaCa-2 and A549 cells described in A were analyzed for anchorage-independent growth in soft agar. The cells were seeded at a density of 5×10^3 cells/well in 6 well plates 48 hours post-siRNA transfection. The cells were supplemented with complete growth medium every 5-6 days, and colonies were counted after 14 days. Each experiment was performed in triplicate, and the results were averaged and graphed.

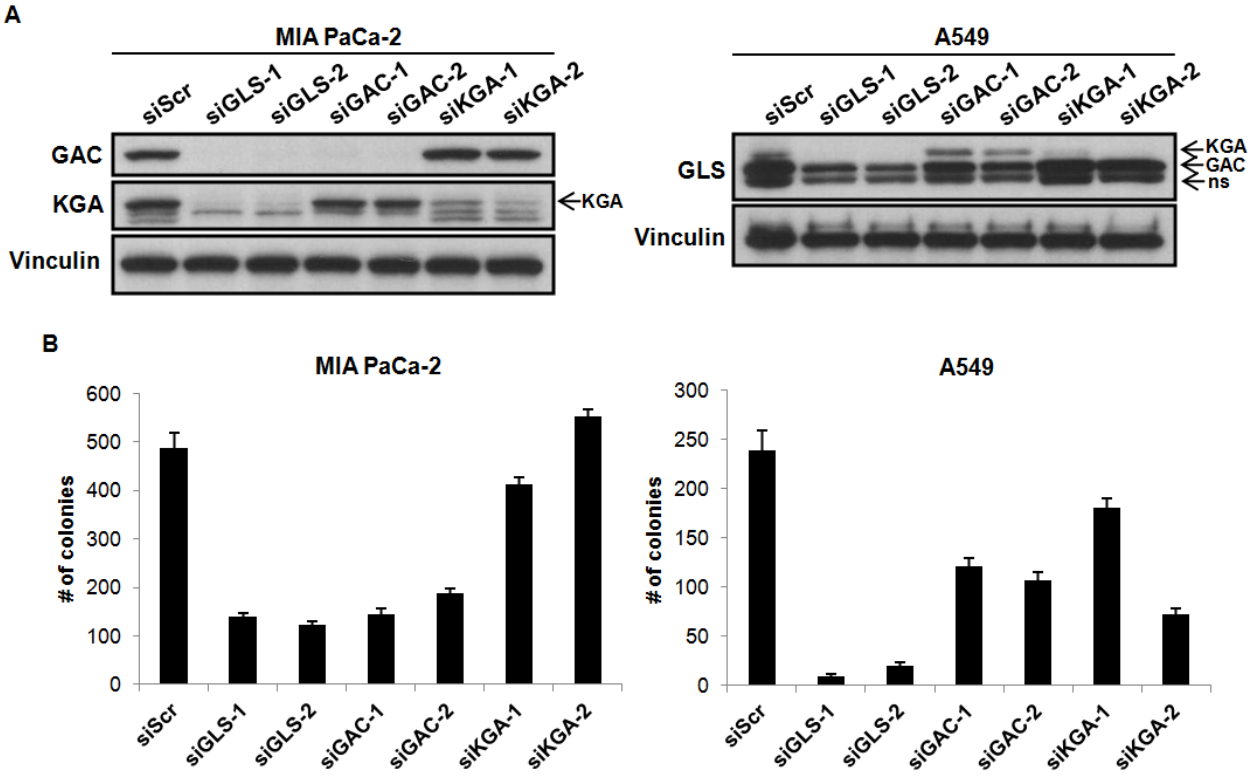
A
MIA PaCa-2
siScr
siGLS-1
siGLS-2
siGAC-1
siGAC-2
siKGA-1
siKGA-2
GAC
KGA
Vinculin
KGA
A549
GLS
Vinculin
KGA
GAC
ns
B
MIA PaCa-2
# of colonies
600
500
400
300
200
100
0
A549
# of colonies
300
250
200
150
100
50
0

Although both isozymes can support the TCA cycle, anaplerosis is thought to be the primary role of GLS, whereas GLS2 has pleiotropic functions in the cell. It can also provide glutamate for glutathione synthesis, and thus plays a crucial role in regulating cellular antioxidants. The subsequent reduction in reactive oxygen species (ROS) is thought to be a major mechanism of GLS2 tumor suppression, although some studies have suggested that GLS2 can also reduce signaling through the PI3K/Akt pathway and act as a transcription factor (15, 26, 27). These varied roles of GLS2 led us to hypothesize that KGA may also have distinct roles in cancer metabolism, and may function as a tumor suppressor given its low expression levels in a majority of cancer cells (Figure 3.1B).

In addition to the contrasting roles of the GLS and GLS2 isozymes in cancer progression, we postulated that GAC and KGA may have distinct functions in transformed cells given that alternative splicing of genes encoding metabolic enzymes has been shown to have important consequences in cancer progression. The Warburg effect is largely brought about by a splicing-induced shift in the expression of two isoforms of pyruvate kinase, namely PKM1 and PKM2. PKM1 is expressed in nearly all non-proliferating cells, and constitutively catalyzes the final reaction of glycolysis (i.e. the conversion of phosphoenolpyruvate to pyruvate). However, PKM1 expression is undetectable in most cancer cells, whereas that of PKM2 is significantly increased in cells exhibiting aerobic glycolysis, an outcome that has been ascribed to alternative splicing. The resulting expression of PKM2, which has very low enzymatic activity, limits flux from glycolysis into the TCA cycle, thus promoting the buildup of glycolytic intermediates that can be shuttled into biosynthetic pathways for cell growth and proliferation (1, 4, 13).

Based on these findings, we felt that the preferential expression of GAC over KGA in cancer cells may be a regulated event designed to promote cancer progression. To compare these

two isoforms, we began by comparing the sequences of each protein, and determined that they are identical apart from their unique C-terminal tails. We then analyzed GAC and KGA for their enzymatic activity and transforming capabilities, and found that they are indistinguishable both in their ability to catalyze the conversion of glutamine to glutamate, and synergize with oncogenic Dbl to induce focus formation in NIH 3T3 fibroblasts. These results suggested that the two isoforms may be functionally redundant, so we next examined their relative contributions to cancer cell proliferation. Using siRNAs that target both GAC and KGA, we observed that the knockdown of GLS is detrimental to the proliferation of MDA-MB231 breast cancer cells and MIA PaCa-2 pancreatic carcinoma cells. However, specific knockdowns of GAC and KGA did not conclusively establish the importance of each individual isoform. Therefore, we carried out soft agar assays to analyze the roles of GAC and KGA in anchorage-independent growth. As these assays more accurately mimic the stressful microenvironment found in tumors, we reasoned that they may better highlight any functional differences between GAC and KGA. We began by testing whether soft agar assays are a valid means of studying GLS-mediated glutamine metabolism and anaplerosis by knocking down total GLS expression, or inhibiting enzyme activity with BPTES, in MIA PaCa-2 cells. We observed that colony formation was significantly inhibited under these conditions, but could be rescued by the addition of dm-αKG, a downstream product of glutamine metabolism and a TCA cycle intermediate. These results verified that the decrease in anchorage-independent growth following GLS knockdown or BPTES treatment was due to a loss in GLS activity and TCA cycle anaplerosis. As such, we continued our comparison of GAC and KGA by knocking down either one or both isoforms in MIA PaCa-2 and A549 lung carcinoma cells, and then assaying their abilities to undergo colony formation in soft agar. We observed that total GLS knockdowns strikingly inhibited anchorage-independent growth in both

cell lines, whereas the individual knockdowns of the GLS isoforms were dependent on their expression levels. In MIA PaCa-2 cells, which predominantly express GAC (see Figure 3.1B), the loss of GAC mimicked the effects of the total GLS knockdowns, whereas KGA knockdowns had very little impact on cell growth. Conversely, the GAC and KGA knockdowns had relatively similar effects in A549 cells, in which GAC and KGA each make up a significant portion of the total GLS pool (Figure 3.6A, B). Thus, it appears that GAC and KGA are functionally redundant in cancer cells, and their relative contributions to the transformed metabolic phenotype are dependent on their expression levels.

Although we have shown that these two GLS isoforms play similar roles in cancer cells, an important question that still remains is why GAC expression is consistently higher than that of KGA in tumor samples and cancer cell lines. We now at least understand the underlying mechanism for this difference in isoform expression. Specifically, the answer likely lies in the regulation of GLS splicing and mRNA degradation. Interestingly, GAC and KGA transcript levels are relatively equal in normal tissues of the central nervous system (CNS), but GAC levels are significantly higher than those of KGA in various CNS tumors, including astrocytoma pilocyticum, ependymoma, subependymal giant cell astrocytoma, ganglioglioma, and oligodendroglioma (28). The reason for this discrepancy appears to have been solved in a recent study of alternative polyadenylation (APA) in several tumor types (29). It is well-known that 3'UTRs are often shortened in cancer cells, especially in oncogenes, and this usually results in their decreased repression by miRNAs (30). Specifically, Xia and colleagues found that the 3'UTR of KGA contains several miRNA binding sites, whereas none are predicted for that of GAC. Furthermore, they observed an APA-coupled 3'UTR shift that leads to a significant reduction in KGA expression and an increase in GAC levels in lung adenocarcinoma, lung

squamous cell carcinoma, and kidney renal clear cell carcinoma. This shift in isoform expression likely uncouples GLS transcripts from repression by the Myc targets miR-23a and miR-23b, allowing GLS to be expressed at higher levels, and likely conferring a selective growth advantage by enhancing glutamine metabolism. Finally, the mechanism underlying APA of GLS transcripts appears to stem from the global up-regulation of *trans*-acting polyadenylation factors, rather than changes in *cis*-acting mRNA sequences (29). Therefore, it appears that differential mRNA regulation is responsible for the differences in GAC and KGA expression levels in cancer cells, despite their functional redundance in the transformed metabolic phenotype.

Materials and Methods

Cell culture

SKBR3, MDA-MB468, BT474, HeLa, U87, and MDA-MB231 cells were cultured in RPMI 1640 supplemented with 10% FBS. GSC cell lines 83 and 1123 were cultured as in (31). HEK293T and A549 cells were maintained in DMEM containing 10% FBS, and MIA PaCa-2 cells were maintained in DMEM supplemented with 10% FBS and 2.5% HS. NIH 3T3 cells were cultured in DMEM supplemented with 10% CS. All cells were incubated in a humidified atmosphere with 5% CO_2 at 37°C. The pZip-neo-GST-Dbl, pcDNA3.1D-V5-GAC, and pcDNA3.1D-V5-KGA constructs were transfected into cells using Lipofectamine according to the manufacturer's instructions, and all siRNAs were transfected into cells using Lipofectamine 2000 according to the manufacturer's instructions. Where indicated, NIH 3T3 cells were treated with 10 μM 968, and MIA PaCa-2 cells were treated with 4 mM dm-αKG and 25 μM BPTES.

Reagents and antibodies

RPMI 1640, DMEM/F12, DMEM, trypsin, FBS, HS, and CS were purchased from Gibco; B-27, penicillin-streptomycin, EGF, Lipofectamine, Lipofectamine 2000, and protein G-agarose beads were from Invitrogen; heparin, glutamine, and dimethyl sulfoxide (DMSO) were from Sigma; and bFGF was from Peprotech. BTPES was a kind gift from Scott Ulrich. Primary antibodies used in this study were anti-GLS (Abgent), anti-V5 (Invitrogen), anti-GAC (custom synthesized by Genscript), anti-KGA (Proteintech), and anti-Vinculin (Sigma). Secondary antibodies conjugated to HRP (anti-mouse, anti-rabbit) were purchased from Cell Signaling.

Western blot analysis

Cells were washed 2 times in cold PBS, then lysed in cell lysis buffer (50 mM HEPES, 200 mM NaCl, 25 mM NaF, 50 mM β-Glycerophosphate, 1 mM $MgCl_2$, 1% Triton X-100, 1 mM DTT, 1 mM Na_3VO_4, 1 µg/mL aprotinin, and 1 µg/mL leupeptin). The lysates were centrifuged at 13,000 rpm for 15 minutes at 4°C, and equal amounts of protein were diluted with Laemmli sample buffer, boiled, and subjected to SDS-PAGE. The proteins were transferred onto PVDF membranes, and the membranes were blocked with 5% nonfat dry milk in TBST (20 mM Tris, 137 mM NaCl, pH 7.4, 0.05% Tween-20). The membranes were incubated with the primary antibodies either overnight at 4°C or for 1 hour at room temperature, then washed 3 times with TBST. Secondary antibodies were diluted in TBST and incubated with the membranes for 1 hour at room temperature. Membranes were washed 3 times in TBST, and visualized on X-ray film using Western Lightning *Plus*-ECL (PerkinElmer).

DNA constructs and siRNAs

Human GAC and KGA constructs were purchased from GeneCopoeia and cloned into the pcDNA3.1D/V5-His-TOPO vector (Invitrogen) according to the manufacturer's instructions. pZip-neo-GST-Dbl was from (8). A negative control siRNA (Stealth^{TM} RNAi Negative Control Medium GC Duplex #2), referred to as siScr, and siGLS-1 were purchased from Invitrogen, and all other siRNAs were purchased from Dharmacon. The sequences for the siRNAs used in this study are as follows: siGLS-1: GCUAAUGGUGGUUUCUGCCCAAUUA; siGLS-2: GCACAGACAUGGUUGGUAU siGAC-1: GGAAAGUCUGGGAGAGAAAUU; siGAC-2: CUAUGAAAGUCUCCAACAAUU; siKGA-1: CCCAAGGACAGGUGGAAUAUU; siKGA-2: CUGGAAGCCUGCAAAGUAAUU.

Immunoprecipitation

MDA-MB231 and HEK293T cells transfected with or without a V5-tagged GAC or V5-tagged KGA construct were collected 48 hours post-transfection, and lysed in cell lysis buffer as described above. Equal amounts of protein (typically 1 mg for MDA-MB231 and 200 µg for HEK293T) were diluted with cell lysis buffer to a concentration of 1 mg/mL, and pre-cleared with protein G-agarose beads for 30 minutes. The lysates were then centrifuged to remove the beads, and the supernatants were incubated with the anti-V5 antibody for 1 hour. Protein G-agarose beads were then added to the lysates and incubated for 1 hour, followed by 3 washes with cell lysis buffer. All incubations and washes were carried out on a rotator at 4°C. 10% of each immunoprecipitated sample was removed and diluted with Laemmli sample buffer, boiled, and subjected to Western blot analysis. The remainder of each sample was analyzed by the Glutaminase activity assay, as outlined below.

Glutaminase activity assay

Following immunoprecipitation, as described above, each sample was analyzed for glutaminase activity as described in (8). The samples were divided into two equal parts, followed by centrifugation and removal of the supernatant. The remaining protein G-agarose beads were incubated in 105 µL of a buffer containing 57 mM Tris-acetate (pH 8.6), 0.225 mM EDTA, 17 mM glutamine, and either water or 150 mM potassium phosphate. The reaction was allowed to proceed for 1 hour (MDA-MB231 cells) or 10 minutes (HEK293T cells) on a rotator at 37°C, and was quenched by the addition of 10 µL 2M HCl followed by a 5 minute incubation on ice. 20 µL of the reaction mixture was then removed and incubated in a buffer containing 114 mM Tris-HCl (pH 9.4), 0.35 mM ADP, 1.7 mM NAD, and 6.3 U/mL GDH. The reaction was carried out for 45 minutes at room temperature, and the absorbance at 340 nm was determined using a water blank. The absorbance of the buffer was subtracted from that of each sample to determine enzyme activity.

Focus formation assay

Focus formation assays were carried out as in (8). Briefly, NIH 3T3 cells were transfected with pZip-neo-GST-Dbl ("Dbl"), V5-tagged GAC, V5-tagged KGA, mock, or the indicated combinations of Dbl and V5-GAC or V5-KGA. The following day, 2.5 x 10^4 cells were seeded into 60 mM dishes in complete medium. The medium was changed to DMEM + 5% CS three days later, and was subsequently replenished every three days. Where indicated, DMSO or 10 µM 968 was added to the cells one day after they were seeded, and each time the medium was replenished. The cells were collected after 12-14 days, fixed in 3.7% formaldehyde in PBS for 20 minutes, stained with 0.4% crystal violet for five minutes, and washed twice with water.

Proliferation assay

MDA-MB231 and MIA PaCa-2 cells transfected with siRNAs for 48 hours were seeded in 6-well plates at 2.5 x 10^4 cells/well in triplicate. The remaining cells were collected for Western blot analysis of siRNA knockdowns. The medium on each well was replenished after 2 days, and the cells were counted on a hemocytometer after 4 days of growth.

Soft agar assay

MIA PaCa-2 cells, or MIA PaCa-2 and A549 cells transfected for 48 hours with siRNAs, were seeded in triplicate in 6-well plates at a density of 5 x 10^3 cells/well in complete growth medium containing 0.3% agarose over a layer of complete growth medium containing 0.6% agarose, with or without BPTES and dm-αKG where indicated. The remaining cells were collected for Western blot analysis of siRNA knockdowns. Fresh growth medium containing 0.3% agarose and DMSO, BPTES, or dm-αKG was added every 5-6 days, and colonies were counted after 14 days on an inverted microscope.

Statistical analysis

For data presented as bar graphs, error bars represent the standard error of the mean (SEM). Statistical significance was calculated in Excel using F-tests for sample variance and Student's t tests for significance. p values < 0.05 were considered statistically significant, and are denoted by asterisks.

Acknowledgements

We thank Kathy Rojas for assistance in cloning the V5-GAC and V5-KGA constructs, and Cerione lab members for helpful discussions and advice. BPTES was kindly provided by Scott Ulrich (Ithaca College, Ithaca, NY).

REFERENCES

1. Vander Heiden MG, Cantley LC, Thompson CB. Understanding the Warburg effect: The metabolic requirements of cell proliferation. Science 2009;324(5930):1029-33.

2. Levine AJ, Puzio-Kuter AM. The control of the metabolic switch in cancers by oncogenes and tumor suppressor genes. Science 2010;330(6009):1340-4.

3. DeBerardinis RJ, Lum JJ, Hatzivassiliou G, Thompson CB. The biology of cancer: Metabolic reprogramming fuels cell growth and proliferation. Cell Metabolism 2008;7(1):11-20.

4. Cairns RA, Harris IS, Mak TW. Regulation of cancer cell metabolism. Nat Rev Cancer 2011;11(2):85-95.

5. DeBerardinis RJ, Cheng T. Q's next: The diverse functions of glutamine in metabolism, cell biology and cancer. Oncogene 2010;29(3):313-24.

6. Hensley CT, Wasti AT, DeBerardinis RJ. Glutamine and cancer: Cell biology, physiology, and clinical opportunities. J Clin Invest 2013;123(9):3678-84.

7. Gao P, Tchernyshyov I, Chang T, et al. c-Myc suppression of miR-23a/b enhances mitochondrial glutaminase expression and glutamine metabolism. Nature 2009;458(7239):762-5.

8. Wang J, Erickson JW, Fuji R, et al. Targeting mitochondrial glutaminase activity inhibits oncogenic transformation. Cancer Cell 2010;18(3):207-19.

9. Robinson M, Mcbryant S, Tsukamoto T, et al. Novel mechanism of inhibition of rat kidney-type glutaminase by bis-2-(5-phenylacetamido-1, 2, 4-thiadiazol-2-yl) ethyl sulfide (BPTES). Biochem J 2007;406:407-14.

10. Katt WP, Ramachandran S, Erickson JW, Cerione RA. Dibenzophenanthridines as inhibitors of glutaminase C and cancer cell proliferation. Mol Cancer Ther 2012;11(6):1269-78.

11. Gross MI, Demo SD, Dennison JB, et al. Antitumor activity of the glutaminase inhibitor CB-839 in triple-negative breast cancer. Mol Cancer Ther 2014;13(4):890-901.

12. Atsumi T, Chesney J, Metz C, et al. High expression of inducible 6-phosphofructo-2-kinase/fructose-2,6-bisphosphatase (iPFK-2; PFKFB3) in human cancers. Cancer Res 2002;62(20):5881-7.

13. Christofk HR, Vander Heiden MG, Harris MH, et al. The M2 splice isoform of pyruvate kinase is important for cancer metabolism and tumour growth. Nature 2008;452(7184):230-3.

14. Szeliga M, Obara-Michlewska M, Matyja E, et al. Transfection with liver-type glutaminase cDNA alters gene expression and reduces survival, migration and proliferation of T98G glioma cells. Glia 2009;57(9):1014-23.

15. Hu W, Zhang C, Wu R, Sun Y, Levine A, Feng Z. Glutaminase 2, a novel p53 target gene regulating energy metabolism and antioxidant function. Proc Natl Acad Sci USA 2010;107(16):7455-60.

16. Shapiro RA, Farrell L, Srinivasan M, Curthoys NP. Isolation, Characterization, and *in Vitro* Expression of a cDNA That Encodes the Kidney Isoenzyme of the Mitochondrial Glutaminase. J Biol Chem 1991;266(28):18792-6.

17. Elgadi KM, Meguid RA, Qian M, Souba WW, Abcouwer SF. Cloning and analysis of unique human glutaminase isoforms generated by tissue-specific alternative splicing. Physiol Genomics 1999;1(2):51-62.

18. Porter LD, Ibrahim H, Taylor L, Curthoys NP. Complexity and species variation of the kidney-type glutaminase gene. Physiol Genomics 2002;9(3):157-66.

19. Srinivasan M, Kalousek F, Farrell L, Curthoys NP. Role of the N-terminal 118 amino acids in the processing of the rat renal mitochondrial glutaminase precursor. J Biol Chem 1995;270(3):1191-7.

20. Srinivasan M, Kalousek F, Curthoys NP. In vitro characterization of the mitochondrial processing and the potential function of the 68-kDa subunit of renal glutaminase. J Biol Chem 1995;270(3):1185-90.

21. Márquez J, de la Oliva, Amada R López, Matés JM, Segura JA, Alonso FJ. Glutaminase: A multifaceted protein not only involved in generating glutamate. Neurochem Int 2006;48(6):465-71.

22. Curthoys NP, Watford M. Regulation of glutaminase activity and glutamine metabolism. Annu Rev Nutr 1995;15(1):133-59.

23. Hart MJ, Eva A, Evans T, Aaronson SA, Cerione RA. Catalysis of guanine nucleotide exchange on the CDC42Hs protein by the *dbl* oncogene product. Nature 1991;354:311-314.

24. Hartwick EW, Curthoys NP. BPTES inhibition of hGA124–551, a truncated form of human kidney-type glutaminase. J Enzyme Inhib Med Chem 2012;27(6):861-7.

25. Vander Heiden MG. Targeting cancer metabolism: A therapeutic window opens. Nat Rev Drug Discovery 2011;10(9):671-84.

26. Liu J, Zhang C, Lin M, et al. Glutaminase 2 negatively regulates the PI3K/AKT signaling and shows tumor suppression activity in human hepatocellular carcinoma. Oncotarget 2014;5(9):2635.

27. Szeliga M, Obara-Michlewska M. Glutamine in neoplastic cells: Focus on the expression and roles of glutaminases. Neurochem Int 2009;55(1):71-5.

28. Szeliga M, Matyja E, Obara M, Grajkowska W, Czernicki T, Albrecht J. Relative expression of mRNAS coding for glutaminase isoforms in CNS tissues and CNS tumors. Neurochem Res 2008;33(5):808-13.

29. Xia Z, Donehower LA, Cooper TA, et al. Dynamic analyses of alternative polyadenylation from RNA-seq reveal a 3′-UTR landscape across seven tumour types. Nat Commun 2014;5.

30. Mayr C, Bartel DP. Widespread shortening of 3′ UTRs by alternative cleavage and polyadenylation activates oncogenes in cancer cells. Cell 2009;138(4):673-84.

31. Mao P, Joshi K, Li J, et al. Mesenchymal glioma stem cells are maintained by activated glycolytic metabolism involving aldehyde dehydrogenase 1A3. Proc Natl Acad Sci USA 2013;110(21):8644-9.

CHAPTER 4

Conclusions

In recent years, rapidly accumulating studies of cancer biology have uncovered many of the major mechanisms that contribute to tumor initiation, growth, metastasis, therapy resistance, and recurrence. Among these are a recently identified sub-population of cancer cells, referred to as cancer stem cells (CSCs), which exhibit self-renewal and tumor-initiating capabilities, and have pleiotropic roles in the development and therapy resistance of various forms of cancer (1-4). Additionally, the process of de-regulated cellular metabolism has become recognized for its critical contributions to neoplastic transformation, and the maintenance of the malignant state (5-7). Therefore, I set out to better understand the molecular basis for these oncogenic events, so as to uncover novel ways of targeting the transformed phenotype.

In the second chapter of this thesis, I examined the role of the CSC marker aldehyde dehydrogenase 1A3 (ALDH1A3), which is thought to be a critical mediator of CSC self-renewal, in glioma stem cells (GSCs) derived from high grade gliomas (HGGs) (8-10). HGGs are particularly malignant and therapy-resistant tumors with a median survival time of only 14.6 months (11, 12). Thus, there is a dire need to better understand the molecular mechanisms underlying the aggressive phenotype of this malignancy, in order to identify novel therapeutic strategies that will promote tumor regression and prevent tumor recurrence. As the GSC marker ALDH1A3 catalyzes the oxidation of retinal to retinoic acid (RA), an important transcriptional regulator, I hypothesized that the induction of RA-regulated genes downstream of ALDH1A3 activity may support the CSC phenotype (13). Specifically, I investigated whether the expression of tissue transglutaminase (tTG), an RA-regulated enzyme that has been implicated in cancer

progression, is dependent on ALDH1A3 catalysis (14-20). I determined that this is indeed the case in highly aggressive mesenchymal (MES) GSCs, and found that the ectopic expression of ALDH1A3 is sufficient to induce tTG expression in ALDH1A3$^-$/tTG$^-$ proneural (PN) GSCs (Figure 4.1).

Although I was unable to establish a direct role for tTG in the aggressive transformed phenotypes of MES GSCs, I postulated that its up-regulated expression may make these cells particularly vulnerable to therapies that cause tTG to adopt an open conformation, which was previously shown to be toxic to NIH 3T3 fibroblasts and HeLa cervical carcinoma cells (21). I determined that tTG-targeted therapies do in fact inhibit the self-renewal and proliferation of MES GSCs, which suggested that tTG may be a suitable target for therapeutic intervention in HGG. I then examined the potential for a tTG inhibitor, namely Z-Don, to sensitize therapy-resistant MES GSCs to the effects of ionizing radiation (IR) and temozolomide (TMZ), which are both clinically used for the treatment of HGG (12). I found that combination therapies involving low doses of Z-Don and either IR or TMZ led to a significant reduction in MES GSC self-renewal and proliferation. Most notably, these combination therapies had a cytotoxic effect that could not be achieved with any of the three monotherapies, suggesting that the addition of a tTG inhibitor to standard HGG treatment regimens may promote tumor regression, and decrease the incidence of tumor recurrence.

While my study of ALDH1A3 and tTG in MES GSCs has identified a role for ALDH1A3 in gene regulation and a therapeutic strategy for targeting these cells, a number of questions still remain to be investigated. First, what are the targets of ALDH1A3-mediated gene expression that support the self-renewal of MES GSCs? A better understanding of the genes induced downstream of ALDH1A3 will allow the development of GSC-targeted therapies that

Figure 4.1. Aldehyde dehydrogenase 1A3 induces the expression of tissue transglutaminase in mesenchymal glioma stem cells.

In MES GSCs, the production of RA by ALDH1A3 leads to the up-regulation of tTG expression. Molecules that induce tTG to adopt an open conformation (e.g. Z-Don) synergize with a chemotherapeutic drug (TMZ) or IR, resulting in cell death. ALDH1A3, aldehyde dehydrogenase 1A3; RA, retinoic acid; TGM2, transglutaminase 2; tTG, tissue transglutaminase; TMZ, temozolomide; IR, ionizing radiation.

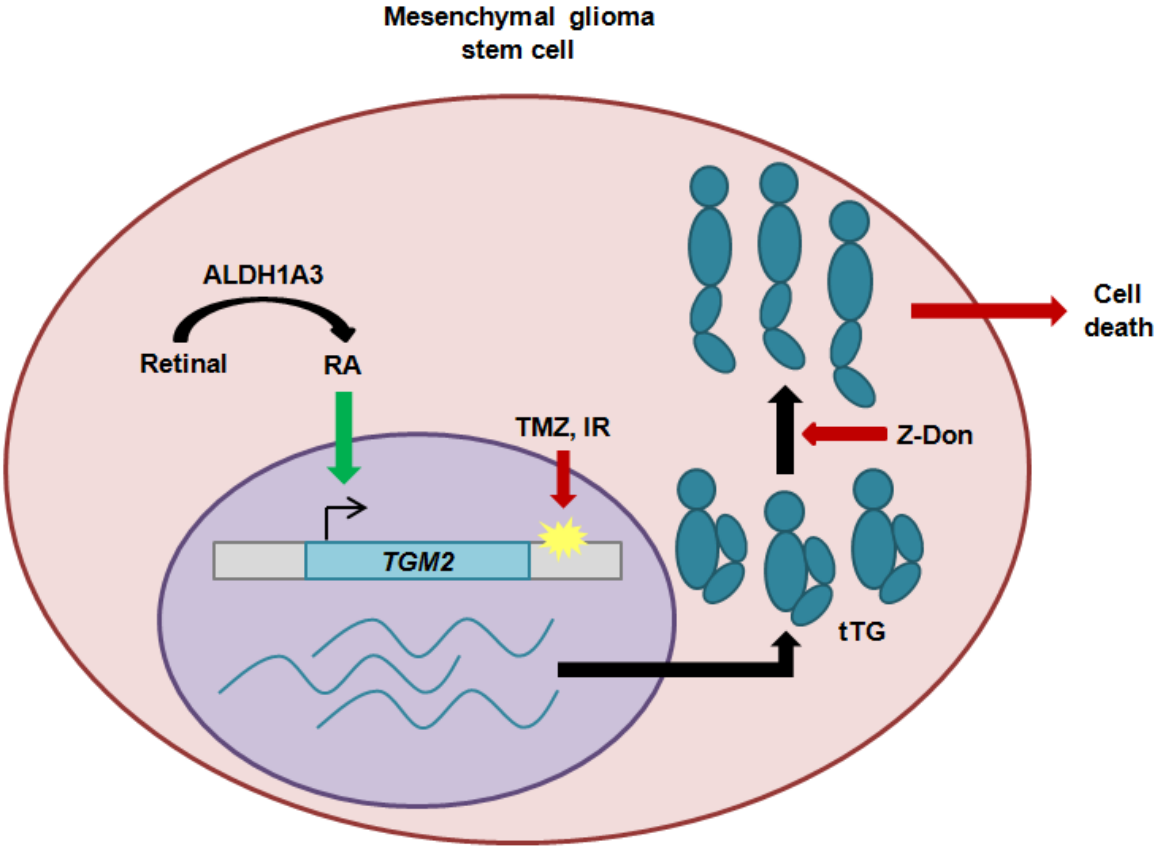
Mesenchymal glioma stem cell
ALDH1A3
Retinal
RA
TMZ, IR
TGM2
tTG
Z-Don
Cell death

may be clinically valuable for achieving a long-term cure for HGG. Secondly, what is the role of tTG in MES GSCs, and are there redundant mechanisms in place that compensate for the loss of tTG? Our finding that the knockdown of tTG does not reduce MES GSC self-renewal, proliferation, or survival was highly unexpected, given the well-characterized roles of tTG in cancer progression (15-20). However, CSCs are known to be resistant to a variety of therapies, which suggests that they have redundant mechanisms in place that protect them from various cellular insults (3, 4). Indeed, I observed that MES GSCs are resistant to the inhibition of PI3K/Akt signaling, highlighting their ability to compensate for a critical signaling pathway that is crucial in a multitude of other cancer cells (unpublished observations). These findings further emphasize the need to develop novel combination therapies that can successfully target and kill CSCs. Interestingly, this may be achieved by targeting glutamine metabolism, which I have discussed in Chapter 3 of this thesis. We have observed that MES GSCs are highly dependent on glutamine metabolism for their enhanced proliferation, as they are sensitive to glutamine starvation and the glutaminase (GLS) inhibitor 968, whereas PN GSCs do not appear to depend on this type of metabolism (unpublished observations). These results suggest the possibility that ALDH1A3 is involved in establishing the Warburg effect, and enhancing glutamine metabolism in MES GSCs. Additionally, MES GSCs express very high levels of a mutant and constitutively active form of the epidermal growth factor receptor (EGFR), referred to as the EGFRvIII, which appears to be necessary for the activation of the transcription factor c-Jun in these cells (unpublished observations). Given that c-Jun was recently found to induce the expression of GLS in breast cancer cells (MJ Lukey, et al., submitted), it is possible that its activation by the EGFRvIII may also lead to an up-regulation of GLS expression, and consequently glutamine metabolism, in MES GSCs. Further investigations will be necessary to understand whether

ALDH1A3 and the EGFRvIII contribute to the transformed metabolic phenotype, and if GLS will be a therapeutic target in these cells.

Work described in the third chapter of this thesis focused on understanding the specific contributions of two major GLS isoforms, namely glutaminase C (GAC) and kidney-type glutaminase (KGA), to the altered metabolism exhibited by many cancer cells. While GAC has been previously suggested to be a therapeutic target in glutamine-addicted cancer cells, the role of KGA in cancer cell glutamine metabolism remained largely unknown (22, 23). However, understanding the importance of each GLS isoform is especially relevant when designing therapeutic strategies that target glutamine metabolism in cancer cells. Therefore, I compared the abilities of GAC and KGA to hydrolyze glutamine to glutamate, contribute to the transformation of fibroblasts, and support the anchorage-independent growth of cancer cells. I found that their enzymatic activities and abilities to synergize with oncogenic Dbl to induce transformation are indistinguishable, suggesting that each isoform is capable of promoting de-regulated glutaminolysis. I also observed that both GAC and KGA contribute to the anchorage-independent growth of MIA PaCa-2 pancreatic carcinoma cells and A549 lung carcinoma cells, though their relative roles in promoting this phenotype appear to depend on their individual expression levels. Importantly, I also found that 968 inhibits Dbl/KGA-induced transformation, providing evidence to suggest that this inhibitor can block the activity of both GAC and KGA, and will be capable of targeting glutamine metabolism in cancer cells expressing either GLS isoform (Figure 4.2).

Although I observed that GAC and KGA are each capable of supporting glutamine metabolism in cancer cells, I was unable to determine the molecular mechanism responsible for their differential expression levels in cancer cells. The indistinguishable activities of these

Figure 4.2. GAC and KGA support glutaminolysis in glutamine-dependent cancer cells exhibiting the Warburg effect.

In cancer cells that depend on the metabolic rewiring of glycolysis and glutaminolysis for their rapid growth and proliferation, the two major GLS isoforms, GAC and KGA, both support glutamine metabolism. Knocking down the expression of these enzymes, or targeting them with the GLS inhibitor 968, results in the decreased proliferation and anchorage-independent growth of these cells. TCA cycle, tricarboxylic acid cycle; αKG, α-ketoglutarate; Glu, glutamate; Gln, glutamine; GAC, glutaminase C; KGA, kidney-type glutaminase.

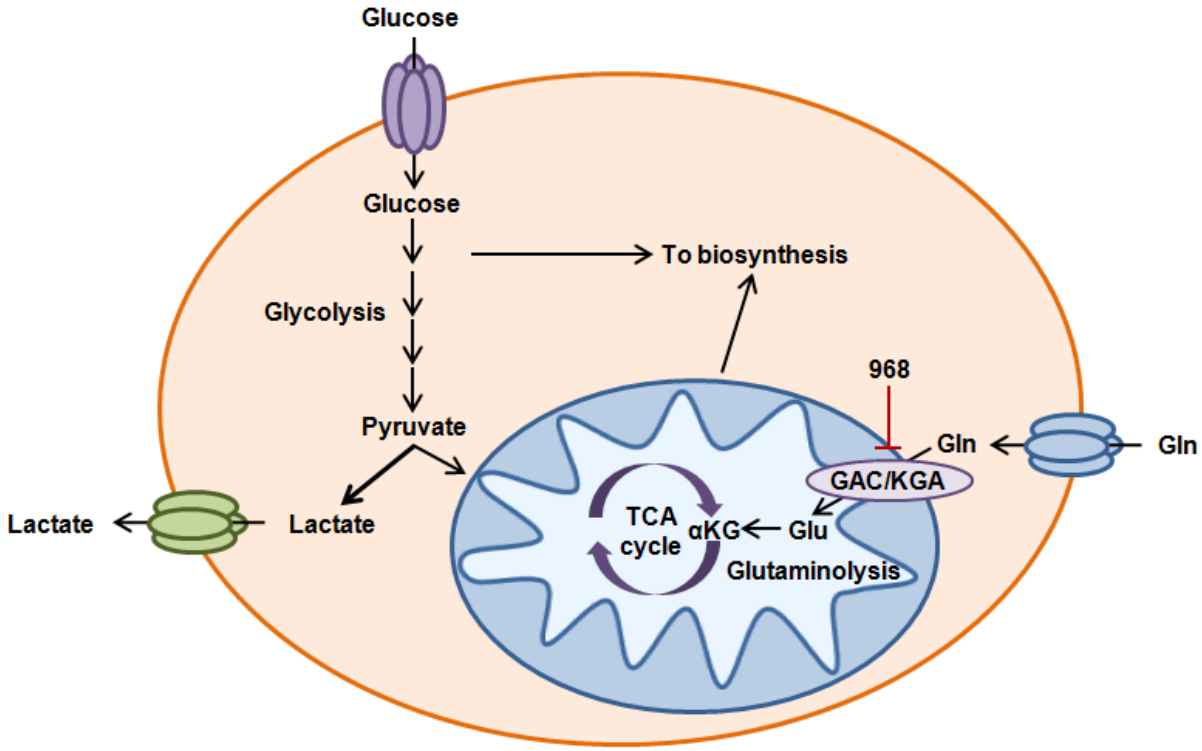
Glucose
Glucose
To biosynthesis
Glycolysis
968
Pyruvate
Gln
Gln
GAC/KGA
Lactate
Lactate
TCA
cycle
αKG
Glu
Glutaminolysis

enzymes in glutamine metabolism suggested that the preferential expression of GAC may stem from the alternative regulation of GAC and KGA transcripts, a hypothesis which has been supported by a recent study of alternative polyadenylation (APA) in cancer cells (24). The global shortening of 3'UTRs in cancer is thought to contribute to the de-regulated expression of many oncogenes through the loss of miRNA repression (25). The shorter 3'UTR of GAC mRNA, which lacks the miRNA binding sites found in the KGA transcript, appears to be favored by the up-regulated APA factors in cancer cells, and thus may be responsible for the differential expression levels of GAC and KGA in these cells (24). This mechanism suggests that the different 3'UTRs of these two isoforms may have evolved to de-regulate, and thus enhance, the expression of GAC in proliferating cells, and this APA appears to be hijacked by cancer cells to promote the elevated glutamine metabolism required for proliferation.

While I have shown that GAC and KGA can both contribute to glutaminolysis, questions still remain as to how these enzymes become activated in cancer cells. One possibility is that their increased expression in cancer cells may drive them into the active tetrameric state by mass action. It is also possible that oncogenic signaling may result in post-translational modifications that activate these enzymes. One such modification that is currently under investigation in our laboratory is the succinylation of Lys164 on GAC/KGA, which may normally help to recruit an E3 ubiquitin ligase that ensures the degradation of these enzymes. However, the up-regulation of Sirtuin 5 (Sirt5), a mitochondrial desuccinylase/demalonylase, in cancer cells has been suggested to de-succinylate GAC, and thus block its degradation and significantly enhance its cellular lifetime (KS Greene, CA Stalnecker, et al., in preparation) (26, 27). It has also been suggested that GAC is regulated by phosphorylation downstream of NF-κB signaling in breast cancer cells (22). Further investigations of these potential post-translational modifications will be necessary

to more fully understand the mechanisms by which cancer cells activate GLS activity, and thereby support glutamine metabolism.

Closing remarks

Recent advances in the study of cancer biology have identified the crucial roles of CSCs and de-regulated metabolism in establishing and maintaining the transformed state. In this thesis, I have built upon these findings by investigating the molecular mechanisms underlying the self-renewal of CSCs, and the regulation of glutamine metabolism. This has enabled me to identify novel therapeutic strategies for targeting the enhanced self-renewal and survival of GSCs that may ultimately improve outcomes for patients suffering from HGG, or other forms of cancer with ALDH1A3^{+} CSCs. Additionally, the characterization of two major GLS isoforms has demonstrated that therapeutic approaches for targeting GLS activity in glutamine-dependent cells must be designed to inhibit the activity of both KGA and GAC. Hopefully, these findings will promote a more complete understanding of CSCs and the transformed metabolic phenotype, and allow the development of therapeutic strategies for the successful treatment of patients suffering from cancer.

REFERENCES

1. Reya T, Morrison SJ, Clarke MF, Weissman IL. Stem cells, cancer, and cancer stem cells. Nature 2001;414(6859):105-11.

2. Pardal R, Clarke MF, Morrison SJ. Applying the principles of stem-cell biology to cancer. Nat Rev Cancer 2003;3(12):895-902.

3. Dean M, Fojo T, Bates S. Tumour stem cells and drug resistance. Nat Rev Cancer 2005;5(4):275-84.

4. Rich JN. Cancer stem cells in radiation resistance. Cancer Res 2007;67(19):8980-4.

5. Vander Heiden MG, Cantley LC, Thompson CB. Understanding the Warburg effect: The metabolic requirements of cell proliferation. Science 2009;324(5930):1029-33.

6. DeBerardinis RJ, Lum JJ, Hatzivassiliou G, Thompson CB. The biology of cancer: Metabolic reprogramming fuels cell growth and proliferation. Cell Metabolism 2008;7(1):11-20.

7. Levine AJ, Puzio-Kuter AM. The control of the metabolic switch in cancers by oncogenes and tumor suppressor genes. Science 2010;330(6009):1340-4.

8. Ma I, Allan AL. The role of human aldehyde dehydrogenase in normal and cancer stem cells. Stem Cell Reviews and Reports 2011;7(2):292-306.

9. Mao P, Joshi K, Li J, et al. Mesenchymal glioma stem cells are maintained by activated glycolytic metabolism involving aldehyde dehydrogenase 1A3. Proc Natl Acad Sci U S A 2013;110(21):8644-9.

10. Shao C, Sullivan JP, Girard L, et al. Essential role of aldehyde dehydrogenase 1A3 for the maintenance of non-small cell lung cancer stem cells is associated with the STAT3 pathway. Clin Cancer Res 2014;20(15):4154-66.

11. Vescovi AL, Galli R, Reynolds BA. Brain tumour stem cells. Nat Rev Cancer 2006;6(6):425-36.

12. Bayin NS, Modrek AS, Placantonakis DG. Glioblastoma stem cells: Molecular characteristics and therapeutic implications. World journal of stem cells 2014;6(2):230.

13. Vasiliou V, Thompson DC, Smith C, Fujita M, Chen Y. Aldehyde dehydrogenases: From eye crystallins to metabolic disease and cancer stem cells. Chem Biol Interact 2013;202(1):2-10.

14. Eckert RL, Kaartinen MT, Nurminskaya M, et al. Transglutaminase regulation of cell function. Physiol Rev 2014;94(2):383-417.

15. Antonyak MA, Li B, Boroughs LK, et al. Cancer cell-derived microvesicles induce transformation by transferring tissue transglutaminase and fibronectin to recipient cells. Proc Natl Acad Sci U S A 2011;108(12):4852-7.

16. Antonyak MA, Li B, Regan AD, Feng Q, Dusaban SS, Cerione RA. Tissue transglutaminase is an essential participant in the epidermal growth factor-stimulated signaling pathway leading to cancer cell migration and invasion. J Biol Chem 2009;284(27):17914-25.

17. Li B, Antonyak MA, Druso JE, Cheng L, Nikitin AY, Cerione RA. EGF potentiated oncogenesis requires a tissue transglutaminase-dependent signaling pathway leading to Src activation. Proc Natl Acad Sci U S A 2010;107(4):1408-13.

18. Boroughs LK, Antonyak MA, Johnson JL, Cerione RA. A unique role for heat shock protein 70 and its binding partner tissue transglutaminase in cancer cell migration. J Biol Chem 2011;286(43):37094-107.

19. Zhang J, Antonyak MA, Singh G, Cerione RA. A mechanism for the upregulation of EGF receptor levels in glioblastomas. Cell Rep 2013;3(6):2008-20.

20. Antonyak MA, Miller AM, Jansen JM, et al. Augmentation of tissue transglutaminase expression and activation by epidermal growth factor inhibit doxorubicin-induced apoptosis in human breast cancer cells. J Biol Chem 2004;279(40):41461-7.

21. Datta S, Antonyak MA, Cerione RA. GTP-binding-defective forms of tissue transglutaminase trigger cell death. Biochemistry 2007;46(51):14819-29.

22. Wang J, Erickson JW, Fuji R, et al. Targeting mitochondrial glutaminase activity inhibits oncogenic transformation. Cancer Cell 2010;18(3):207-19.

23. Katt WP, Ramachandran S, Erickson JW, Cerione RA. Dibenzophenanthridines as inhibitors of glutaminase C and cancer cell proliferation. Mol Cancer Ther 2012;11(6):1269-78.

24. Xia Z, Donehower LA, Cooper TA, et al. Dynamic analyses of alternative polyadenylation from RNA-seq reveal a 3′-UTR landscape across seven tumour types. Nat Commun 2014;5.

25. Mayr C, Bartel DP. Widespread shortening of 3′ UTRs by alternative cleavage and polyadenylation activates oncogenes in cancer cells. Cell 2009;138(4):673-84.

26. Du J, Zhou Y, Su X, et al. Sirt5 is a NAD-dependent protein lysine demalonylase and desuccinylase. Science 2011;334(6057):806-9.

27. Kleszcz R, Paluszczak J, Baer-Dubowska W. Targeting aberrant cancer metabolism–The role of sirtuins. Pharmacological Reports 2015.